Characterization of the Monocyte to Macrophage Differentiation (MMD) protein and its homologue MMD2

Dissertation zur Erlangung des Doktorgrades der Naturwissenschaften (Dr.rer.nat.) der Naturwissenschaftlichen Fakultät III - Biologie und vorklinische Medizin der Universität Regensburg

vorgelegt von

Carol El Chartouni

aus

Beirut - Libanon

Juni 2006

The work presented in this thesis was carried out in the Department of Hematology and Oncology at the University Hospital Regensburg from June 2002 to Februar 2006.

Die vorliegende Arbeit entstand in der Zeit von Juni 2002 bis Februar 2005 in der Abteilung für Hämatologie und Internistische Onkologie des Klinikums der Universität Regensburg.

Promotionsgesuch eingereicht am: 27.06.2006
Tag der mündlichen Prüfung: 8.09.2006
Die Arbeit wurde angeleitet von: PD Dr. Michael Rehli - Prof. Dr. Stephan Schneuwly.

Prüfungsausshuß:
Vorsitzender: Prof. Dr. Christoph Oberprieler

1. Prüfer (Erstgutachten): Prof: Dr. Stephan Schneuwly
2. Prüfer (Zweitgutachten): PD. Dr. Michael Rehli
3. Prüfer: Prof. Dr. Karl Kunzelmann

Table of contents

List of figures

List of tables

Aknowledgment

I would like to thank Prof. Dr. Reinhard Andreesen for taking me as a PhD student and for his truly generous support during all those years.

I would like to thank Prof. Dr. Stephan Schneuwly for accepting to supervise and review my thesis, but also for accompanying me during my first steps in Germany.

I am very grateful to PD Dr. Michael Rehli for his enthusiasm, his continuous guidance and support, for the great atmosphere in our lab, for the many chances he offered me to learn new things, for his infinite patience and for believing in me even in the moments I doubted myself!

I am grateful to Dr. Markus Moser and his lab for his BIG help in doing the whole mount ISH, but also for the helpful tips, discussions and emails concerning the gene targeting.

Many thanks to PD Dr. Wulf Schneider and particularly Oliver Merkel for sharing with me the method for generating stable cell lines. Without his positive "Aura", I wouldn't have been able to see "green".

I thank Prof. Dr. Klaus Pfeffer, for providing me the backbone vector and for his advices in designing the targeting vectors.

I would like to thank everybody in and outside the lab for the wonderful atmosphere, for making me feel at home, for your patience, technical and foremost moral support. In detail:

Many thanks to Dr. Sven Heinz for your precious tips, your last minute rescue, "the music" and reminding me of "always look on the bright side of…life, ♪♪♪", Dr. Achim Ehrnsperger for your ever gentlemen art, Dr. Viola Hähnel for our morning conversations, and Dr.Cindy Swett for not giving up.

Thanks to PhD. Krishna Mondal for introducing the "Horror Evenings", Dr. Ute Schulz for the Glücksbrot, Maja Klug (die Biene) for always smiling, and Elmar Shilling for the "Komplimentäle", Tobias Weil for supporting the dangerous isopropanol ☺, and PD. Dr. Marina Kreutz, Dr. Eva Gottfried, Sabine Pape, Alice Peuker, and all those I forgot to mention, not to forget the whole Forschungsbau H1 where I could find all I needed for the last minute experiments.
Thank to PhD. Hang Thu Pham, first for the help in the Southern blot technique but also for our talks.
Thanks to Dr. Michael Aigner, for his critical review of the chapters, his valuable advices and tips, and for always reminding me that "wirklich jeder hat es geschaft!!!".

Special thanks to Lucia Schwarzfischer for her precious organization skills, her technical and especially her moral support, for offering to buy the knock-out mouse, in case we ever win the lotto ☺, and for the best bier from Sophie Kneitinger !!!
Thanks to my "Schätzchen" and our "Sport-Beauftragte" Monika Lichtinger (you even drove me to run) for our culinary events, and for your precious friendship and endless patience.
Thanks to my "Schatzy" Claudia Gebhart (Miss Schoky Queen) for the original Bavarian courses from Rötz, and for telling me that "olles haut hi".

Thanks to Dr. Maike Bachthaler and to Dr. Katharina Brandl for their precious friendship during all those years. Thanks to Dr. (El) Bauer Richard for many wine-evenings and conversations, not to forget the "Lebanese" words he kept telling me.

And last but not least, the persons living abroad but always in my heart: Dr. Hernàn Rodriguez, and my cousin Victoria Abboud, who kept encouraging me in my plans, my sweet sister Dalia not only for her love.
I am tremendously grateful to my parents, for their support and patience, and for accepting me being so far for so long. I dedicate this work to you because I know it means to you as much as to me!

1. Introduction

1.1. Mononuclear phagocytes in the immune system

The first line of defense that protects us against pathogens is the innate immune system. It is an ancient natural defense mechanism that comprises the physical barriers (skin, mucous membrane, body fluids or normal bacterial flora), blood proteins as well as cellular components (Abul K.Abbas & Andrew H.Lichtman, 2003). The innate immune response to a pathogen is rapid, antimicrobial but incomplete, initiating the slower, more definitive, acquired response of the adaptive immune system (Fearon & Locksley, 1996).

Macrophages were first described as phagocytic cells and are the most ancient cellular component of the innate immune system. They were discovered in 1880 by Elie Metchnikoff in invertebrates (sea stars) and were soon found to exist in vertebrates as well (Tauber, 2003). Macrophages are the terminally differentiated cell type of the mononuclear phagocyte system, which includes the bone marrow monoblasts, promonoblasts as well as the peripheral monocytes (van Furth, 1982). All these cells arise from a common pluripotent stem cell in the bone marrow (Figure 1.1).

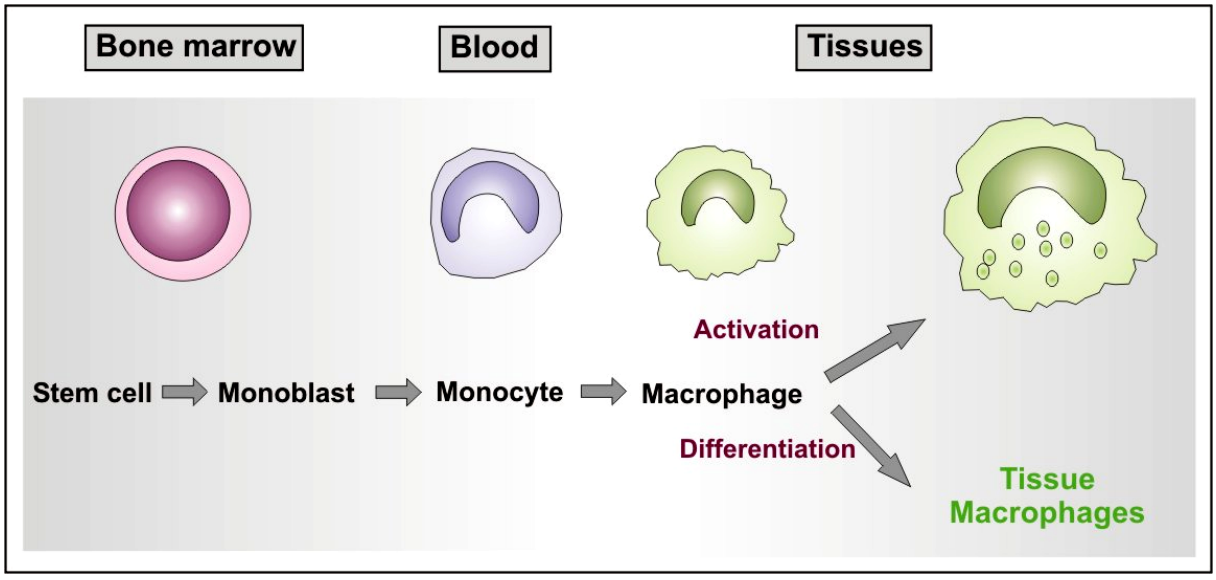

Figure 1.1 Differentiation of mononuclear phagocytes.
Monoblasts develop in the bone marrow from hematopoeitic stem cells. After differentiation, monocytes enter the blood and later migrate to extravascular tissues where they differentiate into macrophages. Depending on external stimuli, macrophages are either activated or differentiated into tissue macrophages (Abul K.Abbas & Andrew H.Lichtman, 2003).

In the bone marrow interleukine 3 (IL-3), granulocytes-macrophage colony-stimulating factor (GM-CSF) and macrophage-CSF (M-CSF) are the major cytokines that direct the maturation of progenitor cells towards monocytes and their release into the bloodstream (Abul K.Abbas & Andrew H.Lichtman, 2003).

1.1.1. Monocyte heterogeneity and differentiation

1.1.1.1. Monocyte heterogeneity

In the blood, at least two major subsets of monocytes exist, each characterized by different markers and properties. Human monocytes are characterized by a differential expression of CD14 and CD16 markers. An inflammatory subset was described as $CD14^{+}CD16^{+}$ and a "classical" subset as $CD14^{hi}CD16^{-}$ (Ziegler-Heitbrock, 2000; Gordon & Taylor, 2005). In mouse, "resident" monocytes were reported to replenish the tissue resident macrophage and dendritic cell (DC) populations under homeostatic conditions and are negative for the monocyte chemotactic protein (MCP)-1 receptor (CCR2) and express high levels of the fractalkine receptor (CX3CR1) (Gordon & Taylor, 2005; Geissmann et al., 2003). Under inflammatory conditions the release of chemokines, such as MCP-1 by activated endothelial and epithelial cells, increases the recruitment of a monocyte subset expressing the MCP-1 receptor at high levels (Gosling et al., 1999; Gu et al., 1998; Boring et al., 1998).

1.1.1.2. Monocyte differentiation

After a short transitory passage in the blood, monocytes attach to the endothelium, roll and diapedese into extravascular tissues, where they differentiate into macrophages and DCs. In culture, monocytes differentiate into macrophages upon exposure to M-CSF (Stanley et al., 1997), and into DCs upon exposure to GM-CSF and IL-4 (Bender et al., 1996; Sallusto & Lanzavecchia, 1994).

However, in vivo, the situation is different because monocytes are under the constant influence of the local microenvironment, whose tremendous variety is reflected in the heterogeneity of these cells (Burke B & Lewis Claire E., 2002). Apart from the influence of cytokine, the endothelium plays a pivotal role in the differentiation of monocytes. In fact, cultured monocytes on unstimulated monolayers of human umbilical vein endothelial cells (grown on a collagenous matrix), diapedese into the subendothelial collagen layer. A proportion of these monocytes "reverse transmigrate" and become DCs, and those that remained differentiated into macrophages. Phagocytosis of particle or exposure to

microorganism enhance the transmigration and differentiation of monocytes. This cytokine independent culture system mimics entry of monocytes from bloodstream into tissues and confirm the influence of the cellular milieu (Randolph et al., 1998).

1.1.2. Macrophage heterogeneity

Macrophages are distributed through the body and form a very heterogeneous cell population, which fulfills various functions. On one side, resident macrophages are responsible for immune surveillance and maintenance of tissue homeostasis. On the other side, upon inflammation, macrophages are activated and thus play a major function in the attenuation and elimination of inflammation and restoring the homeostasis of the inflamed milieu (Burke B & Lewis Claire E., 2002) (see section 1.1.3).

Tissue macrophages are long-lived cells that locally demonstrate modest proliferation activity and whose phenotype and function may depend on the cytokine repertoire produced by surrounding stroma cells as well as the extracellular matrix (endothelial cells, fibroblasts and macrophages) (Gordon et al., 1988; Burke B & Lewis Claire E., 2002). Tissue resident macrophages colonize the whole body. Amongst others are the one described below.

1.1.2.1. Brain macrophages

Microglia, present in the parenchyma of the central nervous system (CNS), constitute the main resident macrophage subset in the brain. In the fetus, microglia plays a central role in structural remodeling by phagocytosing apoptotic cells. In adult, they are characterized by a rapid response to injury and infection (Rezaie & Male, 1999). Microglia contributes to the restoration of damage in the CNS, however they were also associated with multiple sclerosis (MS) and Alzheimer's disease processes (Bar-Or et al., 1999; McGeer et al., 1993). Three other subtypes of macrophages are less abundant in the brain: the perivascular (lining small blood vessels), the meningeal (present in the meninge, membranes surrounding the brain) and the choroids-plexus (present between the blood and the cerebrospinal fluid interface) macrophages. Whereas the meningeal macrophages are involved in restricting the movement of antigens from the blood to the CNS, the two remaining subtypes function mainly as APCs. In addition to endogenous macrophages, there is recruitment of monocytes through the blood-brain barrier (Burke B & Lewis Claire E., 2002).

1.1.2.2. Alveolar macrophages

Alveolar macrophages play a critical role in the defense against airborne pathogens in the lung and are characterized by high capacity to phagocytose. In addition, alveolar macrophages produce a wide range of cytokines, enzymes, as well as reactive oxygen radicals and respiratory burst acting against bacteria (Burke B & Lewis Claire E., 2002).

1.1.2.3. Kupfer cells

Kupffer cells represent the resident macrophages of the liver located in the line sinusoid in direct contact with the blood stream. They play an important role in the clearance of pathogens and soluble substances due to their high phagocytotic capacity. In addition, Kupffer cells were associated with the acute phase protein response which is characterized by fever, tachycardia, shock and changes in concentration of circulating protein. Hepatocytes are the main producers of acute phase proteins under the influence of IL-6 secreted by activated Kupffer cells (Burke B & Lewis Claire E., 2002).

1.1.2.4. Macrophages in peripheral lymphoid organs

The initiation of the adaptive immune response takes place in peripheral lymphoid organs, where antigens are trapped and presented to lymphocytes. Macrophages play a major role in presenting and clearing antigens in lymph nodes and thymus (Charles A.Janeway et al., 2001). In spleen, macrophages form a very heterogeneous population. In the marginal zone, potent phagocytotic macrophages filtrate the blood from foreign antigens as well as effete red blood cells. These marginal zone macrophages express scavenger receptors, which facilitate the clearance of blood borne pathogens (Kraal, 1992). In the white pulp the metallophilic macrophages may play a role in viral infections (O'Riordain et al., 1999; Takahashi et al., 1994).

1.1.2.5. Macrophages of the vascular system

In arteries, macrophages are found within the intima layer and function in maintaining the cholesterol homeostasis in the artery membrane. Cholesterol uptake and its endogenous synthesis is balanced with its metabolism and export outside the cell. Several enzymes, receptors and proteins were found to contribute to this balance. An excess of cholesterol in the blood drives an accumulation of free sterol in macrophages transforming them into so called foam cells, a process that is thought to play a main role in the development of atherosclerosis (Burke B & Lewis Claire E., 2002).

1.1.2.6. Placenta macrophages

Macrophages reside in every organ of the female genital tract and are involved in various processes. Decidual macrophages are abundant in the *deciduas* (endometrial lining developed along the implantation event) and closely associated with extravillous trophoblasts. Decidual macrophages are also involved in the local immune regulation including maternal tolerance against fetal antigens and immune surveillance during pregnancy. Moreover, after the implantation of the embryo, interactions between macrophages and trophoblasts are crucial for the maintenance of pregnancy (Katabuchi et al., 2003; Lea & Clark, 1989).

1.1.3. Macrophages in inflammation

Upon infection, toxin exposure or cell injury, an inflammation is initiated for protection and subsequent repair of damaged tissues (Abul K.Abbas & Andrew H.Lichtman, 2003). Recruited monocytes into inflamed tissues differentiate into macrophages, whose phenotype and function depend on the stimuli.

For a rapid clearance of microbes, macrophages express surface receptors that mediate phagocytosis and subsequent elimination of the pathogen. Amongst others, Toll-like receptors (TLRs) allow the direct recognition of a wide variety of pathogens, such as the bacterial lipopolysaccharide (LPS). LPS is the product of Gram-negative bacteria, which is recognized by TLR4 leading to the alteration of the gene expression in macrophages. This so called "innate" activation involves only the innate immune system and provides macrophages with microbicidial activity and triggers their inflammatory cytokines production, such as IL-1, and tumor necrosis factor (TNF)-α (Abul K.Abbas & Andrew H.Lichtman, 2003).

Once pathogens were eradicated, scavenger receptors (SR) are involved in the clearance of apoptotic cells by inducing phagocytosis and inhibition of pro-inflammatory cytokine production (Fadok et al., 1998), switching off previously activated macrophages. This deactivation process is important to avoid destruction of tissues and persistence of inflammation (Gordon, 2003), and can be achieved with anti-inflammatory cytokines, such as IL-10 (Berrebi et al., 2003).

If inflammation persisted, cells of the adaptive immune system, primed for the pathogen by APCs, trigger macrophages to undergo either a classical or an alternative activation.

1.1.3.1. Classically activated macrophages

"Classically" activated macrophages are found in chronic inflammation, when the innate defense did not succeed in eliminating a microbe. The immune response involves, amongst others, the T helper 1 (Th1) cells of the adaptive immune system with interferon (INF)γ as the key cytokine. INFγ is produced by activated Th1 cells and also by natural killer (NK) cells and primes macrophages for a more efficient killing of intracellular pathogens (Dalton et al., 1993). When primed macrophages encounter a microbial stimulus (such as LPS), they are classically activated and exhibit a phenotype different from the innate activated macrophages (described above). Classically activated macrophages produce pro-inflammatory cytokines (IL-1 and TNFα) (Gordon, 2003). IL-12 secreted by DCs enhances additional INFγ production by Th1 cells, which in turn promote additional classical activation of new macrophages (Abul K.Abbas & Andrew H.Lichtman, 2003). Moreover, the classical activation is coupled with enhanced surface expression of MHC class II and costimulatory molecules as well as increased production of antimicrobial proteins such as elastase, collagenase and lipase. High levels of intracellular reactive oxygen intermediate (ROI) and nitric oxide (NO) are also efficient weapons of the classically activated macrophages against intracellular but also extracellular pathogens (Burke B & Lewis Claire E., 2002; Abul K.Abbas & Andrew H.Lichtman, 2003). Interestingly, as long as the pathogenic stimulus is present, INFγ suppresses an alternative activation of macrophages (described in the following section) keeping a pro-inflammatory state until the eradication of the pathogen (Dickensheets et al., 1999).

1.1.3.2. Alternatively activated macrophages

Alternatively activated macrophages are associated with a suppression of inflammation (Gordon, 2003). T helper 2 (Th2) cytokines, mainly IL-4 and IL-13 induce this phenotype, which is distinct from the deactivation described above (Gordon, 2003; Stein et al., 1992). Alternatively activated macrophages are characterized by an upregulation of mannose receptors (MR), which contribute to clearance of cells debris to avoid the persistence of inflammation and to restore the tissue homeostasis (Taylor et al., 2005). Moreover, their nitric oxide production is reduced resulting from the induction of arginase-I. The later promotes cell growth and collagen production, leading to wound healing of the previously inflamed tissues (Gordon, 2003). The high MHC II molecule expression in alternative activated macrophages enhances the antigen presentation and thus further Th2 cell activation. Alternatively activated macrophages are found in parasitic infection associated with excess fibrosis (Mora et al.,

2006), they inhibit the progression of parasitic infections, thus protecting the host against a disseminated inflammation (Baetselier et al., 2001; Rodriguez et al., 2004).

Taken together, a plausible scenario for macrophage activation is depicted in Figure 1.2. However, in reality the situation is likely to be more complex, because macrophages in vivo not only display different patterns of functions, depending on their microenvironment, but also interact continuously with other components of the immune system. Moreover, the nature of the pathogen inducing the inflammation plays a major conducting role in the polarization of the immune response.

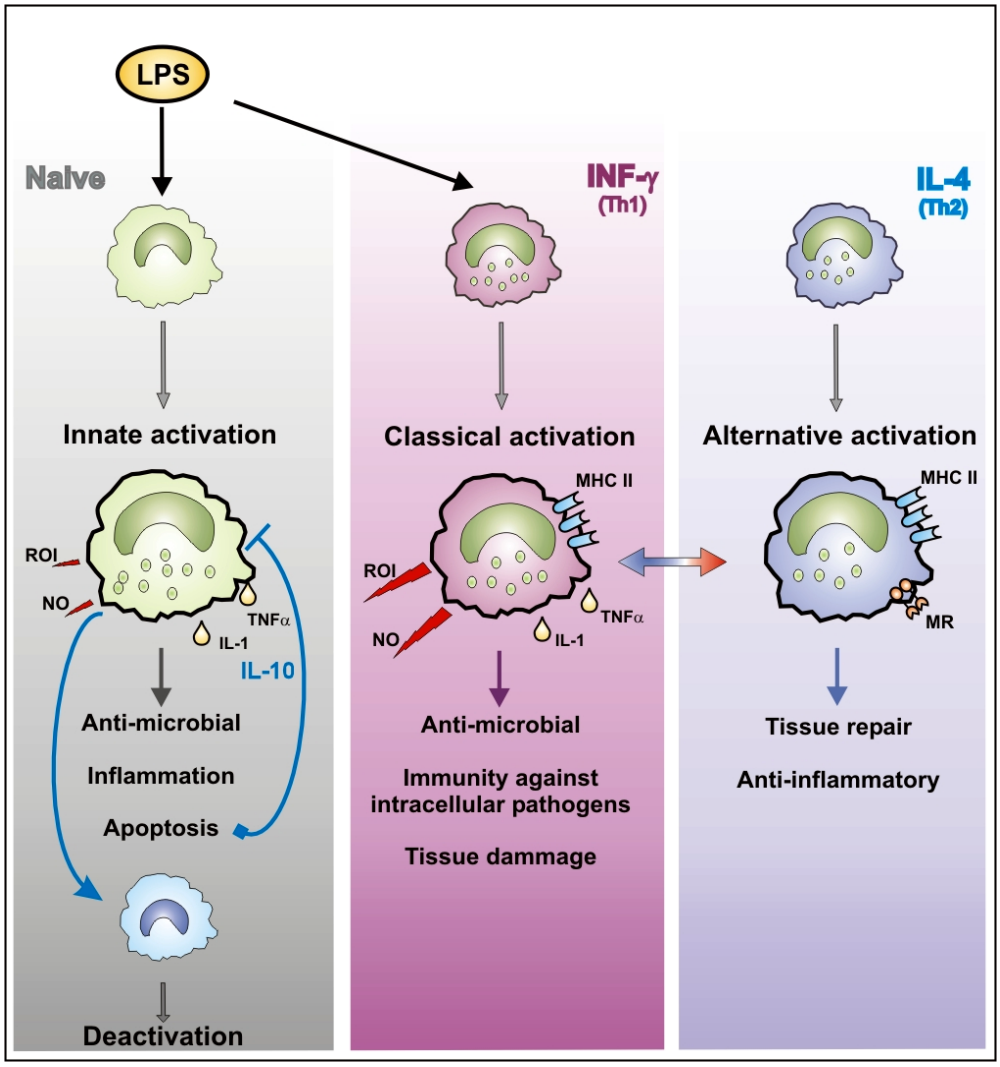

Figure 1.2 Macrophage activation during inflammation.
Recruited macrophages into inflammation sites respond to different stimuli by developing different activation phenotypes. The innate activation (left panel) occurs upon the first pathogenic stimulus. It may be followed by a deactivation under the influence of cytokines, such as IL-10. In an INFγ milieu macrophages are primed and are respond to a second insult by a classical activation phenotype (middle panel), triggering a strong anti-inflammatory response. An IL-4 primed macrophage became alternatively activated (right panel) promoting an anti-inflammatory response and tissue repair. TNF, tumor necrosis factor; MR, mannose receptor; NO, nitric oxide; ROI, respiratory oxygen intermediate.

1.2. MMD, a putative seven transmembrane protein

As detailed above, the differentiation of monocytes to macrophages is a complex process which involves a wide range of proteins, receptors, cytokines, and other mediators. During differentiation and activation, macrophages acquire many new properties and functions not only as cellular components of the innate immune system, but also as important accessory cells in the adaptive immune response. They play also a crucial role in tissue remodeling and healing. This complexity in function reflects a phenotype heterogeneity, which is illustrated by a broad range of specific markers.

Our lab has been focusing on the identification and characterization of new marker proteins, which may provide more insights into the molecular mechanisms underlying the differentiation of macrophages and their newly acquired functions. In this context, a Representational Difference Analysis (RDA) of cDNA was performed leading to the identification of new genes expressed in macrophages and not in monocytes (Rehli M, 1996). Amongst others, the human monocyte to macrophage differentiation (*hMMD*) gene was identified as absent in monocytes but high expressed in macrophages. *hMMD* was isolated, cloned and used to screen a cDNA library to obtain its complete nucleotide sequence (Rehli et al., 1995).

The full-length human MMD (hMMD) cDNA encodes a putative polypeptide of 238 amino acids. Transmembrane prediction analysis of the deduced human MMD protein sequence revealed a seven transmembrane (7TM) domain with paralogues in different species. Blast search showed that hMMD shared 99% amino acid sequence identity with the mouse orthologue mMMD, and both share a conserved UPF0073 motif. The UPF0073 motif was termed after Hemolysin (Hly)-III, which is a protein produced by *Bacillus cereus*, that forms pores in cell membranes (Baida & Kuzmin, 1996). It is considered as a virulence factor of this bacterium, driving the lysis of erythrocytes.

After starting with this project, the full open reading frame (ORF) of mouse and human MMD homologues were published as the monocyte to macrophage differentiation factor 2 (MMD2). Mouse and human *MMD2* genes also encode predicted 7TM proteins, which share a high level of sequence identity (94%) and contain the same UPF0073 motif. Beside a study associating MMD2 with testis development, the function of this protein is still unclear (Menke & Page, 2002).

Recently, Tom Tang Y. et al. (Tang et al., 2005) defined a new protein family, the Progestin and AdipoQ Receptors (PAQRs), which were characterized by a 7TM domain wholly encompassed within the UPF0073 motif. This family includes eleven proteins with conserved amino acid residues and a broad range of functions. MMD and MMD2 were termed as PAQR11 and PAQR10 respectively.

1.3. PAQR family

The PAQR family was identified by performing a tBLASTn analysis using the sequence of the adiponectin receptors, AdipoR1 and 2 (Tang et al., 2005). The input of this assembly analysis was a collection of public and private expressed sequence tags (ESTs) as well as predicted exons from the human genome and it allowed the identification of weak but relevant sequence similarities (Altschul et al., 1997).

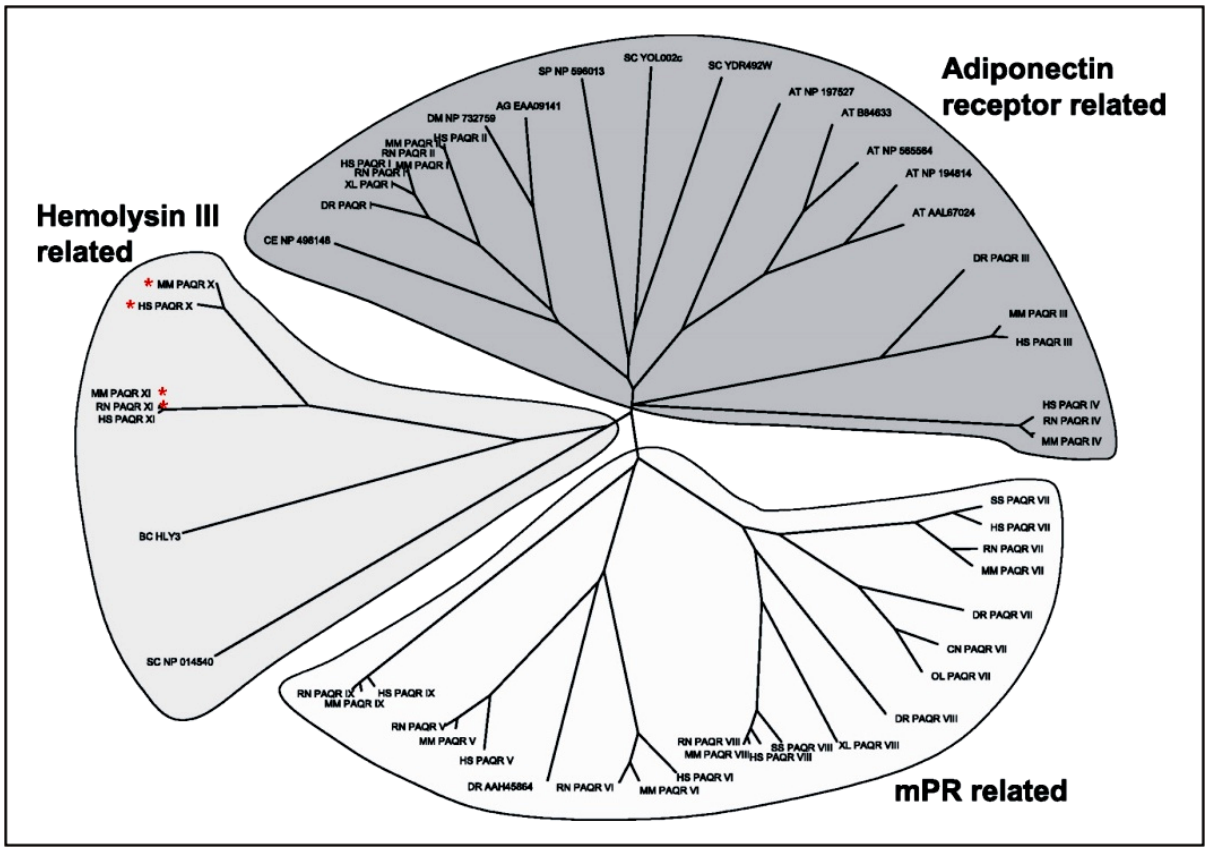

Figure 1.3 Phylogenetic analysis of PAQR family proteins.
MMD and MMD2 (red stars) belong to Hemolysin III proteins diverging from the rest of PAQR family. The protein name prefixes relate to source species of the sequence: HS, *Homo sapiens*; MM, *Mus musculus*; RN, *Rattus norvegicus*; SC, *Saccharomyces cerevisiae*; SP, *Schizosaccharomyces pombe*; CE, *Caenorhabitis elegans*; DR, *Danio rerio*; XL, *Xenopus laevis*; DM, *Drosophila melanogaster*; BC, *Bacillus cereus*; AG, *Anopholes gambiae*; AT, *Arabiodopsis thaliana*; CN, *Cynoscion nebulosus*; OL, *Oryzias latipes*; SS, *Sus scrofa* (Fernandes et al., 2005).

PAQR family members 1 to 11 are structurally and topologically distinct from the G protein-coupled receptors (GPCRs) (Tang et al., 2005). Within the protein sequence of PAQRs, N- and C-terminal regions show very low sequence homology, but a significant portion of amino acid residues were conserved in the transmembrane region. MMD and MMD2 represent the most divergent proteins of this receptor family with the greatest sequence similarities to bacterial Hly-III (Tang et al., 2005). Based on phylogenetic analyses PAQR1-9 were classified as adiponectin receptor and membrane progesterone receptor (mPRs) related proteins (Figure 1.3) (Fernandes et al., 2005; Tang et al., 2005).

1.3.1. Adiponectin receptor related proteins

1.3.1.1. Adiponectin receptors, PAQR1 and PAQR2

AdipoR1 and *AdipoR2* encode proteins that include a 7TM domain characterized with the PFAM conserved UPF0073 motif and show marked conservation from yeast to mammals. Although no significant sequence homology was detected with other PAQR proteins, at the protein sequence level, human and mouse AdipoR1 and AdipoR2 share 96.8% and 95.2% identity respectively (Yamauchi et al., 2003a).

In mouse, the AdipoR1 transcript is mainly expressed in the skeletal muscle but also in the lung, liver, spleen, heart, kidney and very weak in the brain and testis. By contrast, AdipoR2 expression is restricted to the liver and very weak in the heart, lung and skeletal muscle (Yamauchi et al., 2003a).

In human, the Reference Database for Expression Analysis (RefEXA) (www.lsbm.org) reported a high transcript expression of AdipoR1 in the peripheral blood and bone marrow. Interestingly, both AdipoRs were found highly expressed in monocytes and slightly upregulated in macrophages (Figure 1.4).

Although not much is known about the downstream signaling of these receptors, it was reported that the peroxisome proliferator-activated nuclear receptors (PPARs) α and γ regulate AdipoRs expression in macrophages and adiponectin concentration in the plasma (Chinetti et al., 2004; Tsuchida et al., 2005).

The adiponectin protein (also called adipocyte complement related protein (Acrp30), or AdipoQ) is the known ligand of AdipoRs, synthesized and secreted exclusively by adipose tissues. It shares significant homology to subunits of the complement factor C1q with a collagenous structure at the N-terminus and a globular domain at the C-terminus (Hu et al., 1996; Scherer et al., 1995). Adiponectin is abundantly present in the human and mouse

plasma (Arita et al., 1999) and exerts anti-inflammatory, anti-atherogenic and insulin-sensitizing (Hu et al., 1996) effects. The two latest were identified in mouse models studies (Kubota et al., 2006; Combs et al., 2004; Yamauchi et al., 2003b).

The anti-inflammatory effect was illustrated by a suppression of LPS-induced TNFα production (Ouchi et al., 2001) and induction of anti-inflammatory cytokine secretion (IL-10) by macrophages (Kumada et al., 2004). However another study reported that adiponectin anti-inflammatory effects is rather modulated by the induction of TNFα and IL-6 production thus rendering macrophages resistant to pro-inflammatory stimuli (Tsatsanis et al., 2005).

In the bone marrow, secreted adiponectin was found to suppress the proliferation of myelomonocytic progenitor, thus influences the hematopoeisis, in addition it inhibits the phagocytic activity of macrophages (Yokota et al., 2000).

The protective effect of adiponectin against atherosclerosis disease is mediated by the inhibition of the surface expression of adhesion molecules in endothelial cells in response to TNFα. Consequently, the attachment of monocytes to aortic endothelial cells is blocked (Ouchi et al., 1999; Kawanami et al., 2004). The migration and proliferation of smooth muscle cells, which is the second factor promoting the formation of atherosclerosis, may also be hindered by adiponectin (Matsuda et al., 2002). In macrophages, adiponectin inhibits the cholesterol ester accumulation and the uptake of oxidized LDL. Thus, it negatively influences the development of foam cells, which are the main cellular component of the atherosclerotic plaque (Ouchi et al., 2001).

It is still not known if this wide range of adiponectin function is only mediated by AdipoRs. It seems that other "missing links" may mediate the signal inside the cell and their identification may drop more light in the function of the PAQR1 and PAQR2 (Yamauchi et al., 2003a).

1.3.1.2. PAQR3, PAQR4

PAQR3 is a predicted 7TM protein, ubiquitously expressed in all human tissues and without any attributed function (Tang et al., 2005). Fernandes M.S. et al (Fernandes et al., 2005) found that PAQR3 expression in the endometrium and myometrium was constant during pregnancy and after labor, suggesting its role in tissue homeostasis (Fernandes et al., 2005). In *Drosophila* the PAQR3 orthologue, CG7530, with unknown function, was associated with resistance to oxidative stress (Monnier et al., 2002).

To date, PAQR4 has been related to adiponectin receptors without any known function. Its transcript was found in all human tissues outside the breast (Tang et al., 2005).

1.3.2. Membrane progestin receptor (mPR) related proteins

1.3.2.1. PAQR5, 7 and 8

The novel putative mPRα, β and γ, also termed PAQR 7, PAQR 8 and PAQR 5 were identified in fish and human as progestin binding proteins (Zhu et al., 2003a; Zhu et al., 2003b). Progestin, a synthetic modification of progesterone, is a hydrophobic signaling molecule able to diffuse through the plasma membrane and binds to the progesterone receptor (PR) within the cell nucleus. Progestin binding promotes the dissociation of heat shock proteins from the nascent receptor, which dimerizes and gets phosphorylated. This active form of the PR recruits and stabilizes transcription factors at the target gene promoter, leading to its transcription. This "classical" also called "genomic" mechanism of action of steroid hormones is well known (Li et al., 2004).

However, steroid membrane receptors on the cell membrane were found to be responsible for the rapid "non-genomic" steroid action (Orchinik et al., 1992). It was reported that mPRs are such steroid receptors with high affinity for progesterone and characterized by rapid association and dissociation rates (Zhu et al., 2003a). mPRs were predicted to have a 7TM domain with extracellular N-terminal and intracellular C-terminal tails, and thus resembling the GPCRs (Tang et al., 2005). PAQR5, 7 and 8 orthologues share high protein sequence identities, comparable with AdipoR1 and 2 orthologues:

- Mouse/Human mPRα: 83%
- Mouse/Human mPRβ: 94%
- Mouse/Human mPRγ: 92%

Although mPRs were believed to be plasma membrane proteins, mPRα was described to be localized in the intracellular tubuloreticular network (Fernandes et al., 2005), and mPRβ (also termed lysosomal membrane protein in brain (LMPB)-1) was associated to lysosomes (Suzuki et al., 2001). The cellular localization of mPRγ is still unknown.

On the RNA level, mPRα expression was detected in kidney and reproductive tissues (placenta, uterus, testis, and ovary), whereas mPRβ is restricted to the neural tissues, and mPRγ to the kidney, colon, and lung. This differential expression pattern of mPR subtypes may reflect various physiological functions. It has been suggested that mPRα might play a role in pregnancy (Chapman et al., 2006; Fernandes et al., 2005) as well as in the acrosome reaction and the hyperactivity of human sperm in response to progesterone (Revelli et al., 1994; Zhu et al., 2003a). mPRβ was described in association with a form of juvenile

myoclonic epilepsy (JME) in human (Suzuki et al., 2001).To date the function of mPRγ has still not been identified.

Also, little is known about the signaling cascade following the binding of progestin to mPRs. It was found that in sea trout, mPR has a rapid influence on the oocyte maturation by activating an inhibitor G-protein which decreases the intracellular cyclic adenosine monophosphate (cAMP) (Zhu et al., 2003b).

1.3.2.2. PAQR6

PAQR6 was also related to the membrane progestin receptors on the basis of protein sequence homology, however, its function has not yet been defined. Tom Tang Y. et al (Tang et al., 2005) found that PAQR6 transcript is restricted to brain, although they did not include the female reproduction system in their mRNA expression analysis.

1.3.2.3. PAQR9

PAQR9 was first described by Fernandes M.S. et al (Fernandes et al., 2005) in the context of the female reproduction system. So far no function has been attributed to the protein. A high expression of PAQR9 mRNA was found in placenta and cycling endometrium. In addition PAQR9 transcript was predominant in the liver, brain, testis, heart, thymus, in the adult bone marrow, skeletal muscle and kidney (Tang et al., 2005). Although PAQR9 was classified in the mPR family, it is not known in which mechanism it may be involved.

Finally, the discovery of the novel PAQR family introduced three subgroups of receptors which include proteins related to adiponectin, membrane progestin and to the *Bacillus cereus* Hly-III. Although PAQRs share a conserved protein architecture and key amino acid residues, they differ in their transcript expressions and function (for the one that has been described). While PAQR1 and PAQR2 were associated with lipid metabolism, PAQR5, PAQR7 and PAQR8 appeared to be involved in the nongenomic action of steroids, but little is known about PAQR3, PAQR4, PAQR6 and PAQR9 ligands and functions (Table 1.1). The Reference Database for Expression Analysis (www.lsbm.org) reported a high RNA expression of PAQR1, and PAQR2 in monocytes and macrophages. However, PAQR8 and PAQR11 were less expressed in monocytes but at least 2-fold upregulated in macrophages (Figure 1.4).

Table 1.1 PAQR family in human and mouse

PAQR	Synonyms	Reported ligand	Reported functions
1	AdipoR1	Adiponectin	Associated with antidiabetic metabolic effects
2	AdipoR2		
3	--	?	?
4	--	?	?
5	mPRγ	Progestin	?
6	--	?	?
7	mPRα	Progestin	Role in the hyperactivity of the human sperm
8	mPRβ or LMPB-1		Associated with the JME and the placenta cycle
9	--	?	?
10	**MMD2**	?	?
11	**MMD**	?	?

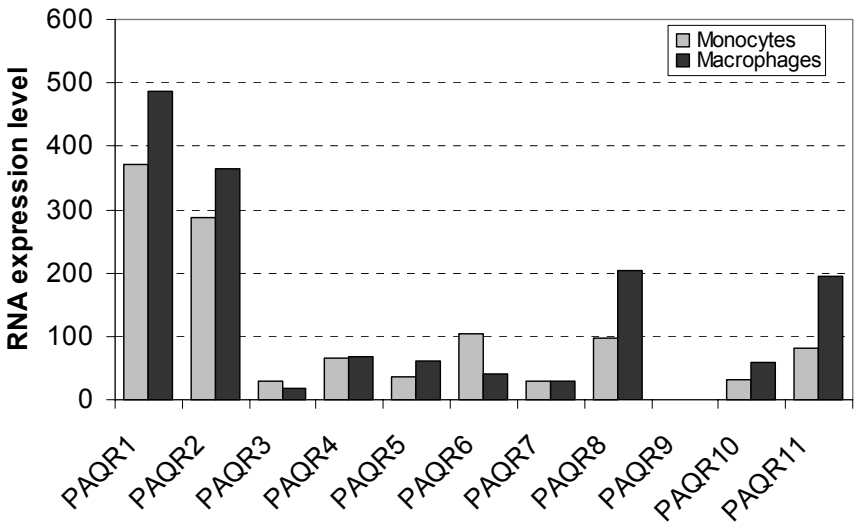

Figure 1.4 RNA expression levels of PAQRs in human monocytes and macrophages.
PAQR1 and PAQR2 are highly expressed in monocytes (grey) and slightly upregulated in macrophages (black). PAQR8 and PAQR11 expressions are at least 2-fold upregulated, in contrast to PAQR6 which is down-regulated in macrophages. The residual PAQRs expression is less significant. No data are reported concerning PAQR9 expression. Values used to generate this diagram were taken from the Reference Database for Expression Analysis (RefEXA) and indicate the mRNA expression level obtained from microarray data of Affimetrix GeneChip U133A (www.lsbm.org).

2. Research objectives

The gene **M**onocyte to **M**acrophage **D**ifferentiation-associated (MMD) was originally identified in our lab during a differential screen for macrophage-differentiation associated transcripts. The MMD gene encodes a hydrophobic orphan seven transmembrane protein that is highly conserved during evolution. As its homologue MMD2, it contains a conserved Hemolysin III domain. The biological function of both MMD genes is unclear, however, due to their exceptional degree of conservation, it was hypothesised that this gene family may have an important function.

The aim of this thesis was to characterize MMD properties and functions, in particular during monocyte to macrophage differentiation, using both molecular and biochemical approaches. Thereby, a major objective was to establish tools, including over-expressing cell lines and knock-out ES cells to enable further studies on the biological function of the highly conserved MMD gene product.

3. Material

3.1. Equipment

Autoclave	Technomara, Fernwald, Germany
Centrifuges	Heraeus, Hanau; Eppendorf, Hamburg, Germany
Densitometer	Molecular Dynamics, Krefeld, Germany
Electrophoresis equipment	Biometra, Göttingen; BioRad, Munich, Germany
Electroporation system and cuvettes	Biometra, Götingen; BioRad, München
Heat sealer (Fermant 400)	Josten & Kettenbaum, Bensberg, Germany
Stratalinker® UV Crosslinker	Stratagene, Germany
Incubators	Heraeus, Hanau, Germany
Laminar air flow cabinet	Heraeus, Hanau, Germany
Luminometer (Sirius)	Berthold Detection Systems, Pforzheim, Germany
Microscopes	Leitz, Heidelberg, Germany
PCR thermocyclers	MJ Research, Hessisch Oldendorf, Germany
pH-Meter	Knick, Berlin, Germany
Power supplies	Biometra, Göttingen; Bachofer, Reutlingen, Germany
Spectrophotometer	Perkin Elmer, Überlingen, Germany
Typhoon™	Amersham Biosciences, Germany
Thermomixer	Eppendorf, Hamburg, Germany
Ultracentrifuge Optima L-70	Beckman, Munich, Germany
Water purification system	Millipore, Eschborn, Germany

3.2. Material

Cell culture flasks and pipettes	Costar, Cambridge, USA
Cryo tubes	Nunc, Wiesbaden, Germany
Sterile micropore filters	Millipore, Eschborn, Germany
Nylon transfer membrane	Roche, Germany
Nitrocellulose membrane (Protran)	Schleicher & Schuell, Dassel, Germany
PVDF membrane (Immobilon-P)	Millipore, Eschborn, Germany
Hyperfilm	Amersham Biosciences, Buckinghamshire, UK
Whatman 3MM paper	Whatman, Maidstone, UK.
Micro test tubes (0.5, 1.5, 2 ml)	Eppendorf, Hamburg, Germany
Multiwell cell culture plates and tubes	Falcon, Heidelberg, Germany

3.3. Chemicals

Unless noted otherwise, chemicals included in these studies were purchased either from Sigma Chemicals (Deisenhofen, Germany) or from Merck (Darmstadt, Germany). Ready-made buffers and cell culture media were obtained from Biochrom (Berlin, Germany) or from Invitrogen (Karlsruhe, Germany). Water was generally of Millipore-purified/distilled quality. When denoted, ultra-pure, DEPC-treated H_2O_{USB} purchased from USB Corp. through Amersham (Braunschweig, Germany) was used.

3.4. DNA oligonucleotides

Oligonucleotides primers were generated by the following companies: TIB Molbiol (Berlin, Germany); Metabion (Martinsried, Germany); and Qiagen (Hilden, Germany).

General primers

T7	5'-TAATACGACTCACTATA-3'
M13 (-20) forward	5'-TTG TAA AAC GAC GGC CAG TG-3'
M13 reverse	5'-GGA AAC AGC TAT GAC CAT GAT-3'

Primers for Northern blot probe PCRs

North-Mous.MMD_S	5'-AAACGATTCCATTGACGC-3'
North-Mous.MMD_AS	5'-AACCACAATGACTTGAACCG-3'
North-Mous.MMD2_S	5'-ATATCCCTGACCATGGTAGG-3'
North-Mous.MMD2_AS	5'-TTCTGATAGAGGAAGACCCTGC-3'
North-Hum.MMD1_S	5'-ATCTCTGCAGGTCCTCATTCATG-3'
North-Hum.MMD1_AS	5'-AATGACTTAACCATTGGGCACC-3'
North-Hum.MMD2_S	5'-AGATGAGGGATGGTGAATGG-3'
North-Hum.MMD2_AS	5'-TTAAGTATGGAGCAGGGAGC-3'
North-H2-MMD2_S	5'-ACCCACTACTATGCCATCTGG-3'
North-H2-MMD2_AS	5'-AGGACTCTTTGCCAGATTCTTC-3'

Primers for tagged-MMD in pIRES-hrGFP-1a

Tag241pIRES_S	5'-ATATGCGGCCGCCATGCGGTTCAGGAATCG-3'
Tag241pIRES_AS	5'-AAGTCTCGAGTAAATGCCGAATAAAGTCTGTGG-3'
MMD241-int_AS	5'-AGAAAATCCCATCGTGAGATAG-3'
EF1seq_AS	5'-ATGGTTCATGAAACGCTG-3'
EF1alpha_S	5'-TAGTTCTCGAGCTTT TGGAGT-3'
End MMD_S	5'-AGCCTTGGTGGTGACATCAA-3'
HA tag-S	5'-AATGCGGCCGCTCATGTACCCATACGATGTTCCAG ATTACGCTATGCGGTTCAGGAATCG-3'
MMD-stop-AS	5'-CCCTCGAGTCATAAATGCCGAATAAAGTCTG-3'
myc tag-S	5'-ACTCATCTCAGAAGAGGATCTGTTGAGAACAGTGG AGCATTGT-3'

Primers for tagged-MMD in pIRES-hrGFP-1a (continued)

myc tag-AS	5’-CAGATCCTCTTCTGAGATGAGTTTTTGTTCGTGGCT CTTCTTCCATGATACTA-3’
Flag-tag_S	5’-AATGCGGCCGCGCCACCATGGATTACAAGGATGAC GATAAGATGCGGTTCAGGAATCGATTC -3’
HAc-term_AS	5’-AAGTCTCGAGTCAAGCGTAATCTGGAACATCGTATG GTATAAATGCCGAATAAAGTCTGT-3’
Mu2-stop-AS	5’-CCCTCGAGTCATAAATGCCGAATAAAGTCTG-3’
Myc1-tag_S	5’-GAACAAAAACTCATCTCAGAAGAGGATCTGGACTG CTGGGAGAAGATAACA-3’
Myc1-tag_AS	5’-CAGATCCTCTTCTGAGATGAGTTTTTGTTCATCAGA CAGCCGATGGAG-3’

Primers for tagged-MMD in pQCXIP

pQCXIP 5’ primer	5’-ACGCCATCCACGCTGTTTTGACCT-3’
pQCXIP 3’ primer	5’-AAGCGGCTTCGGCCAGTAACGTTA-3’
BamHI-stopMMD-AS	5’-CGCGGATCCGCTCATAAATGCCGAATAAAGTCTG-3’

Primers for targeting construct I

LKA_S	5’-ACTGGCGGCCGCGTGATTGGTCAGAATAGATACTG GC-3’
LKA_AS	5’-TGTTCTGGCACTAGGCAGC-3’
LA_S	5’-ATCTGTCGACCGCAGGTACACAGCCCG-3’
LAn_AS	5’-TACACTCGAGCTTGTGTCTCGGGCTCCC-3’
geno5’-dd3f_S	5’-CTTGTTTAGGTGGCCTGGAGG-3’
geno5’-dd3f_AS	5’-GGTGAACAGCTCCTCGCCC-3’
geno3’-dd3f_S	5’-GTCATTCGTTTGAGGCCACC-3’
geno3’-dd3f_AS	5’-CACAACTGTCAGGCCATGCC-3’

Primers for targeting construct II

1.Arm5’-1_S	5'-ATATGCGGCCGCCCACCTCTTAGACTCACATTACA GG-3'
1.Arm5’-1_AS	5'-AAAAGTGGCTAGCGTGCATAG-3’
1.Arm5’-2_S	5'-AATAAGCCCTGCCTCACTAACCATC-3’
1.Arm5’-2_AS	5’-ACTTATTGCCTATGGGATGAGAGTGC-3’
1.Arm5’-3_S	5’-ATTCCTAGTAGGGTATGAGCCACGC-3’
1.Arm5’-3_AS	5'-CGCGGATCCCCGATGGTTCATGAAACTGTGGA-3'
intArm1_S	5’-ATCAAAGTCAACTAGGGGCAG-3’
intArm1_AS	5’-ATCAGCTCATTACTACACTCCTTGG-3’
intArm2_S	5’-ATCCAGCTTACCCATTCATCG-3’
intArm2_AS	5’-AAGCTCGAGGACAAGTTCAC-3’
intArm3_S	5’-ATCATGGGAATGGAGAATGTG-3’
intArm3_AS	5’-AGTAGAGGGCCTGTCGGACTAG-3’
5’South1_S	5’-ATCAATGCGGTTCAGGAATCG-3’
5’South1_AS	5’-TCACCCACTTAGAAACATTAAAGCC-3’

Primers for targeting construct III

5'probe-NcoI_S	5'-ATGTCACAGTGTCAAAAGATTGG-3'
5'probe-NcoI_AS	5'-ATTGAAAAAGACACCTGTTACTAGC-3'

Primers for targeting construct IV

SA-Not_S	5'-ATAAGAATGCGGCCGCGGTAAGATAGCATCCTGTACC-3'
SA-EcoR_AS	5'-CCGGAATTCATAGATGCAAATGACAAAGG-3'
Laex6-1_S	5'-ACGCGTCGACGGGAACTTCAGTATAAGAGTGTTACATTA-3'
LAex6-1_AS	5'-ATTGCTATTTGGAAAGTCTACAGG -3'
LA 6ex6-2_S	5'-AATAATGAATTAAAGCTGCGGGC-3'
LA ex6-2_AS	5'-ATGTTACTGAAGAAGTACCCTCACAAC-3'
LA ex6-3_S	5'-TAGTAAGGAATATGCAACCTGACAAG-3'
LA ex6-3_AS	5'-ACGCGTCGACAGCAACTGGCTTCAGGAAAAG-3’
Southex6_S	5’-TTCAGCACAGCATAGAAGCCAG-3’
Southex6_AS	5’-TAGCTAAGCCTATACTTCAAATGG-3’
SA-in	5’-ACTATAGTTTCTCCCCTAGACC-3’
LA ex6-1-in	5’-AGTCTCCTATTGAACGGAAAC-3’
LA ex6-3-in	5’-AATACTACCGGTTGAACC-3’

Light cycler MMD primer

MMD-S	5’-GTGACATCAATGAATAACACTGACGGAC-3’
MMD-AS	5’-TGAAGAACACAACTCCCAAGCAG-3’

3.5. Antibodies

Monoclonal antibodies

Mouse anti-FLAG M2 (IgG1)	SIGMA-ALDRICH, Germany
Rat anti-HA high affinity (clone 3F10)	Roche, Germany
Mouse anti-cMyc	Werner Falk
(FITC)-conj. rat anti-mouse CD107a (LAMP-1)	BD Biosciences Clontech, Germany

Polyclonal antibodies

Alexa Fluor® 546 goat anti-mouse IgG (H+L)	Molecular Probes, Inc. USA
Alexa Fluor® 546 goat anti-rat IgG (H+L)	Molecular Probes, Inc. USA
Rabbit anti-rat HRP	DakoCytomation, Denmark
Goat anti-mouse HRP	DakoCytomation, Denmark

3.6. Enzymes and kits

Restriction endonucleases, DNA polymerases and protease inhibitors were purchased from ROCHE (Germany)and New England Biolab (Frankfurt Germany), unless noted otherwise.

DIG Easy Hyb.	Roche, Germany
DIG Easy wash and block buffer set	Roche, Germany
Lipofectamin transfection reagent	Invitrogen, Karlsruhe, Germany
DNA molecular weight standard	Invitrogen, Karlsruhe, Germany
Mouse ES cell transfector® kit	Amaxa biosystems, Cologne, Germany

NucleoSpin® Extract II	Macherey-Nagel, Düren, Germany
NucleoSpin® Plasmid Quick Pure	Macherey-Nagel, Düren, Germany
PCR DIG probe synthesis kit	Roche, Germany
Plasmid preparation kits	Qiagen, Hilden, Germany
QIAEX II gel extraction kit	Qiagen, Hilden, Germany
Qiagen-Effectene transfection reagent	Qiagen, Hilden, Germany
RetroMax™ System	IMGENEX, San Diego, USA
RNeasy Midi kit	Qiagen, Hilden, Germany

3.7. Molecular weight standards

DNA Ladder 1 kB Plus was purchased from Invitrogen (Karlsruhe, Germany). For Southern blot analysis, DIG-labeled DNA Molecular Weight Marker III, was purchased from Roche, (Germany). The Kaleidoscope Prestained standard protein marker was purchased from BioRad (Munich, Germany).

3.8. Plasmids

pCR®2.1-TOPO	Invitrogen, Karlsruhe, Germany
pEF6/V5-HIS-TOPO	Invitrogen, Karlsruhe, Germany
pBluescript II KS+	Stratagene, La Jola CA, USA
pIRES-hrGFP-1a	Stratagene, La Jola CA, USA
pQCXIP	BD Biosciences Clontech, Germany
pCLEco	IMGENEX, San Diego, USA
pCL-10A1	IMGENEX, San Diego, USA

3.9. E.coli strains

The following bacterial strains were used:

TOP10	F- mcrA Δ(mrr-hsdRMS-mcrBC) Φ80lacZΔM15 ΔlacX74 recA1 deoR araD139 Δ(ara-leu)7697 galU galK rpsL (StrR) endA1 nupG
DH10B	F-mcrA Δ(mrr-hsdRMS-mcrBC) Φ80lacZΔM15 ΔlacX74 recA1 deoR araD139 Δ(ara-leu)7697 galU galK rpsL endA1 nupG

3.10. Antibiotics

Antibiotic	Selection	Working concentration	Stock solution
Ampicillin	Prokaryotic cells	50-100 µg/ml	100 mg/ml in H_2O
Neomycin (G420)	Eukaryotic cells	200-350 µg/ml	10-50 mg/ml
Puromycin	Eukaryotic cells	1 mg/ml	4 µg/ml in PBS

3.11. Animal cell lines culture

Murine cell lines

NIH 3T3	Swiss mouse embryo fibroblast (DSMZ no. ACC 59)
RAW 264.7	Mouse monocyte-macrophage BALB/c (ATCC TIB-71)
P815	Mouse mastocytoma (ATCC TIB 64)
BV-2	Mouse microglia (Zürich, W.Milipiero)
HT-2	Spleen helper T-cell, IL-2 dependent (ATCC CRL-1841)
J774A.1	Mouse monocytes-macrophage BALB/c (DSMZ no. ACC 170)
ES	E14.1 embryonic stem cells (129/Ola mouse)
EF	Embryonic fibroblast (CD1 mouse)
EFneo	Embryonic fibroblast (Nc1 neomycin resitant +/- mouse)

Human cell lines

THP-1	Human acute monocytic leukemia (DSMZ no. ACC 16)
HL-60	Human acute myeloid leukemia (DSMZ no. ACC 3)
Hep G2	Hepatocellular carcinoma (ATCC HB-8065)
Mono-Mac-6	Human acute monocytic leukemia (DSMZ no. ACC 124)
CaCo-2	Human colon adenocarcinoma (DSMZ no. ACC 169)
HT-29	Human colon adenocarcinoma (DSMZ no. ACC 299)
U-937	Human hystiocytic lymphoma (DSZM no. ACC5)

3.12. Databases research

PubMed	www.ncbi.nlm.nih.gov/entrez
Ensembl Browser	www.ensembl.org
BLAST	www.ncbi.nlm.nih.gov/BLAST
ClustalW	www.ebi.ac.uk/clustalw
ExPASy Proteomic	www.expasy.org
USCS Gen. Browser	www.genome.ucsc.edu
LSBM	www.lsbm.org
SymATLAS	www.symatlas.gnf.org

4. Methods

Unless otherwise mentioned, all methods were based on protocols described in the Current protocols of Molecular Biology (Ausubel Frederick et al., 2006), and in the Molecular cloning laboratory manual (Sambrook & Russel, 2001).

4.1. General molecular biology

4.1.1. Bacterial culture

4.1.1.1. Bacterial growth medium

E.coli strains were streaked out on solid LB-agar with antibiotic and grown overnight. Single colonies were then picked and grown in liquid cultures overnight. For blue/white screening of insert-containing clones after transformation, 40 µl of X-gal was dispersed on the pre-warmed LB plates, that were incubated at 37°C for an additional 30 min prior to use. The transformation was then spread out using a Drigalski spatula.
Liquid cultures were grown overnight, at 37°C with shaking at 200 rpm, in LB medium with the appropriate antibiotics (see section 3.10).

LB medium	10 g	NaCl
	10 g	Bacto Tryptone (Difco)
	5 g	Yeast extract
	Add H_2O to 1 l, autoclave.	
LB-agar plates	15 g	Agar
	10 g	NaCl
	10 g	Bacto Tryptone (Difco)
	5 g	Yeast extract
	Add H_2O to 1 l, autoclave, cool to 50°C and add antibiotic.	
	Pour the agar solution into 10cm Petri dishes, and store inverted at 4°C.	
X-gal	40mg	X-gal (5-bromo-4-chloro-3-indolyl-β-D-galactoside)
	In 1 ml DMF, store in a brown bottle at -20°C in the dark.	

4.1.1.2. Preparation of chemically competent E.coli

The desired bacterial strain was streaked out on solid LB agar with antibiotic, grown overnight and a single bacterial colony was picked into 5 ml Ψ Broth. Bacteria were grown at 37°C with shaking to an OD550 of 0.3, and the 5 ml culture was used to inoculate 100 ml

Ψ Broth prewarmed to 37°C. After growing to an OD550 of 0.48, cells were chilled on ice and pelleted at 1300 g and 4°C for 5-10 min. The pellet was loosened up by vortexing and resuspended in 30 ml ice-cold TfBI. After incubation on ice for 5 min, cells were collected by centrifugation (5 min, 4000 g, 4°C) and resuspended in 4 ml ice-cold TfBII. The suspension was dispensed into 50 µl aliquots and frozen at -80°C.

Required buffers:

Ψbroth	**2%**	20 g	Bacto Tryptone (Difco)
	0.5%	5 g	Bacto Yeast Extract (Difco)
	0.4%	8,18 g	$MgSO_4.7H_2O$
	10 mM	0.745 g	KCl
	Adjust to pH 7.6 with KOH and add H_2O to 1 l.		
TfBI	**100 mM**	6.045 g	$RbCl_2$
	50 mM	4.5 g	$MnCl_2$
	30 mM	1.472 g	KOAc
	10 mM	0.735 g	$CaCl_2.2H_2O$
	15%	75 ml	Glycerol
	Adjust to pH 5.8 with 0.2 M HOAc		
	Add H_2O to 500 ml, filter sterilize and store at 4°C.		
TfBII	**10 mM**	1.047 g	MOPS/NaOH, pH 7.0
	10 mM	0.605 g	$RbCl_2$
	75 mM	5.513 g	$CaCl_2$
	15%	75 ml	Glycerol
	Add H_2O to 500 ml, filter sterilize and store at 4°C.		

4.1.1.3. Transformation of chemically competent E.coli

Chemically competent *E.coli* (50 µl) were thawed on ice, 1-25 ng plasmid DNA in 2-5 µl volume was added and the suspension was mixed gently and incubated on ice for 30 min. Cells were heat-shocked in a water bath at 42°C for 130 s, immediately cooled on ice for 2 min and 250 µl SOC medium was added. To express the resistance, bacteria were incubated for 1 h at 37°C with shaking and 50-150 µl of the transformation were plated and incubated overnight at 37°C on LB-agar containing the antibiotic necessary for selection of transformed cells.

Required medium:

SOC medium	**2%**	20 g	BactoTrypton (Difco)
	0.5%	5 g	BactoYeastExtract (Difco)
	10 mM	0.6 g	NaCl
	3 mM	0.2 g	KCl
	Add H_2O to 1 l, autoclave and add to the cooled solution:		
	10 mM	10 ml	$MgCl_2$ 1M, sterile filtered
	10 mM	10 ml	$MgSO_4$ 1M,sterile filtered
	20 mM	10 ml	Glucose 2 M, sterile filtered.

4.1.1.4. Glycerol stock

For long-term storage, bacteria were stored in 20% glycerol by adding 500 µl liquid culture to 200 µl of 80% glycerol, mixing and freezing at -80°C.

4.1.2. Plasmid isolation from E.coli

To check if the isolated single *E.coli* colonies contained the correct plasmid, a DNA mini-prep was carried out using NucleoSpin® Plasmid Quick Pure Kit from Macherey-Nagel following the supplied instructions. To isolate larger amounts of ultra pure DNA (100 µg) for transfection experiments, plasmids were isolated using QIAGEN Plasmid Midi, Maxi and Mega Kits.

4.1.3. Molecular cloning

Direct cloning of PCR-products was done using the TOPO-TA Cloning kit (Invitrogen) according to the manufacturer's instructions. Alternatively DNA fragments were PEG-precipitated (see section 4.1.3.3) and the precipitate as well as the cloning vector were digested with the necessary endonuclease. For directional cloning, restriction sites were introduced by adding the appropriate recognition sequences to the primer sequences The cut fragment and vector were gel-purified (see section 4.1.3.4), and combined in a 10 µl ligation reaction at a 3- to 5-fold molar excess of insert to vector, using 25-50 ng of vector. Ligation was carried out overnight at 16°C with 1U T4 DNA ligase buffer. Two µl of the reaction was used to transform chemically competent *E.coli* (see sections 4.1.1.2 and 4.1.1.3).
Successful insertion of the fragment into the vector was checked by preparing plasmid DNA from liquid cultures (see section 4.1.2). To check for correct insertion and sequence integrity, plasmid constructs were sequenced using vector-specific primers.

4.1.3.1. PCR

The polymerase chain reaction (PCR) allows in-vitro synthesis of large amounts of DNA by primed, sequence-specific polymerization of nucleotide triphosphates catalyzed by DNA polymerase. PCRs were generally performed in PCR tubes in 20-100 µl of reaction volume in a MJ research PTC 200 thermocycler (Biozym). The "calculated temperature" feature was used to decrease temperature hold times. The nucleotide sequences of the utilized primers are given in 3.4. The primer annealing temperatures varied between 57 and 65°C.
Typical reaction parameters for analytical PCR were:

Action		PTC 200	
Initial Melting		95°C	2 min
20-35 Cycles	Melt	95°C	15 sec
	Anneal	65°C	15 sec
	Extend	72°C	1 min
Final Extension		72°C	5-7 min
Cool to		15°C	∞

If PCRs were performed from bacterial colonies, the initial melting step was prolonged to 2 min. To avoid generating unspecific products during the first heating phase, reaction tubes were transferred into thermocycler, once the block temperature reached 95°C.
Required:

DNA polymerase	**0.04-0.67 U/µl**	Taq DNA polymerase or Expand High Fidelity polymerase mix with the supplied reaction buffer
Primers	**0.2-1 µM**	Sense-/antisense primers (10-100 µM)
dNTPs	**0.2-0.25 mM**	dATP, dCTP, dGTP, dTTP (25 mM each).

4.1.3.2. PCR-based site specific mutagenesis

For site-specific mutagenesis of single sites, and to generate tagged-internally constructs, two overlapping fragments containing the desired mutation at their ends were generated by PCR using sense/antisense mutant primers (primer I-AS and primer II-S), which contained the mutation in the centre of the oligonucleotide together with fragment-specific (outer) primers featuring endonuclease restriction sites for directional cloning in two separate reactions (primer I-S and primer II-AS respectively). The PCR products were gel-extracted together to give 20 µl of gel extract (GE) which served as template for a second PCR employing the outer primers (Primer I-S and primer II-AS) to assemble the two fragments at their overlapping portion. The ensuing PCR product was PEG-precipitated and TOPO cloned into the pCR2.1 vector. The insert was sequenced to confirm the incorporation of the mutation and the integrity of the sequence, then subcloned into the desired vector.
To facilitate incorporation of the mutation into the PCR product, the first round of PCRs was performed with *Taq* polymerase which does not possess a 3'→5' proofreading activity. For maximum accuracy, the second PCR was carried out using a DNA polymerase mix (Expand High Fidelity, Roche) with proofreading activity.

PCR-Reactions:	**PCR 1**	**PCR 2**	**PCR 3**
DNA template	1 µg	1 µg	20 µl GE PCR1+2
10x Taq Buffer	10 µl	10 µl	-
10x HiFi Buffer	-	-	10 µl
dNTP (10 mM each)	2 µl	2 µl	2 µl
Primer I-S (10 pmol/µl)	5 µl	-	5 µl
Primer I-AS (10 pmol/µl)	-	5 µl	5 µl
Primer II-S (10 pmol/µl)	-	5 µl	-
Primer II-AS (10 pmol/µl)	5 µl	-	-
H_20	to 98 µl	to 98 µl	to 98 µl
Taq	2 µl	2 µl	-
HiFi	-	-	2 µl

To avoid producing amplification errors due to high cycle numbers, PCRs were performed in quadruplicates for 6, 9, 12 and 15 cycles and the product generated by the lowest number of cycles was used for the residual the procedure. PCRs were performed using the following program:

Action		**PTC 200**	
Initial Melting		95°C	3 min
20-35 Cycles	Melt	95°C	15 sec
	Anneal	65°C	20 sec
	Extend	72°C	1:10 min
Final Extension		72°C	7 min
Cool to		15°C	∞

4.1.3.3. Precipitation of DNA using PEG

To precipitate DNA from small volumes, e.g. PCR reactions or endonuclease digestion, one volume of PEG-mix was added to the DNA-containing solution, vortexed and incubated for 10 min at RT. After centrifugation (10 min, 13000 rpm, RT), the supernatant was discarded and the precipitated DNA was washed by carefully adding 200 µl 100% EtOH to the tube wall opposite of the (often invisible) pellet, followed by a centrifugation step (10 min, 13000 rpm, RT) and careful removal of the supernatant. The pellet was dried and resuspended in H_2O at half to three-quarters of the initial volume.

PEG-mix	**26.2 %**	26.2 g	PEG 8000
	0.67 M	20 ml	NaOAc (3 M) pH 5.2
	0.67 mM	660 µl	$MgCl_2$ (1 M)
	Add H_2O to 250 ml.		

4.1.3.4. Purification of DNA fragment by gel extraction

DNA fragments were purified by running on an ethidium bromide-containing agarose gel, excising the band containing the fragment under UV illumination and subsequent gel extraction using QIAEX II Gel Extraction Kit (Qiagen) or NucleoSpin® Exract II following the manufacturer's instructions.

4.1.3.5. Agarose gel electrophoresis

The required amount of agarose as determined according to table 3.1 and table 3.2 was added to the corresponding amount of TAE (1x). The slurry was heated in a microwave oven until the agarose was completely dissolved. The ethidium bromide was added after cooling the solution to 50-60°C. The gel was cast and mounted in the electrophoresis tank and covered with TAE (1x). DNA-containing samples were diluted 4:1 with DNA loading dye (5x), mixed and loaded into the slots of the submerged gel. Depending on the size and the desired resolution, gels were run at 40-100 V for 30 min to 3 h.
Required buffers:

TAE (50x)	**2 M**	252.3 g	Tris
	250 mM	20.5 g	NaOAc/HOAc, pH 7.8
	50 mM	18.5 g	EDTA
	Add H_2O to 1 l.		
EDTA (0.5 M)	**0.5 M**	18.6 g	EDTA/NaOH, pH 8.0
	Add H_2O to 100 ml.		
DNA loading dye	**50 mM**	500 µl	Tris/HCl, pH 7.8
DNA-LD (5x)	**1%**	500 µl	SDS (20%)
	50 mM	1 ml	EDTA (0.5 M), pH 8.0
	40%	4 ml	Glycerol
	1%	10 mg	Bromophenol blue
	Add H_2O to 10 ml, and store at 4°C.		
1.0% Agarose	**1%**	1 g	Agarose (Biozym)
	Add 1x TAE to 100 ml, and till agarose dissolves.		
	Cool to 50°C and add 2.5 µl Ethidium bromide (10 mg/ml) (Sigma).		

Table 4.1 Agarose concentration for different separation ranges

Efficient range of separation (kb)	Agarose in gel (%)
0.1-2	2.0
0.2-3	1.5
0.4-6	1.2
0.5-7	0.9
0.8-10	0.7

4.1.3.6. Restriction endonuclease digestion

To verify the presence and orientation of plasmid-insert, or to clone insert DNA into a plasmid, DNA was digested with appropriate restriction enzymes. Enzymes and their buffers were purchased from Roche or New England Biolabs (Germany). The digestion of plasmid DNA or PCR products was carried out using 5 U enzyme/1 µg DNA in 20 µl at 37°C for 2 hours. Digestion of genomic DNA was performed overnight with 1.5 U/µg DNA in 30 µl reaction volume.

4.1.3.7. Dephosphorylation of DNA with alkaline phosphatase

To prevent the self ligation, digested vectors were treated with CIAP (calf intestinal alkaline phosphatase, Roche) at 37°C for 30 min before gel extraction.

4.1.3.8. Fill in 5'-overhang with Klenow DNA-polymerase

To ligate two DNA fragments cut with two incompatible enzymes, blunt ends were generated by filling the 5'- or the 3'-overhangs (see section 4.1.3.9). To fill in 5'-overhanging ends of DNA fragments, digested DNA was mixed with 1 µl of dNTPs (0.5 mM each), 4 U Klenow fragment and H_2O to a total volume of 20 µl, and incubated for 15 min at 30°C. The inactivation of Klenow was done by heating for 10 min at 75°C. The DNA fragment with blunt ends was then either digested with a second enzyme or purified and used for ligation.

4.1.3.9. Generation of blunt ends with T4 DNA-polymerase

To fill in 3'-overhanging ends of DNA, T4 polymerase was used. Digested DNA was incubated with T4 polymerase at 11°C for 20 min. T4 polymerase was then inactivated for 20 min at 70°C.

4.1.3.10. DNA sequencing and sequence analysis

Sequencing was performed by Entelechon or GeneArt (Regensburg, Germany). Database searches in GenBank were performed with BLAST v2.11.1 at the NCBI (URL: http://www.ncbi.nlm.nih.gov/BLAST/).

4.1.3.11. Generation of different MMD tagged constructs

Mouse MMD construct tagged C-terminally with 3xFLAG was prepared as following. Briefly mMMD cDNA, previously cloned into pGEM3, was amplified by PCR using "Tag241pIRES_S" and "Tag241pIRES_AS" primers, introducing NotI and XhoI restriction

sites respectively. In addition the Stop codon at the C-terminus of mMMD cDNA was removed to allow fusion of 3xFLAG-tag with mMMD protein. The PCR product was digested with NotI and XhoI and inserted into pIRES-hrGFP-1a vector upstream of 3xFLAG-tag sequence. MMD-3xFLAG construct was used as template to generate additional constructs.
For this purpose, PCR reactions were performed with pIRES-MMD-3xFLAG as template and using different primer pairs, introducing NotI restriction site upstream of the ATG start codon, and XhoI downstream of the insert. PCR products were purified via gel extraction and cloned into the pCR2-1-TOPO vector. After sequence confirmation, the insert was cut with NotI and XhoI restriction enzymes and cloned into pIRES-hrGFP-1a vector. A schematic presentation of the cloning strategies are depicted in Figure 5.12.

- *Cloning of pIRES-HA-MMD*

To tag MMD N-terminally with an HA-eptitope, a PCR reaction was performed using "HA tag-S" primer containing NotI site followed by a start codon and HA-tag sequence. A stop codon was introduced at the C-terminus of mMMD with antisense "Mu2-stop-AS" primer to prevent the translation of 3xFLAG-tag (Figure 5.12C)

- *Cloning of pIRES-HA-MMD-3xFLAG*

For tagging MMD at the N- and C-terminus with HA and 3xFLAG respectively, the same PCR amplification reaction was performed as described above but using "Tag241pIRES_AS" antisense primer to allow transcription of 3xFLAG-tag (Figure 5.12B).

- *Cloning of pIRES-FLAG-MMD-HA*

To incorporate a single FLAG-tag (in contrast to 3xFLAG usually used) at the N-terminus and an HA-tag at the C-terminus of mMMD, a PCR reaction was performed with "Flag-tag-S" as sense primer inserting a NotI restriction site upstream of FLAG-tag. The antisense primer, "HAc-term-AS" incorporates the HA-tag sequence followed by a stop codon and a XhoI restriction site (Figure 5.12D).

- *Cloning of pIRES-HA-MMD(c-Myc2)-3xFLAG*

To incorporate an additional c-Myc-tag in the second extramembrane loop of MMD protein, a PCR-based site specific mutagenesis was done (see section 4.1.3.2). It consists in generating initially two PCR products with pIRES-MMD-3xFLAG as template. The first reaction was done using "HA-tag-s" and "myc-tag-AS" (containing c-Myc sequence) primers. The second

PCR reaction was performed using "myc-tag-S" and "Tag241pIRES_AS". After gel extraction both PCR products were mixed and used as template for the third reaction done with primers "HA-tag_s" and "Tag241pIRES_AS" (Figure 5.12E).

- *Cloning of pIRES-MMD(c-Myc2)-3xFLAG*

In order to tag MMD with c-Myc at the second extramembrane loop and 3xFLAG on the C-terminus, a PCR-based site specific mutagenesis was performed, as described above using "Tag241pIRES_S" and "myc-tag-AS" primers for the first PCR, and "myc-tag-S" and "Tag241pIRES-AS" primers for the second PCR. After gel extraction of the PCR product, it was used as template in the third PCR done with primers "Tag241pIRES_S" and "Tag241pIRES_AS" (Figure 5.12F).

- *Cloning of pIRES-HA-MMD(c-Myc2)*

For the creation of this construct, the first PCR product of pIRES-HA-MMD(c-myc)-3xFLAG was mixed with a PCR product, generated using primers "myc-tag-S" and "MMD-stop-AS". This mix was used as template for the third PCR reaction with primers "HA-tag-s" and "MMD-stop-AS" (Figure 5.12G).

- *Cloning of pIRES-MMD(c-Myc2)*

To generate a MMD tag construct with only c-Myc integrated in the second extramembrane loop, again a PCR site specific mutagenesis was carried out. The first PCR product of pIRES-MMD(c-myc)-3xFLAG was mixed with the second PCR product of pIRES-HA-MMD(c-myc), and used as template for a third reaction using primers "Tag241pIRES_S" and "MMD-stop-AS" (Figure 5.12I).

- *Cloning of pIRES-MMD(c-Myc1)*

In this construct c-Myc tag was integrated in the first extramembrane loop of MMD protein. Following the same PCR reactions as described above except that "myc1-tag-S" replaced "myc-tag-S" primer (Figure 5.12H).

4.1.4. RNA related molecular methods

It is important to prevent the introduction of RNases in all RNA related molecular methods. Therefore, gloves, RNase-free pipettes, tips and tubes were used. All aqueous solutions were prepared using water treated with diethylpyrocarbonate (DEPC). DEPC (0.1%) was added to

the water, mixed and incubated overnight to eliminate protein (including RNases). Afterwards the inactivation of DEPC by autoclaving twice for 20 min was necessary to eliminate its toxicity.

4.1.4.1. Isolation of RNA by GTC-Phenol-Chloroform extraction

Up to $1.5x10^7$ cells were lysed per 3 ml of solution D. Adherent cells were directly lysed in the culture vessel followed by scraping with a sterile rubber policeman. Suspension cells, after pelleting and discarding the supernatant, were resuspended in the residual medium before addition of solution D. The lysate was transferred to sterile 14 ml centrifuge tubes, and DNA was sheared by passing the lysate 10 times through a 20G (0.9 mm x 40 mm) needle fitted to a syringe. Acetate (0.1 volumes of 2 M) was added to the lysate which at this point could be stored at -20°C. For each 1 ml solution D, 1 ml phenol and 0.2 ml $CHCl_3$/IAA were added. The RNA was extracted into the aqueous phase by vigorous shaking, phase separation on ice (15 min) and centrifugation (20 min, 10000 g, 4°C). The upper aqueous phase was carefully aspirated without disturbing the protein-containing interphase and combined with an equal volume of cold 100% isopropanol in a fresh tube. Total RNA was precipitated by mixing thoroughly, incubation at -20°C for at least 1 h and centrifugation for 20 min at >10000 g and 4°C. The supernatant was discarded, the RNA pellet dissolved in 0.3 ml per 1 ml lysate of solution D, transferred to a sterile 1.5 ml screw-cap micro centrifuge tube and precipitated a second time by adding an equal volume of isopropanol. After mixing and incubation for > 1 h at -20°C, a centrifugation step followed for 20 min at >10000 g and 4°C. The supernatant was discarded and the pellet was washed twice each with 1 ml of 80% ethanol (15 min, 10000 g, 4°C), dried and dissolved in H_2O_{DEPC}. RNA yield and purity were determined on a spectrophotometer and its integrity was assessed by running 1 µg of RNA on an agarose/formaldehyde gel (intact RNA has a 28S:18S rRNA band intensity ration of 2:1, and the highest RNA density around 2 kb).

Required solutions:

Solution D	**4 M**	47.2 g Guanidine thiocyanate (GTC)
	25 mM	2.5 ml Sodium citrate 1 M/HCl, pH 7.0
	0.5 %	1.67 ml Sodium N-lauroylsarcosine solution (30%)
	Add H_2O_{DEPC} to 100 ml, store at 4°C for up to 3 months.	
	Add 7.2 µl/ml β-mercaptoethanol (fume hood) directly before use.	
2 M Acetate	**2 M**	16.4 g $NaOAc \cdot 3H_2O$
	Dissolve in 40 ml H_2O_{DEPC}, adjust to pH 4.0 with 2 M	
	Add H_2O_{DEPC} to 100 ml.	

Phenol unbuffered, saturated with H_2O_{DEPC}:	Melt redistilled phenol in water bath Add **2x** Shake well and let sit overnight. Top water layer should be ¼ of the phenol phase.	 0.1% 8-Hydroxyquinoline 40% H_2O_{DEPC}
$CHCl_3$/IAA (49:1)	**1x vol** **49x vol**	2 ml Isoamyll-alcohol 98 ml Chloroform
100% Isopropanol	Stored at 4°C	
80% Ethanol	**80 %** Add H_2O_{DEPC} to 100 ml, chill on ice.	80 ml Ethanol

4.1.4.2. Isolation of total RNA with Qiagen RNeasy Midi Kit

Alternatively, for Northern blots and microarray analysis, RNA was isolated using the RNeasy Mini and Midi Kit (Qiagen) according to the manufacturer's instructions.

4.1.4.3. Formaldehyde agarose gel

The agarose was dissolved in MOPS/H_2O_{DEPC} by heating in a microwave oven, and cooled to 60°C. Formaldehyde was added while stirring the solution under a fume hood and the gel was cast, mounted in an electrophoresis tank and overlaid with 1x MOPS as electrophoresis buffer. RNA samples were prepared by diluting with four volumes RNA loading buffer (1:4), denaturing for 20 min at 65°C and brief incubation on ice. Samples were centrifuged and loaded into the gel slots. Gels were run at 40-60 V; for subsequent Northern blotting, they were run overnight at 13-16 V.

Required buffers:

MOPS (20x)	**0.4 M**	42 g	MOPS/NaOH, pH 7.0
	100 mM	4.1 g	NaOAc
	20 mM	3.7 g	EDTA
	Add H_2O_{DEPC} to 500 ml, stored in the dark.		
RNA loading buffer	**50%**	10 ml	Formamide, deionised
	2.2 M	3.5 ml	Formaldehyde (37%)
	1x	1 ml	MOPS (20x)
	0.04%	0.8 ml	Bromophenol blue (1% in H_2O)
	1%	0.2 g	Ficoll 400, Pharmacia (dissolve in 2 ml H_2O)
	Add H_2O_{DEPC} to 20 ml, stored in 1 ml aliquots at -20°C		
	Add 5 µl/ml Ethidium bromide (10 mg/ml) before use.		

4.1.4.4. Northern blot - RNA transfer

Following separation on formaldehyde/agarose gels, the RNA was transferred to nylon membranes by capillary elution. A nylon membrane (Magna NT, MSI) was cut to gel size, wetted with H_2O, and briefly soaked in 20x SSC. The RNA gel was placed upside-down on two layers of 20x SSC-soaked Whatman 3MM filter papers on a glass plate, the ends of which were reaching into a buffer reservoir placed below and filled with 20x SSC. The membrane was laid on top of the gel, avoiding to trap air bubbles. One corner of the membrane was marked by cutting it off. Plastic stripes were placed on the membrane borders to avoid short-circuiting the capillary flow past the membrane to the two layers of 20x SSC-soaked Whatman filters which were put on top of the membrane and the plastic covers. A 6-8 cm stack of cellulose wadding was placed on top to draw the 20x SSC through the gel and the membrane. The cellulose was weighed down with a glass. After an overnight transfer, completeness of the transfer was checked under UV illumination. The gel lanes, 18S and 28S rRNA bands were marked with a soft pencil. RNA was fixed to the membrane by UV-crosslinking with $1.20x10^6$ mJ/cm^2 (Autocrosslink) in a Stratalinker.
Required buffer:

SSC (20x)	**0.3 M**	88 g $Na_3Citrate \cdot 2H_2O$/HCl, pH 7.0
	3 M	175 g NaCl
	Add H_2O to 1 l and autoclave.	

4.1.4.5. Northern blot hybridization

Northern blot prehybridization and hybridization steps were pursued with ULTRAhyb™ solution (Ambion) because of its high sensitivity and low background. Northern blot membranes were prehybridized in a total volume of 25 ml ULTRAhyb solution (prewarmed at 65°C) with continuous shaking at 42°C for 3 h. The radioactive probe was denaturated for 10 min at 95°C and chilled out on ice for 2 min. It was then added ($2.5x10^6$ cpm/25ml) directly to the prehybridization solution. Blots were hybridized overnight at 42°C, the following day rinsed twice each with fresh NWB1 for 5 min at RT. The overall radioactivity was then measured with a Geiger counter. Blots with values over 0.1-5 Bq/cm^2 were further rinsed with NWB2 at 50°C till the overall radioactivity was reduced. Thereafter blots, with a small amount of wash buffer, were heat-sealed in plastic bags, fixed with adhesive tape in an exposure cassette with a storage phosphor screen and exposed for up to three days. The screen was later scanned using a Typhoon™ phosphoimage (Amersham Biosciences, Germany).

MTN blots contain 2 µg polyA$^+$ RNA per lane, which allows a specific and sensible detection of RNA transcripts in various tissues.
Required buffers:

Northern Wash Buffer 1 (NWB1)	**2x SSC** **0.05% SDS**	SSC (20x) SDS (20%)
Northern Wash Buffer 2 (NWB2)	**0.1x SSC** **0.1% SDS**	SSC (20x) SDS (20%)

4.1.4.6. Stripping Northern blots

For rehybridization of blots with different DNA probes, the radioactively labeled DNA was removed by stripping the membrane. This was done by incubating it in heated H_2O (90°C) with 0.5% SDS for 10 min. Afterwards, blots were dried and kept ready for a subsequent hybridization, or were stored at -20°C for later use.

4.1.4.7. Generation of specific radioactive DNA probes

To generate probes for hybridization of Northern blots, DNA fragments were PCR-amplified from the 3'-untranslated Region (UTR) of MMD cDNAs, where the lowest similarity grade between the homologues was found. This is important to prevent cross-hybridization between MMD and MMD2 in mouse and human. As a template cDNA, mouse MMD cDNA was previously cloned into pGEM3 vector in our lab. Mouse MMD2 (in pBS vector), human MMD and MMD2 (in pCMV-SPORT6) cDNAs were purchased from the German Resource Center for Genome Research (RZPD) under the following clone IDs:

- Mouse MMD2: IRAKp961O 0461Q2
- Human MMD: IRAKp961D1732Q2
- Human MMD2: IMAGp998H2211791

Afterwards the PCR products were labelled with ^{32}P by Hartman Analytic (Braunschweig, Germany).

4.1.4.8. Reverse transcription (RT) and quantitative real time-PCR (qRT-PCR)

To quantify mRNA transcript of tagged-mMMD in stably transfected NIH3T3 cells (see section 5.3.2.1), or of mMMD in BMM after stimulation (see section 5.2.3), and in cell lines after siRNA silencing (see section 5.5), qRT-PCR was performed. For this purpose, total RNA was first transcribed. This was achieved by using the M-MLV reverse transcriptase

(Promega, Germany) combined with the random decamers (Ambion, Germany) in a total reaction volume of 20 µl. The reaction was pursued as follows:

RT PCR reaction:
1 µg Total RNA
1 µl Random decamers
1 µl dNTPs (10 pmol/ml)
Add H_2O_{USB}, incubate for 5 min at 65°C, cool on ice, and centrifuge
4 µl M-MLV Buffer (5x)
Mix, and incubate for 2 min at 42°C
1 µl M-MLV Reverse transcriptase
Incubate for 50 min at 42°C followed by 15 min at 70°C.

Quantitative RT- PCR was performed using QuantiTect SYBR green kit (Qiagen, Germany) and the LightCycler® apparatus (Roche, Germany) following the manufacturer's instructions. The primers used in the PCR reaction were generated by Metabion.
The quantitative real-time PCR program was:

Action		LightCycler	
Initial Melting		94°C	15 min
55 Cycles	Melt	94°C	15 sec
	Anneal	57°C	15 sec
	Extend	72°C	25 sec
Melting point		60°C	90°C
Cool to		4°C	∞

The amplification was carried out in a total volume of 20 µl containing 10 µl SYBR green 2x PCR mix, 1 µl of each of the sense and antisense primers, and 2 µl of the cDNA (5-fold diluted). A standard curve was generated for each primer pair by amplifying four dilutions (1; 1:10; 1:50; 1:100) of the most concentrated sample (also 5-fold diluted). The *Hprt* housekeeping gene served as an internal control and was used to normalize for differences in the amount of cDNA. The slope of the standard curve was an indicator of the amplification efficiency, and should be between 3.3 and 3.8. Standard curves were subsequently used to calculate the relative abundance of each transcript in each sample. The measurements were performed in duplicates.

4.1.5. Gene silencing by short interference RNA

siRNA involves the use of dsRNA to target a post-transcriptional degradation of the mRNA of the gene of interest, thereby inhibiting the protein synthesis and leading to gene silencing. Short siRNA duplexes (22-23 nucleotides) are the effector molecules. Once introduced into a cell, they are incorporated into a nuclease complex to form the so called RNA induced silencing complex (RISC). RISC targets the endogenous homologous transcript by base pair interaction cleaving the mRNA (Elbashir et al., 2001).

siRNA silencing experiment of mouse MMD was conducted using siRNA duplexes purchased from QIAGEN (Germany). siRNA duplexe (30 pmol) was transfected into NIH3T3 or RAW264.7 cell lines ($1.5x10^5$ cells/well) using Invitrogen Lipofectamine™ RNAiMAX transfection reagent following the manufacturer's instructions. As negative control, a non silencing duplexe was provided and separately transfected. At different time points after transfection (48, 72 and 96 h) cells were harvested and used to isolate total RNA, which were reverse transcribed into cDNA. Afterwards, mMMD expression was controlled by performing a qRT-PCR analysis (see section 4.1.4.8).

4.1.6. Whole-mount in situ hybridization

Whole-mount in situ hybridization (ISH) was performed to determine the spatial and temporal distribution of MMD and MMD2 in mouse embryo. Therefore embryos were isolated, pretreated and hybridized to digoxigenin (DIG) labeled RNA. Detection was performed by using an enzyme-conjugated antibody to DIG (Ausubel Frederick et al., 2006).

4.1.6.1. Isolation of embryos

Mouse embryos were dissected free of any extra-embryonic membranes at 10, 11, and 13 dpc (day post coitus) (see section 4.5.2.2). In order to preserve their morphology, they were fixated in a 6-well culture plate with 5 ml 4% PFA_{PBS} overnight at 4°C, and afterwards washed twice in PBT at RT for 5 min before proceeding with the dehydration.

- *Dehydration:*

To improve the permeabilization of the tissues and increase the sensitivity of the ISH, fixed embryos were dehydrated by successive washes in 25%, 50%, 75% and 100% methanol/PBT at RT for 5 min each. It is possible to store fixed embryos in 100% methanol at -20°C for up to 3 months. Before proceeding with the rehydration step, brain ventricle cavities were

punctured carefully in order to avoid a high background signal due to trapped antibodies in these cavities.

➢ *Rehydration:*

To rehydrate the embryos, a reverse order of the methanol/PBT series was performed, and samples were then washed twice in PBT at RT for 5 min.

➢ *Proteinase K treatment and postfixation:*

In order to facilitate the hybridization of the riboprobe with its complementary RNA, embryos were treated with proteinase K (10 µg/ml PBT) at 37°C. The length of the treatment depends on the embryos age in dpc. Late-stage embryos are more difficult to permeabilize.

- For embryos at 10 dpc: 13 min
- For embryos at 11-13 dpc: 15 min

Digestion was stopped by adding freshly prepared glycin (2 mg/ml in PBT) (Sigma) and incubating for 10 min at RT. After washing twice each for 5 min in PBT, embryos were postfixed with freshly prepared 0.2% glutaraldehyde/4% paraformaldehyde in PBT for 20 min at RT. This step was necessary to stabilize digested tissues and conserve their morphology during subsequent hybridization. After washing (2x 5 min with PBT at RT), embryos were separated and each transferred carefully to a 1.5 ml microfuge tube to proceed with hybridization (see section 4.1.6.3).

Required reagents:

4% PFA	**4%**	4 g Paraformaldehyde (PFA) Add 66 ml warmed H_2O_{DEPC} (60°C), cover and stir. In the fume hood add 1 drop 2 N NaOH, the solution will clear. Add 33 ml 3x PBS, adjust pH to 7.2 with HCl. Cool to RT, aliquot and store at -20°C.
20% PFA	**20%**	20 g Paraformaldehyde (PFA) Prepared as a 4% PFA solution. Aliquot and store at -20°C.
PBT (1x)	**1x** **0.1%**	100 ml PBS (1x) (Gibco) 200 µl Tween 20.
0.2% Glutaraldehyde /4% PFA	**0.2%** **4%**	120 µl Glutaraldehyde (25%) (Sigma) 3 ml PFA (20%) Add 11.9 ml 1x PBT, aliquot and store at -20°C.

4.1.6.2. Synthesis of sense and antisense RNA probe

Sense and antisense DIG-labeled RNA probes were generated using an RNA in vitro transcription kit (Roche). The cDNA containing plasmid template was linearized by digestion with the appropriate restriction enzyme 5' or 3' of the cDNA region of interest, to prepare sense or antisense RNA probes, depending on the orientation of the cDNA in the plasmid.
MMD cDNA, cloned in pGEM3 vector, was cut either with XbaI or HindIII restriction enzymes to be used as template for the RNA in vitro transcription reaction to generate MMDas and MMDs probes respectively. MMD2 cDNA purchased in pCMV-SPORT6 vector (RZPD, Germany) was cut either with EcoRI or NotI to generate MMD2as and MMD2a probes respectively (Table 4.2; Figure 4.1).

Table 4.2 DNA template and restrictions enzymes used for the generation DIG-RNA probes.

DIG-RNA probe	DNA template	Restriction enzyme	RNA polymerase
MMD antisense	pGEM3-MMD	XbaI	Sp6
MMD sense	pGEM3-MMD	HindIII	T7
MMD2 antisense	pCMV-Sport6-MMD2	EcoRI	T7
MMD2 sense	pCMV-Sport6-MMD2	NotI	Sp6

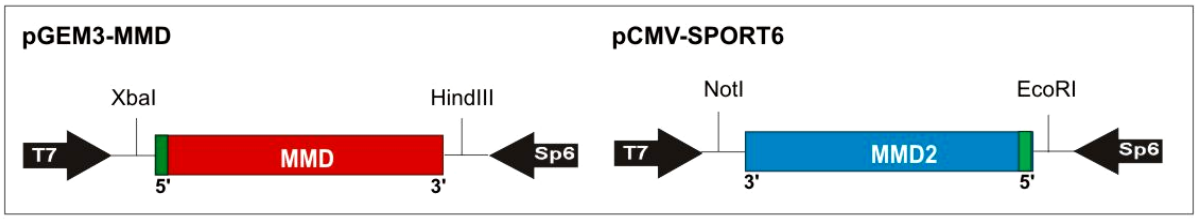

Figure 4.1 Structure of pGEM3-MMD and pCMV-SPORT6-MMD2 vectors.
MMD and MMD2 inserts are depicted in the MCS of the template vector. T7 and Sp6, are RNA polymerase promoters used in the in vitro RNA transcription.

Digested template DNA was examined by agarose gel electrophoresis to confirm that the cleavage was complete, phenol/chloroform extracted, precipitated with 1/10 3 M Na-acetate pH 5.2, plus 2 volumes 100% ethanol. The DNA pellet was dissolved in 20 µl H_2O_{DEPC}.
In vitro DIG-labeling of RNA probes was performed in 20 µl reaction according to Roche's protocol. Reagents were mixed at RT in the order described below, and incubated at 37°C for 2 h. RNA transcript was synthesized from linearized DNA template using bacteriophage

polymerase, and later purified by Na-acetate/Ethanol precipitation. DIG-labelled RNA probes were stored at -80°C.

Probe labelling reaction:	**1x**	2 µl 10x transcription buffer
	20 U	0.5 µl RNase inhibitor
	1x	2 µl 10x DIG-nucleotide mix
	2 µg	2 µl linearised DNA (1 µg/µl)
	Add 11.5 µl $H_2O_{DEPC.}$	
	2 µl	T7 or Sp6 RNA polymerase.
	Reagents were mixed in the described order at RT	
	2 h incubation at 37°C. Add the following:	
	40 U	1 µl RNase inhibitor
	10 U	1 µl RNase free DNase
	15-30 min incubation at 37°C.	
	Add 180 µl H_2O_{DEPC}, and the following:	
	10 µg/µl	1 µl tRNA
	10%	20 µl Na-acetate (3M), pH 5.2
	3x volume	600 µl 100% ethanol
	Mixed and incubated at -70°C for at least 30 min	
	Spined at 12000 rpm at 4°C for 20 min.	
	Pellet dissolved in 40 µl $H_2O_{DEPC.}$	

4.1.6.3. Hybridization procedure on whole-mount

- *Prehybridization:*

Each embryo was incubated in 500 µl prewarmed hybridization solution (Hyb.mix) for 1 hour at 70°C to block non-specific hybridization sites.

- *Hybridization:*

Digoxigenin-labeled riboprobe (0.5 µg) (see section 4.1.6.2) was denaturated at 80°C for 2 min and transferred directly from the heating block to 500 µl prewarmed fresh Hyb.mix replacing the old Hyb.mix solution in the embryo tube. The hybridization followed overnight at 70°C.

Required solution:

Hyb. mix solution	**50%**	50 ml deionised formamide (Roche)
	5x	25 ml SSC (20x), pH 4.5
	50 µg/ml	500 µl tRNA (10 mg/ml) (Roche)
	1%	5 ml SDS (20%)
	50 µg/ml	100 µl Heparin sodium (50 mg/ml) H3393 (Sigma)
	Add H_2O_{DEPC} to 100 ml, aliquot and store at -20°C.	

4.1.6.4. Post-hybridization and detection procedures

➢ *Post-hybridization washes:*

The hybridization solution was removed and embryos were carefully washed with 1 ml solution I, II and III as follows:

- 2x 30 min with solution I (prewarmed to 70°C) at 70°C.
- 1x 10 min with solution I + solution II (1:1) (prewarmed to 70°C) at 70°C.
- 3x 5 min with solution II at RT.
- 1x 30 min incubation in solution II + 100 µg/ml RNase A at 37°C.
- 1x 5 min with solution II at RT.
- 1x 5 min with solution III at RT.
- 2x 30 min with solution III (prewarmed to 65°C) at 65°C.

➢ *Blocking and antibody incubation:*

After removal of nonspecifically bound riboprobes, embryos were washed carefully 3x 5 min with MAB at RT, to equilibrate the samples. A 3 hours incubation step followed in MAB/BR/NSS reagent at RT, to block nonspecific antibody binding.
Embryos were then incubated with anti-DIG-AP Fab fragment solution (previously prepared) overnight at 4°C. The next day, samples were washed 3x 5 min at RT with MAB (cooled at 4°C). Embryos were then transferred into 15 ml tubes and further washed with MAB every hour all day at RT, to be left in the buffer overnight at 4°C with very gentle agitation.

➢ *Visualization of hybridized RNA:*

MAB was removed carefully and embryos were washed 3x 10 min with NTMT at RT, later transferred into a 12-well plate and incubated with BM purple AP substrate (Roche) containing Levamisol (0.5 mg/ml) for 5 h at dark. After the signal has developed embryos were washed with PBT, and stored in 4% PFA/PBS at 4°C.
Required solutions:

Solution I	**50%**	20 ml Formamid (Roche)
	5x	8 ml SSC (20x), pH 4.5
	1%	4 ml SDS (10%)
	Add H_2O_{DEPC} to 40 ml.	
Solution II	**0.5 M**	8 ml NaCl (5M)
	10 mM	0.8 ml Tris (1M), pH 7.5
	0.1%	80 µl Tween 20
	Add H_2O_{DEPC} to 80 ml.	

Solution III	**50%**	20 ml Formamid
	2.5x	4 ml SSC (20x), pH 4.5
	Add H_2O_{DEPC} to 40 ml.	
Maleic acid buffer (MAB)	**100 mM**	11.6 g maleic acid
	150 mM	8.8 g NaCl
	Add H_2O_{DEPC} to 900 ml, adjust pH to 7.5 with ~20 ml NaOH (10 N)	
	0.1%	1 ml Tween 20
	2 mM	500 mg Levamisole (Sigma L-9756)
	Add H_2O_{DEPC} to 1000 ml.	
MAB/BR	**2%**	200 mg Blocking reagent (BR) (Roche)
	Add 9 ml MAB, dissolve at 70°C and cool on ice.	
MAB/BR/NSS	**10%**	1 ml Normal Sheep Serum (NSS) (Sigma S-3772)
	Add MAB/BR to 10 ml. It should be prepared fresh on day of use.	
MAB/Ab	**10%**	5 µl NSS
	1.5 U	2 µl AP-conjugated anti-Digoxigenin (Roche)
	Add 500 µl MAB/BR, and incubate for 1h at 4°C.	
	Antibody was recovered by spinning for 10 min at 4°C.	
	Add to the supernatant 6 ml MAB/BR and 60 µl NSS (1%), vortex.	
NTMT	**100 mM**	2 ml NaCl (5M)
	100 mM	10 ml Tris.Cl (1M), pH 9.5
	50 mM	5 ml $MgCl_2$ (1M)
	0.1%	0.1 ml Tween 20
	Add to 100 ml H_2O_{DEPC}. NTMT should be fresh prepared.	

4.2. Protein biochemical methods

4.2.1. Preparation of cell protein extracts from mammalian cells

4.2.1.1. Extraction of whole cellular protein

NIH3T3 cells were scrapped, and washed twice with cold PBS to remove residual proteins of the FCS that cause high background signals by binding unspecifically the antibody. The cell pellet volume was estimated, after removing the supernatant completely, and the pellet was resuspended on ice with 1x volume sample buffer (2x). Samples were denatured by incubating at 95°C for exactly 3 min, centrifuged at 10000 rpm for 1 min and stored on ice or directly loaded on the gel (see section 4.2.2)

Required buffer:

Sample buffer (2x)	**20%**	10 ml Glycerol
	125 mM	5 ml Tris buffer (1.25 M), pH 6.8
	4%	2 g SDS
	10%	5 ml 2-mercaptorethanol
	0.02%	10 mg Bromophenol blue
	Add to 50 ml H_2O and dissolve. Stored at 4°C.	

4.2.1.2. Extraction of cellular membrane protein

In order to extract only membrane protein, NIH3T3 cell pellet was prepared as described above and gently resuspended on ice in 1x volume of ice-cold EP-w/o. Two volumes of ice-cold EP-NP was added, the sample was incubated on ice for 15 min and centrifuged at 13000 rpm for 5 min at 4°C. The supernatant containing the cytoplasmic fraction was collected, mixed with 1x volume sample buffer (2x) and incubated at 95°C for exactly 3 min.
Required buffers (prepared fresh on day of use and stored on ice):

Extraction buffer:	**100 mM**	1 ml Tris (1 M) pH 7.4
(EP) 2x	**4 mM**	200 µl EGTA (0.2 M)
	2 mM	20 µl $MgCl_2$ (1 M)
	Add H_2O to 10 ml.	
EP-w/o(1x):	**1x**	500 µl EP (2x)
(freshly prepared)	**1 mM**	10 µl DTT (100mM)
	2.5 µg/ml	2.5 µl Leupeptin (1 µg/µl)
	1 µg/ml	1 µl Pepstatin (1 µg/µl)
	2 µg/ml	1 µl Aprotinin (2 µg/µl)
	1 mM	10 µl PMSF (100 mM)
	1 mM	10 µl Sodium-o-vanadate (100 mM)
	Add H_2O to 1 ml (465 µl).	
EP-NP (1x)	same as EP-w/o	
	1%	100µl NP-40 (10%)
	Add H_2O to 1 ml (365 µl).	

4.2.2. Discontinuous SDS-PAGE

Protein samples were separated by using a discontinuous gel system, which is composed of stacking and separating gel layers that differ in salt and acrylamide concentration.

Table 4.3 SDS-PAGE stock solutions

Stock solution	Separating gel stock solution	Stacking gel stock solution
Final AA concentration	**13.5%**	**5%**
Stacking gel buffer	-	25 ml
Separating gel buffer	25 ml	-
SDS (10%)	1 ml	1 ml
Rotiphorese Gel 30 (30%)	45 ml	16.65 ml
H_2O	Add H_2O to 100 ml	

Table 4.4 SDS-PAGE gel mixture

Stock solution	Separating gel 13.5%	Stacking gel 5%
Stock solution	10 ml	5 ml
TEMED	10 µl	5 µl
AP (10%) fresh prepared	50 µl	40 µl

The separating gel was cast the day before electrophoresis, and overlaid with water-saturated isobutanol until polymerized. Isobutanol was exchanged for separating gel buffer diluted 1:3 with water and the gel was stored overnight at 4°C. The following day, the stacking gel was poured on top of the separating gel, and the comb inserted immediately. After polymerization, the stacking gel was mounted in the electrophoresis tank, which was filled with 1x Laemmli buffer. Meanwhile, the protein lysate (prepared as described above) was thawed on ice, cleared by centrifugation and loaded in the wells. The gel was run with 25 mA/110 volts till the sample buffer bands reached the surface of the stacking gel, then the current was increased to 200 volts and the gel was run for 2-4 h. Proteins were then resolved through the separating gel according to their size.

Required buffers and solutions.

Separating gel buffer **1.5 M** 90.83 g Tris/HCl, pH 8.8
Add H_2O to 500 ml.

Stacking gel buffer **0.5 M** 30 g Tris/HCl, pH 8.8
Add H_2O to 500 ml.

SDS (10%) **10%** 10 g SDS
Add H_2O to 500 ml.

Ammonium persulfate AP (fresh prepared) **10%** 100 mg Ammonium persulfate
Add H_2O to 1 ml.

Laemmli buffer (5x)	**40 mM**	15 g Tris
	0.95 M	21 g Glycin
	0.5%	15 g SDS
	Add H_2O to 3000 ml.	

4.2.3. Western blot analysis

After separation by SDS-PAGE, proteins were blotted electrophoretically onto PVDF membrane (Immobilon-P, Millipore) using a three-buffer semi-dry system. The membrane was cut to gel size, moistened first with methanol followed with buffer B, and placed on top of two sheets each of 3x Whatman3MM filter paper soaked with buffer A (bottom, on the anode) and buffer B, respectively. The SDS-PAGE gel was removed from the glass plates, immersed in buffer B and placed on top of the membrane. Another 3x Whatman 3MM filter papers soaked with buffer C were placed on top of the gel followed by the cathode. Air bubbles in-between the layers were avoided. Protein transfer was conducted for 1 h at 0.8 mA/cm^2 gel surface area.

Required buffers and materials:

Buffer A	**0.3 M**	36.3 g Tris, pH 10.4
	20%	200 ml Methanol
	Add H_2O to 1000 ml.	
Buffer B	**25 mM**	3.03 g Tris, pH 10.4
	20%	200 ml Methanol
	Add H_2O to 1000 ml.	
Buffer C	**4 mM**	5.2 g ε-amino-n-caproic acid, pH 7.6
	20%	200 ml Methanol
	Add H_2O to 1000 ml.	

4.2.4. Immunostaining of blotted proteins

Blotted membranes were blocked either with 5% milk in PBST (for FLAG and c-Myc staining) or in TBST +1% BSA (for HA staining) for 1 h at RT then washed once for 5 min with PBST or TBST before incubation at RT for 1 h with the primary antibody. After washing 3x 10 min with the appropriate washing buffer, the membrane was incubated for 1 h at RT with a horseradish-peroxidase (HRP)-coupled secondary antibody, detecting the isotype of the first antibody. The working concentrations and conditions of each antibody are given in the following table. A last 3x 10 min washing steps preceded the visualization of bound antibody

using ECL kit. Blots were exposed to an autoradiography film (Hyperfilm^{TM} ECL, Amersham) for 5 seconds to 30 min depending on the signal intensity.

Table 4.5 Antibody dilution for Western blot analysis.

Primary antibody	Dilution factor	Secondary antibody	Dilution factor
Mouse anti-Flag M2	1:4000 in 5% $milk_{PBST}$	Rabbit anti mouse HRP	1:10 000 in 5% $milk_{PBST}$
Rat anti-HA	1:100 in 1% BSA_{TBST}	Rabbit anti-rat HRP	1:1500 in 5% $milk_{TBST}$
Mouse anti-c-myc	1:200 in 5% $milk_{PBST}$	Goat anti mouse HRP	1:10 000 in 5% $milk_{PBST}$

Required buffers and materials:

TBS (2x)	**20 mM**	9.16 g Tris /HCl, pH 7.4
	150 mM	35.1 g NaCl
	Add H_2O to 2000 ml.	
TBST (1x)	**1x**	500 ml TBS
	0.1%	1 ml Tween 20
	Add H_2O to 1000 ml.	

4.2.5. Immunocytochemistry

NIH3T3 cells were transiently transfected (see section 4.4.1) with various tagged MMD in Lab-Tek^{TM} 2-wells chamber slides (Nalge Nunc International, USA) and further stained as described below. Additionally, to examine the orientation of MMD within the lipid membrane bilayer, NIH3T3 cell lines stably over-expressing tagged MMD were generated using a retroviral transfection system (see section 4.4.2). NIH3T3 cells were seeded in chamber slides ($5x10^4$ cells/chamber) and cultured at 37°C for 48 h to reach around 80% confluency before proceeding with the staining. Coating of chamber slides with a 0.2% gelatin solution before cell seeding improved the cell adherence during the staining procedure.

4.2.5.1. Fixation and permeabilization

Cells were washed twice with PBS at RT, then fixed on ice for 8 min with 2% paraformaldehyde (PFA) (freshly prepared from a 4% stock solution), followed by 3x 5 min washing with PBS at RT. Afterwards cells were either incubated with ice cold acetone/methanol (1:1) for 1 min to achieve a complete membrane permeabilization or with digitonin for selectively perforating the plasma membrane.

Digitonin is a mild non-ionic detergent that aggregates with cholesterol creating pores in the lipid membranes. Since the endoplasmic reticulum (ER) contains a reduced amount of

cholesterol compared to the plasma membrane, digitonin is capable, at low concentration and short incubation, to disrupt the plasma membrane leaving the ER intact. Digitonin solution should be fresh prepared. Short incubation between 10 and 20 seconds was enough to disrupt the cytoplasmic membrane of NIH3T3 leaving the ER membrane intact.
Required solutions:

Gelatine	**0.2%**	0.2 g Gelatine (Sigma)
	Add H_2O to 50 ml and autoclave.	
Digitonin	**0.003%**	0.003 g Digitonin (Sigma)
	Add 100% ethanol to 100 ml and dissolve by vortexing.	
	Fresh prepared.	

4.2.5.2. Blocking and antibody staining

After permeabilization, cells were washed 3x 5 min with PBS, and blocked in blocking buffer for 1 h at 4°C. They were then stained with the primary antibody, washed 3x 10 min with PBS to remove unbound antibodies, followed by the fluorescence-labelled secondary antibody incubation in the dark. The incubation with antibodies followed in blocking buffer for 1 h at 4°C and their concentrations are given in the following table. Cells were then washed 3x 10 min with PBS and for staining of lysosomes incubated with FITC-conjugated LAMP-1 antibody (CD107a) in a 1:1000 dilution in blocking buffer for 1 h at 4°C. For nuclei staining, cells were incubated with DAPI working solution at RT for 3 min in the dark. After final washing steps of 3x 5 min, the upper structure of the chamber slide was removed, slides were mounted with DakoCytomation Fluorescent mounting medium (Dako, Hamburg), and stored at 4°C in the dark until pictures were taken at the fluorescence microscope "Axioskop 2 plus" from Zeiss.
Required buffer and solution:

Blocking buffer	**3%**	3 g BSA (Sigma)
	2.5%	2.5 ml FCS
	Add PBS to 100ml. Prepared fresh.	
DAPI working solution	**5 ng /ml**	1 µl DAPI (0.5 µg/ml) (Sigma)
	Add 99 µl Glycerin /PBS (1:3).	
	Prepared fresh and stored in the dark.	

Table 4.6 Antibody dilution for immunocytochemistry

Primary antibody	Dilution factor	Secondary antibody	Dilution factor
Mouse anti-Flag M2	1:2500	Alexa Fluor® 546 goat anti-mouse	1:1000
Rat anti-HA	1:400	Alexa Fluor® 546 goat anti-rat	1:1000
Mouse anti-c-myc	1:200	Alexa Fluor® 546 goat anti-mouse	1:1000

4.3. General cell culture methods

4.3.1. Cell culture conditions and passaging

4.3.1.1. Cell culture medium and supplements

If not noted otherwise, cells were cultured in RPMI 1640 (PAA) or DMEM (Gibco) supplemented with 10% inactivated FCS, L-Glutamine (2 mM), sodium pyruvate (1 mM), antibiotics (50 U/ml penicillin and 50 µg/ml streptomycin), 2 ml vitamins and non-essential amino acids and 50 µM β-mercaptoethanol (Table 4.7). FCS was previously incubated at 56°C for 30 min in order to inactivate the complements. An exceeding incubation time and a higher temperature should be avoided because some other necessary heat sensitive growth factors could be damaged. Each batch of FCS was tested before use.

Table 4.7 Cell lines growth and subculture conditions.

Cell lines	Growth medium	Subculture conditions
RAW264.7	RPMI (Biochrom)	Split by scraping
NIH3T3	DMEM high glucose (PAN)	Split by trypsination
HEK293T	DMEM + GlutaMax (Gibco)	Split by trypsination
BV-2	DMEM (Gibco)	Split by scraping
J-774A.1	DMEM (Gibco)	Split by scraping
P815	RPMI (Biochrom)	Shaking the flask
HT-2	RPMI (Biochrom) + IL-2	Cell in suspension

4.3.1.2. Cell passaging

Cell cultures were split 1:4 to 1:8 in fresh medium every 2-4 days. Adherent cells were washed once with PBS and either scrapped or disaggregated by incubation with 0.05% Trypsin /0.02% EDTA/PBS (3 ml per 75 cm^2 culture vessel area) at 37°C for 5 min until cells detached. Trypsin was then inactivated by adding 6 ml medium with 10% FCS.

4.3.2. Assessing cell vitality

The number of viable and dead cells was determined by trypan blue exclusion. The cell suspension was diluted with trypan blue solution and the cells counted in a Neubauer haemocytometer. The concentration of viable cells was then calculated using the equation:

Number of viable cells/ml $C = N \times D \times 10^4$

With : N: average of unstained cells per corner square (1mm containing 16 sub-squares)

D: dilution factor

Required solution:

Trypan blue solution:	**0.2% (w/v)**	Trypan blue in 0.9% NaCl solution.

4.3.3. Freezing and thawing cells

Cells were harvested and suspended at 4-6x 10^6 cells/ml in 800 µl ice-cold medium, including 10% FCS. After inverting the mix and transferring it in cryo-vials, 160 µl DMSO (Sigma) and 640 µl FCS were added and the tubes were rapidly inverted to mix cells properly. To allow gradual freezing at a rate of 1°C/min, the cryo-vials were placed in isopropanol-filled cryo-containers (Nalgene) and frozen at -20°C for only 2 h then transferred to -80°C for 48 h. For long-term storage, samples were transferred to liquid nitrogen (-196°C).

4.3.4. Mycoplasma assay

Cells were routinely checked for mycoplasma contamination by ELISA with a Mycoplasma Detection Kit (Roche, Germany) or by a biochemical test with a MycoAlert® Mycoplasma detection assay (Cambrex, Rockland USA) according to the manufacturer's instructions.

4.3.5. Mouse bone marrow macrophage preparation

Mouse bone marrow-derived macrophages (BMM) were extracted from the femurs of 8- to 12-week-old mice. Cells from several animals were pooled before plating into non-charged bacteriological plates ($5x10^5$ cells/ml culture media). After five days the medium was changed and cells were harvested on day 6 and replated at a density of $10x10^6$ cells/20 ml media in 10-cm tissue culture dish. Experimental time courses were started on day 7. Afterwards cells were harvested and total RNA was isolated (Rehli et al., 2005).

Required cell culture medium:

BMM growth medium:	**500 ml**	RPMI with supplements (see section 4.3.1.1)
	200 ng/ml	rCSF (Cetus)
	10%	50 ml FCS (PAN Biotech).

4.4. Transfection of mammalian cells

4.4.1. Transient transfection

4.4.1.1. Effectene transient transfection

To introduce different tagged-MMD constructs into NIH3T3 cell line, Effectene™, a cationic lipid transfection reagent, was used following Qiagen instructions. One day prior to transfection $5x10^4$ NIH3T3 cells were seeded per well into chamber slides or into a 6-well culture plate. On day 2, 0.5 µg DNA diluted in 150 µl EC buffer were supplemented with 8 µl *Enhancer*, shortly vortexed and incubated at RT for 5 min. The *Enhancer* facilitates DNA condensation. Afterwards 25 µl Effectene was added, vortexed and further incubated for 10 min at RT to allow the formation of the Effecten-DNA complex. Finally, 800 µl normal growth medium was added to the mix and applied to the cells. On day 4, the cell lysate was prepared or an immunocytochemistry staining was performed.

4.4.1.2. Lipofectamine transient transfection

NIH3T3, HEK293T as well as RAW264.7 transfection with various tagged MMD constructs was carried out using Lipofectamin™ 2000 according to Invitrogen's instructions. In brief, for transfection in 6-well plates, for each well the following solutions were taken:

- Solution A: 1 µg DNA was mixed with 100 µl Opti-MemI.
- Solution B: 7 µl Lipofectamin was mixed with 100 µl Opti-MemI.

Combined together, solutions A + B were incubated for 30 min at RT, 800 µl Opti-MemI was added, and the transfection cocktail applied into $1.5x10^5$ cells/well seeded on day prior to transfection. After 5 h, transfection mix was removed and replaced with normal growth medium. After 48 h, transient transfected cell were ready for further experiments.

4.4.2. Retroviral stable cell transfection

To generate NIH3T3 cell lines stably expressing tagged MMD, a combination of the RetroMax™ System (Imgemex) and the retroviral vector pQCXIP from BD Biosciences (Clontech) was used. The procedure is based on a transient cotransfection of a packaging cell line, HEK293T, with pCL-ECO, a RetroMax packaging vector, and pQCXIP containing the gene of interest. Once introduced into the packaging cell line, pCL-ECO vector produces the viral Gag-Pol elements and the ecotropic viral envelope (Eco) at high level. The envelope

allows viral particles to infect specifically mouse and rat target cells by binding to receptors only present on the surface of these cells. The retroviral vector, pQCXIP, expresses a viral genomic transcript containing a CMV immediate early promoter, the gene of interest, an Internal Ribosomal Entry Site (IRES) and the puromycin selection marker. In addition, these elements are fused with a retroviral packaging signal Ψ^+, which allows the packaging of Gag-Pol and envelope viral proteins into viral particles. Once released into the culture medium of the packaging cell line, the replication-defective virus is capable of infecting mouse target cell lines. After genomic integration, the gene of interest is then expressed constitutively along with a puromycine resistance gene, which allows the selection of positive cells (Figure 4.2).

4.4.2.1. Generation of retroviral constructs

To generate retroviral expression vectors, HA-MMD and MMD-3FLAG cDNA were cloned separately into the pQCXIP vector as follows:

Mouse MMD cDNA fused with 3xFLAG at the C-terminus was cut from pIRES-MMD-3xFLAG construct(Figure 5.12A) with BstEII and KpnI restriction enzymes, and subcloned into the BamHI-KpnI sites of pQCXIP vector.

The construction of pQCXIP-HA-MMD vector was accomplished by amplifying mMMD (cloned previously in pGEM3) by PCR using “HA-tag-S” and “BamHI-stopMMD-AS” primers. The PCR product (containing HA-tag sequence at its N-terminus) was intermediately cloned into pCR2-TOPO vector. After sequencing, NotI-BamHI fragment was subcloned into NotI-BamHI site of pQCXIP vector.

4.4.2.2. Transfection of the packaging cell line HEK293T

As a transduction control, EYFP gene (Enhanced Yellow Fluorescent Protein) cloned into pQCXIP was used. After successful infection, cells expressing EYFP protein were visualized via the fluorescence microscope. An empty retroviral vector was also used to produce a negative control cell line.

Two independent cell lines stably producing tagged-MMD or EYFP were generated following two different transfection protocols. The following plasmids pQCXIP-HA/MMD, pQCXIP-MMD/3xFLAG, pQCXIP-EYFP or pQCXIP were cotransfected with the RetroMax packaging vector pCL-ECO.

➢ *Transient transfection of HEK293T with $CaCl_2$/HeBS*

Following the protocol described in (Schneider-Brachert et al., 2004), $3x10^6$ HEK293T cells were seeded 48 h prior to transfection into 10-cm tissue culture dishes to reach 80% confluency. At least 1 h prior to transfection, DMEM medium was replaced with 10 ml DMEM + GlutaMaxI (Gibco) to increase the transfection efficiency. The transfection mix, containing 30 µg of each the expression and the packaging plasmids diluted in a total water volume of 450 µl, was prepared. After adding 50 µl $CaCl_2$, the DNA/$CaCl_2$ mix was dripped into a 15 ml tube containing 500 µl 2xHeBS under slight vortexing. The DNA/$CaCl_2$/HeBS mix was added immediately to HEK293T cells. After 6 h incubation, the DNA mix was replaced with normal growth medium. The retroviral supernatant was collected after 48 h.
Required buffers and solutions:

2x HeBS	**50 mM**	11.9 g HEPES
	280 mM	16.4 g NaCl
	1.5 mM	0.27 g Na_2HPO_4
	Add H_2O to 1000 ml and adjust pH to 7.05 with NaOH (10 N). Filter, aliquot and store at -20°C.	
$CaCl_2$	**2.5 M**	183.7 g $CaCl_2.2\ H_2O$
	Add H_2O to 500 ml , filter, aliquot and store at -20°C.	

➢ *Transient transfection of HEK293T with Lipofectamine™*

Following the protocol described in section 4.4.1.2, $3x10^5$ HEK293T cells were seeded in 6-well culture plates 24 h prior to transfection. Duplicates for each sample were done. The packaging and the tagged-MMD expression vectors (2 µg each) were mixed with 200 µl Opti-MEM® to form the solution A. The solution B was prepared by adding 200 µl Opti-MEM® to 14 µl Lipofectamine™. Both solutions were mixed and incubated for 30 min at RT. After adding 1.2 ml Opti-MEM®, the transfection mix was transferred to each well and cells were incubated for 5 h. Afterwards Opti-MEM® mix was replaced with 5 ml growth medium. The retroviral supernatant was also collected 48 h after transfection.

4.4.2.3. Transduction of the targeting cell line

In order to transduce the target cell line, $3x10^5$ NIH3T3 cells were seeded in a 6-well culture plate at the day of transfection (for each construct two wells were prepared). Virus particles containing medium was harvested from transfected HEK293T and passed through a sterile HT Tuffryn low protein-binding 45 µm filter (PALL Gelman Laboratory, USA).

To enhance the infection efficiency, Polybrene (4 µg/ml growth medium, Chemicon) was added, which is a polycation molecule that binds to the cell surface and neutralizes its surface charge facilitating the penetration of the retrovirus. The infection solution (2.5 ml /well)) was diluted 1:1 with normal growth medium and added to NIH3T3 cells. The rest of the viral supernatant was stored at 4°C and used after 6 h to perform a second infection overnight. Another infection round was pursued the next day by collecting a new HEK293T supernatant.

4.4.2.4. Selection and expansion of stable cell lines

Once the infection was completed, the target cells were incubated with normal growth medium for 24 h to recover. Afterwards, cells were selected with 4 µg/µl puromycin for 48 h. After all cells of the non-transfected control were dead, cells carrying GFP or MMD were then transferred into culture flasks, expended and frozen.

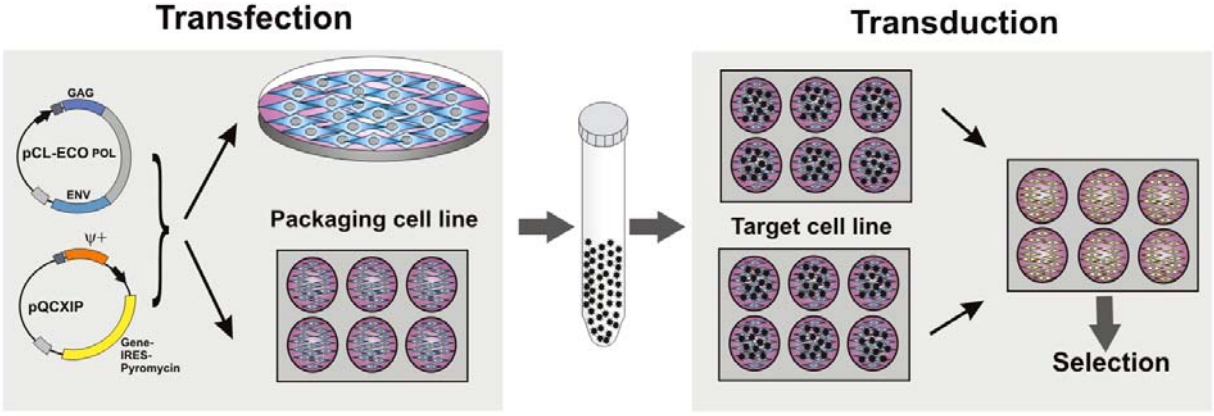

Figure 4.2 The retroviral transfection system
The packaging vector, pCL-Eco and the expression vector, pQCXIP, were transfected into the packaging cell line, which produced replication deficient retroviral particles in the supernatant. These were collected and used to transduce a target cell line, integrating into its genome to stably express the gene of interest.

4.5. Gene targeting protocols

4.5.1. Cloning of targeting vectors

In the course of this work, five "replacement" targeting consctructs were generated, which contains elements described in section 5.4.2.

4.5.1.1. Targeting vector I

The targeting vector I, TOPO-[KA-GFP-Neo-LA]-TK (13.2 kb) was prepared as follows:

(1) The short arm, KA, was amplified by PCR from E14.1 genomic DNA using the primer pair: "KA-S" (with 5'NotI site) and "KA-AS" (with 3' BamHI site). After checking the PCR product by sequencing, the 500-bp fragment was subcloned into pBS-loxP-Neo-loxP vector using NotI-BamHI restriction sites, resulting in pBS-[KA-Neo] construct.
(2) The GFP reporter gene in pCR2-TOPO vector was cut using BamHI and EcoRI restriction enzymes and ligated into the BamHI-EcoRI site of pBS-[KA-Neo] construct in frame with the short arm of *mMMD* gene.
(3) The long arm, LA, was also amplified by PCR from E14.1 genomic DNA using "LA_S" and "LAn_AS" primers (introducing 5'SalI and 3'XhoI restriction sites). The 2500-bp PCR product was cloned into pCR2.1-TOPO vector.
(4) The fragment [KA-GFP-Neo] was then cloned into NotI-SalI site of TOPO-LA vector.
(5) The negative selection TK-cassette was prepared from pGEM7-TK vector by digestion with KpnI, and ligated into KpnI site of TOPO-[KA-GFP-Neo-LA] construct in the same orientation of the Neo-cassette.

4.5.1.2. Targeting vector II

In the targeting vector II, TOPO-[LLA-GFP-Neo-LA]-TK (17 kb), the short 500-bp arm (KA) of the targeting vector I has been replaced by a longer 4600-bp arm to improve the recombination efficiency. For this purpose, the "long long arm" (LLA) was generated in three steps as follows:
(1) The first fragment of LLA was amplified from ES genomic DNA using "1.Arm5'-1_S" (introducing a 5'NotI site) and "1.Arm5'-1_AS" primers, and afterwards subcloned into pCR2.1-TOPO vector.
(2) The second fragment of LLA was also generated by PCR using "1.Arm5'-2_S" and "1.Arm5'-2_AS" primers, and subcloned into pCR2.1-TOPO vector.
(3) The last fragment was amplified using "1.Arm5'-3_S" and "1.Arm5'-3_AS" primers (introducing a 3'BamHI site). Each fragment of LLA was checked for mutation by sequencing.
(4) The pBS-[KA-GFP-Neo] construct from step 2 section 4.5.1.1, was digested with NotI and BamHI restriction enzymes to excise the KA short arm.
(5) The 1.step fragment cut with NotI-NcoI together with the 2.step fragment, cut with NcoI-BamHI were subcloned into the pBS-[GFP-Neo] prepared in the previous step.
(6) The 3.step fragment of LLA, cut with BamHI, was subcloned into the construct of step 5 (cut with BamHI), to yield pBS-[LLA-GFP-Neo].

(7) [LLA-GFP-Neo] fragment was excised using NotI and SalI restriction enzymes and ligated between NotI and SalI sites into TOPO-[LA]-TK vector.

4.5.1.3. Targeting vector III

Taking advantage of the results of previous targeting vectors, the targeting vector III, pBS-[SA3-GFP-Nep-LA]-DT (11.1 kb) was generated as follows:
(1) The pCR2.1-TOPO backbone was suspected to be inappropriate for amplification and purification of large constructs. Therefore, the [GFP-Neo-LA] fragment was excised from TOPO-[KA-GFP-Neo-LA] using BamHI-XhoI restriction enzymes, and ligated into an empty pBS vector. The resulting construct is pBS-[GFP-Neo-LA].
(2) The PCR product, SA3 of LLA (targeting construct II, section 4.5.1.2, step 3) was taken as short arm for the targeting construct III: it was cut from pCR2.1-TOPO vector with BamHI, and subcloned into pBS-[GFP-Neo-LA].
It was reported that the DT-ApA cassette leads to a more efficient elimination of negative clones, which integrated randomly the targeting vector (Yanagawa et al., 1999), therefore:
(3) the DT-ApA negative selection cassette was excised with KpnI from the pBS-DT-ApA vector and ligated into the KpnI site of pBS-[SA3-GFP-Neo-LA] downstream of the long arm (LA).

4.5.1.4. Targeting vector IV

In the construct IV, pBS-[SAex5-Neo-LAex6]-DT, the short homologous arm (1.4 kb) was positioned between exons IV and V, and the long arm (4.4 kb) upstream of exon VI of mMMD gene. The cloning procedure was carried out as follows:
(1) The SAex5 was generated by PCR amplification using "SA-Not_S" and "SA-EcoR_AS" primers. The PCR product was then subcloned into the NotI-EcoRI site of pBS-Neo vector.
(2) DT-ApA cassette was subcloned into pBS-[SAex5-Neo] construct using the KpnI site, to yield pBS-[SAex5-Neo-DT].
(3) LA-ex6 long arm was generated in a single PCR reaction with the "Laex6-1_S" and "Laex6-3_AS" primers and by using the Herculase® enhanced DNA polymerase (Stratagene, Germany). Afterwards, the PCR product was cloned into pCR2.1-TOPO vector and controlled by sequencing using the following primers: "Laex6-1_in", "Laex6-1_AS", "Laex6-2_S", "Laex6-2_AS", "Laex6-3_S", and "Laex6-3_in". Finally, the LAex6 long arm was cut with SalI and ligated into SalI site located between the Neo and DT cassettes of pBS-[SAex5-Neo-DT] vector. The resulting construct has the size of 11.8 kb.

4.5.1.5. Targeting vector V

The elements of targeting vector V, TOPO-[KA-GFP-Neo-LA], are the same described in section 4.5.1.1 but without the TK negative selection cassette, which was excluded to minimize its toxicity and increase the number of clones after positive selection. Additionally, the size of the vector is reduced which may positively influence the transfection efficiency.

4.5.2. Mouse Embryonic Fibroblast (MEF) cell culture

4.5.2.1. Setting up mating

To prepare mouse embryonic fibroblast (MEF), fertile female mice were mated with fertile C57BL6 males. To enhance the ovulation, the male mouse was isolated in a cage and 4 h later a female was transferred into the same cage and kept there overnight. A successful copulation was controlled in the early morning by a simple visual examination of the vulva looking for a plug. The plug is a coagulum of particular component of the male ejaculate that blocks the entrance of the vagina. Once it was detected, the potentially pregnant female was isolated, controlled for pregnancy and sacrificed to isolate mouse embryos after 14.5 days post-coitus (dpc). To prepare neomycin resistant EF, C57BL6 male were mated with an available knock-out female mouse (Rehli et al., 2005), which expressed the neomycin resistant (neo^R) gene constitutively from a gene targeted mutation, giving birth to embryos heterozygous for the neo^R gene.

4.5.2.2. Isolation of embryo

To isolate mouse embryos, a pregnant mouse was killed by cervical dislocation and transferred under a laminar flow hood. The mouse was laid on its back, the belly swabbed with 70% ethanol, and the uterus dissected out by using sterile forceps and avoiding contact with the fur to minimize bacterial contamination. The uterus was then placed into a Petri dish filled with sterile PBS to remove blood, transferred to a second Petri dish where the embryos were isolated out of the embryonic sac. From each embryo, head and internal red organs were cut and discarded, and the residual body was transferred into a fresh Petri dish containing PBS.

4.5.2.3. Preparation of MEF cells

- *Protocol I*

MEF cells used in the first two targeting experiments were prepared from isolated embryo bodies as following: embryos were cut into small pieces, gently pushed through a metal sieve which was rinsed continuously with PBS. Cells were collected and washed twice with PBS, centrifuged (8 min, 300 g) and cultured in MEF growth medium on 15 cm culture dishes for 48 h (3 embryos on 1x15 cm plate). Afterwards cells were detached from the plates by incubation with trypsin/EDTA for at least 10 min and split at a 1:2 ratio. After an incubation for another 48 h, cells were frozen in liquid nitrogen (5 vials/2x15 cm plates).
The day before MEF cells were needed, one vial was thawed and cultured. Once confluency reached, plates were incubated at 37°C for 2.5 h in MEF medium supplemented with 10 μg/ml mitomycin-C (Medac, Hamburg) to inactivate their mitosis. Mitomycin treated MEFs can be used for up to 3 days.

- *Protocol II*

The protocol II (personal communication with Dr. Markus Moser Max Planck Institute, München) was followed to prepare MEF neomycin resistant cells, which were used during neomycin selection in most of the targeting experiments. Isolated embryos were cut into small pieces and incubated in a 50 ml tube with 20 ml trypsin/EDTA for 15 min. MEF medium was then added to inactivate trypsin and with a 25 ml pipette, embryo debris were pipetted up and down till the tissues disassociate. MEF medium was added and cells were then cultured in T175 flask (2 embryos/T175 flask). The next day cells were split at a ratio of 1:4, and 48 h later at a ratio of 1:2. Once 100% confluency was reached, cells were trypsinized and collected in 50 ml tubes filled with MEF medium.
To inactivate mitosis, they were exposed to 4000 rads (376 seconds) of γ-irradiation. Afterwards mitotic inactivated MEFs were centrifuged, the cell pellet was dissolved in MEF medium, with an equal volume of 2x Freezing medium, and immediately frozen overnight at -80°C (3 vials /T175 flask). The next day cells were transferred into liquid nitrogen.
Independently of the protocol, the cell density used to obtain a confluent MEF monolayer culture depended on the size of the plate as following:

Table 4.8 MEF cell density on different size tissue culture plates.

MEF cells	Number of MEF plates or flasks	Medium (ml/plate or well)
$1.5x10^5$	1x 14 cm plate or T175 flask	25
	3x 10 cm plates or T75 flask	10
	3x 24-well plates	1

Required media:

MEF growth medium:	**500 ml**	DMEM (Cat. No. 41960-029, Invitrogen)
	2 mM	5 ml L-Glutamine (100x) (Invitrogen)
	5 µM	500 µl β-Mercaptoethanol (1000x)
	1x	5 ml penicillin (50 U/ml) and streptomycin (50 µg/ml)
	5%	50 ml FCS (PAN Biotech)
MEF freezing medium: **(2x, fresh prepared)**	**60 %**	6 ml MEF growth medium (with 5% FCS)
	20%	2 ml FCS
	20%	2 ml DMSO (Sigma).

4.5.3. Embryonic stem (ES) cell culture

4.5.3.1. General conditions of ES cell culture and freezing

ES cells require special conditions to maintain their full developmental potential and their capability to contribute to the germ line. ES cells were cultured at 37°C with 7% CO_2, supplied daily with fresh ES medium supplemented with LIF (Leukemia Inhibitory Factor), which prevented their differentiation. Additionally, for long-term culture, ES cells were grown on a monolayer of MEF cells providing them with additional growth factors. ES cells culture should be subconfluent and were split in a 1:4 ratio. Passaging was kept at a minimum because prolonged culture may decrease ES cell contribution to the germ line. Cultured inappropriately, ES cells can accumulate mutations, thus increasing their growth rate on the cost of their pluripotency (Nagy et al., 2003).

For freezing ES cells, a pellet of $2x10^6$ cells was dissolved in an equal volume of ES growth medium and ES freezing medium (2x), immediately transferred into cryovial, placed into cryo container at -80°C overnight, and on the next day, stored in liquid nitrogen.

The embryonic stem E14.1 cell lines used in the targeting experiments were kindly provided by Prof. Dr. Klaus Pfeffer (Düsseldorf, Germany) and Dr. Marina Karaghiosoff (Vienna, Austria).

Required media:

ES growth medium:	**500 ml**	DMEM (Cat. No. 41960-029, Invitrogen)
	2 mM	5 ml L-Glutamine (100x) (Invitrogen)
	5 µM	500 µl β-Mercaptoethanol (1000x)
	1x	5 ml penicillin (50 U/ml) and streptomycin (50 µg/ml)
	5%	50 ml FCS (PAN Biotech)
	$5x10^5$ U	50 µl ESGRO-LIF (10^7 U/ml) (ESG-1107, Chemicon).
ES freezing medium: (2x, fresh prepared)	**60%**	6 ml ES growth medium (with 15% FCS)
	20%	2 ml FCS
	20%	2 ml DMSO (Sigma).

4.5.3.2. Testing serum batches

It is crucial to culture ES cells with FCS batches that do not influence their morphology and growth. To select an appropriate FCS, three batches, recommended for ES cell culture, were ordered from PAN Biotech GmbH (Aidenbach, Germany), and tested as following: ES cells were plated at low density with different concentration of FCS (10%, 15% and 30%). Their density and morphology was monitored for 5 days after ES colonies appearance and during three passages. The FCS batch P231610-ES conserved morphology and ES cells and plating efficiency in high FCS concentration (30%) after 5 days, and was chosen for ES cell culture.

4.5.4. ES cell electroporation

Preceding electroporation, MEF coated culture plates were prepared with the appropriate cell density (Table 4.8). Two different electroporation protocols were carried out.

- *Amaxa ES cell electroporation*

ES cell electroporation was performed by Amaxa Nucleofactor (Amaxa Biosystems, Köln, Germany) following the instructions of the manufacturer. In brief, ES cells split on the previous day, were trypsinised and plated for 30 min to allow MEF cells to adhere. The supernatant was centrifuged and cell pellet was dissolved in Nucleofactor solution mixed with 5, 10 or 15 µg linearized plasmid DNA in a total volume of 100 µl. The electroporation was performed immediately and cell-DNA mix was transferred with 500 µl warmed medium on two previously prepared MEF plates with ES growth medium (day 0). The number of ES cells electroporated varied depending on the experiment (see section 5.4.3).

➢ *BioRad ES cell electroporation*

One day after splitting the ES cells, they were trypsinized, counted, washed and resuspended in PBS before addition of the DNA. Cell number and DNA concentration varied depending on the experimental setup (see section 5.4.3). The cell-DNA suspension was transferred into a 0.4 cm BioRad cuvette and subjected to electroporation. Afterwards cells were cultured on MEF coated plates with ES growth medium (day 0).

4.5.5. Antibiotic selection

Positive selection with G418 was initiated 48 h after electroporation (day 2). Negative selection started with ganciclovir one day later (day 3) with a daily medium change. G418/G420 (PAN Biotech GmbH, Germany) concentration was tested for each new batch, and when using neomycin resistant MEF cells. The final concentration of the antibiotic varied between 200 and 300 µg/ml ES growth medium. Gancyclovir (Cymeven, Syntex GmbH-Roche, Germany) working concentration was 25 µg/ml. The selection time varied from 9 to 11 days, and picking was started when round clones with a shiny, well-defined border appeared.

4.5.6. Picking, expansion and freezing of ES cell clones

Picking ES clones was performed under the microscope in the laminar flow hood. Each individual drug-resistant clone was picked from the selection plate containing PBS using a pipette with a yellow tip adjusted to a volume of 20 µl. Clones were transferred into a 96-well plate, after picking 12 clones, 50 µl trypsin/EDTA was added into each clone-containing well and the plate was incubated for 7 min at 37°C. ES growth medium (50 µl) was added to the well, and cells of each clone were separated by pipetting up and down, and transferred into a MEF coated 48-well plate containing 500 µl ES growth medium.

Once ES-cell clones reached confluency (usually after 2-3 days), they were split into 2x 48-well plates as follows: each well was washed once with PBS and incubated with 100 µl trypsin 5 min at 37°C. Each clone was treated separately to avoid cross-contamination. After adding 500 µl ES growth medium, the cell suspension was homogenized and divided into 2x 48-well plates:

- A-plate: coated with MEF cells (planned for freezing)
- B-plate: coated with gelatin without MEF cells (planned for genotyping).

When cells of the A-plate have reached 80% confluency, each well was washed once with PBS, cells were trypsinized and after 10 min incubation at 37°C, ES growth medium and freezing medium were added. Cells were well suspended, and plates sealed with parafilm and frozen at -80°C. It is crucial that cells from the A-plate conserve their non-differentiated morphology (grown on MEF, supplemented with LIF). If a specific clone turned out to be positive, the corresponding plate would be thawed and cells subjected to injection. The B-plates were used only to prepare genomic DNA for genotyping (see section 4.5.7)

4.5.7. Screening of ES cell clones

4.5.7.1. Genomic DNA purification

To purify genomic DNA from ES cells for clone screening, two different methods were used:

- *Genomic DNA extraction with phenol-chloroform extraction*

For genomic DNA extraction, confluent ES cells in 48-well plates were washed once with PBS and incubated at 37°C overnight with 500 µl lysis buffer per well (plates were sealed with parafilm to prevent drying). The cell lysate was subjected to one phenol extraction, followed by 2x phenol/chloroform/isoamyl alcohol (in a 25:24:1 ratio) and 2x chloroform extractions (1 volume each, with 3 min centrifugation steps at 13000 rpm). Genomic DNA was precipitated by the addition of 2 volumes of 100% ethanol and 1/10 volumes of sodium acetate 3 M pH 5.2. After incubating at -20°C for 30 min, the precipitated genomic DNA was pelleted at 13000 rpm for 5 min. After a 70% ethanol wash, genomic DNA was resuspended in 100 µl H_2O and stored at 4°C. DNA concentration and quality was assessed with the spectrophotometer.

Lysis buffer I:	**100 mM**	5 ml	Tris-HCl (1 M), pH 8.5
	5 mM	0.5 ml	EDTA (0.5 M)
	200 mM	5 ml	NaCl (2M)
	1%	2.5 ml	SDS (20%)
	0.1 mg/ml	5 mg	Proteinase K (Roche)
	Add H_2O to 50 ml. Fresh prepared.		

- *Rapid and direct genomic DNA extraction from 48-well plates*

The following method allowed the rapid extraction of genomic DNA directly from plates. ES cells were previously cultured on 0.2% gelatin-coated 48-well plates until the medium turned yellow. The plates were rinsed with 500 µl PBS, and then 200 µl lysis buffer II was added. They were then sealed with parafilm and incubated at 50°C overnight in a humid atmosphere

inside a closed Tupperware containing wet paper towel. The next day, after shortly centrifuging the plate at 2500 rpm, 20 µl NaCl was added to each well followed by 2.5 volumes 100% ethanol. Gentle shaking at RT for 30 min resulted in the precipitation of DNA as a filamentous network. Plates were then centrifuged and gently inverted to discard the supernatant while the DNA stayed attached to the bottom. After washing wells 3x with 500 µl 70% ethanol, plates were inverted and the ethanol was discarded. Finally after drying in a laminar hood, 70 µl TE was added to each well and the dissolved genomic DNA was transferred into microfuge tubes and stored at 4°C. DNA concentration and quality was assessed again with the spectrophotometer.

Lysis buffer II:	**10 mM**	250 µl	Tris-HCl (2 M), pH 7.5
	10 mM	1 ml	EDTA (0.5 M), pH 8
	10 mM	250 µl	NaCl (2 M)
	0.5%	250 µl	Sarcosyl (Merck)
	1 mg/ml	50 mg	Proteinase K (Roche)
	Add H_2O to 50 ml. Fresh prepared.		

4.5.7.2. DIG-labeling of southern probes

DIG-DNA probes were used to screen ES clones from which genomic DNA was prepared following protocol I (see section 4.5.7.1), because large amounts of digested genomic DNA (15 µg) are required to get clear bands by non-radioactive Southern blot analysis. DIG-labeling was carried out using the PCR DIG Probe Synthesis kit following the manufacturer instructions (Roche). As template, a genomic DNA region (about 500 bp) positioned outside of the homologous region of the targeting constructs was chosen to be amplified from the genomic DNA using a mix of DIG-dNTPs and unlabeled dNTPs. Presence and size of the DIG labeled PCR product were then controlled by agarose gel electrophoreses, and the specific DNA band was extracted from the gel. The DIG-labeled probe was titrated as described in the manufacturer protocol.

PCR reaction mix:	300 ng	Genomic DNA
	5 µl	10 pmol/µl Sense primer
	5 µl	10 pmol/µl Anti-sense primer
	2.5 µl	10 mM dNTP
	2.5 µl	PCR DIG mix (Roche)
	5 µl	10x Taq buffer
	0.75 µl	High Fidelity polymerase
	Add H_2O to 50 µl.	

4.5.7.3. Radioactive labeling of Southern probes

Radioactive labeled DNA probes were used to screen ES clones where genomic DNA was extracted following protocol II (see section 4.5.7.1). The DNA probes were first generated by PCR. As described in section 4.5.7.2, a genomic DNA region (about 500 bp) positioned outside the homologous region of the targeting constructs was chosen as template. The ensuing PCR product 25 ng was radioactively labeled by random prime second-strand synthesis with Klenow fragment. After labeling, unincorporated nucleotides were removed by MicroSpin™ G-25 column (Amersham, Germany) following the manufacturer's protocol. The radioactively labeled DNA probes were denatured at 95°C for 5 min before hybridization.

Labeling reactions:
25 ng DNA
1 µl Random 9-mer (Ambion, Germany)
Add H_2O to 28 µl, incubate at 95°C for 10 min.
Cool down on ice, and spin down quickly.
4 µl 10x Klenow buffer
2 µl dNTPs (without dATPs)
1 µl exo^- Klenow (Roche, Germany)
5 µl [α-32P]-dATP.
Mix, spin and incubate at 37°C for 20 min.
Add 2 µl dNTPs. Mix and incubate at 37°C for 10 min.

4.5.7.4. Screening clones by Southern blot analysis

Southern blotting is the transfer of DNA from a gel to a membrane. First genomic DNA was digested overnight with the appropriate enzyme in a final volume of 30 µl. Digested samples were analysed on an agarose gel which was run for 4 h with 90 V to allow a good separation of DNA bands. After photographing the gel, the blotting procedure was started as following:

- DNA depurination: shaking the gel 1x 10 min in 0.25 M HCl.
- Washing the gel 1x with Millipore water.
- DNA denaturation: shaking the gel 2x 15 min in denaturation buffer.
- DNA neutralization: shaking the gel 2x 10 min in neutralization buffer.
- Blotting overnight using a positively charged nylon membrane (Roche), following the Northern blotting procedure described in section 4.1.4.4 with some modifications (Figure 4.3).
- DNA fixation on the membrane by UV crosslinking (Stratalinker).
- Washing the membrane: 1 h with 2x SSC.
- Drying the membrane: 1 h at RT.

- Prehybridization in 10 ml DIG-Easy Hyb (Roche) for 2 h at 42°C (for DIG-labeled probe), in 10 ml Rapid-hyb buffer (GE Healthcare biosciences) for 3 h at 65°C (for radioactively labeled probe).
- Probe denaturation: 5 min at 95°C.
- Hybridization: probe was added into 10 ml hybridization buffer, incubated overnight at 42°C or 65°C for DIG- or radioactively labeled probes respectively.
- Membrane washing: 2x 10 min with washing buffer I at RT.
- Membrane washing: 2x 15 min with washing buffer II (prewarmed at 68°C) at 68°C.
- Visualization of DIG-probe-target hybrids was performed using chemiluminescence assay (Roche). Afterwards labeled membranes were fixed in an exposure cassette with a storage phosphor screen and exposed overnight to up to three days. The cassettes were later scanned on a phosphoimager Typhoon™ (Amersham Biosciences).

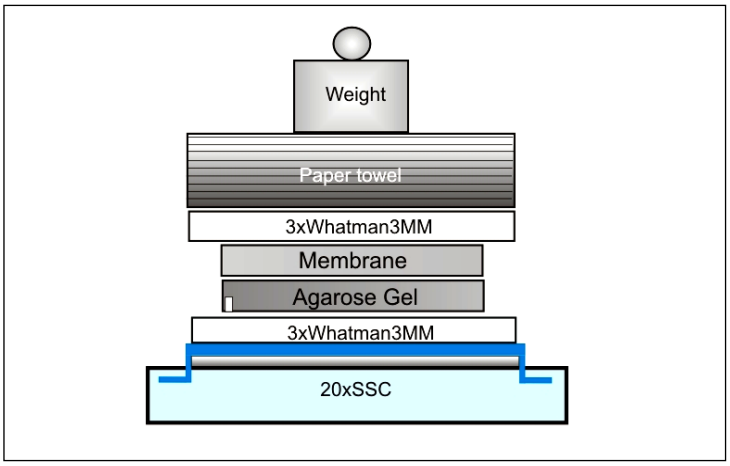

Figure 4.3 Southern blot, DNA transfer to nylon membrane.
The digested DNA was transferred to a nylon membrane. The DNA gel was placed upside-down on 3 layers of 20xSSC-soaked Whatman 3MM filter papers on glass plates. The membrane was laid on the top of the gel, covered with 3 layers filter papers soaked with 20xSSC. A cellulose wadding was placed on top and pressed with a glass plate.

Required buffers and solutions:

Denaturation solution	**0.5 M**	40 g NaOH
	1.5 M	175.32 g NaCl
	Add H_2O to 2 l.	
Neutralisation solution	**1.5 M**	175.32 g NaCl
	1 M	121.14 g Tris
	Add H_2O to 2 l.	
Southern Blot Washing buffer I	**2x**	100 ml 20x SSC
	0.1%	5 ml 20% SDS
	Add H_2O to 1 l.	
Southern Blot Washing buffer II	**0.1x**	5 ml 20xSSC
	0.1%	5 ml 20% SDS
	Add H_2O to 1 l.	

5. Results

To get more insights into the structure of *monocyte to macrophage differentiation* (*MMD*) and *MMD2* genes, the mouse nucleotide sequence was studied and aligned with its orthologues. To profile their expression, Northern blot analyses of RNA from different human and mouse tissues and cell lines were carried out. In addition a whole-mount in situ hybridization was performed in mouse embryo to study MMD and MMD2 transcripts expression during the embryogenesis. To determine mouse MMD (mMMD) protein cellular localization, various tagged MMD cDNA were transiently or stably expressed in a mouse cell line. In an attempt to define the likely function of mMMD, ES cell culture was established in our lab in the course of this PhD work, and different targeting vectors were designed, generated, and electroporated into ES cells to produce a MMD knock-out ES cells. Finally by using siRNA, the silencing of mMMD gene was achieved in two mouse cell lines, which may provide a tool for studying its function.

5.1. Genomic organization of *MMD* and *MMD2* genes

5.1.1. Analysis of mouse *MMD* and *MMD2* genes

- *Mouse MMD*

The mouse *MMD* gene (m*MMD*) is located on the chromosome 11D and comprises 7 exons with the ATG start codon positioned in exon I (Figure 5.1). The full-length cDNA has about 2.6 kb encoding 238 amino acids with a predicted molecular weight of 28 kDa.

- *Mouse MMD2*

The mouse *MMD2* (m*MMD2*) gene was recently identified as a homologue to *MMD*, with a conserved gene organization (6 exons and ATG start codon also in exon I) (Figure 5.1). The MMD2 transcript is about 2 kb long and the ORF is located on chromosome 5qG2. It encodes a protein of 247 amino acids with a predicted molecular weight of 29 kDa.

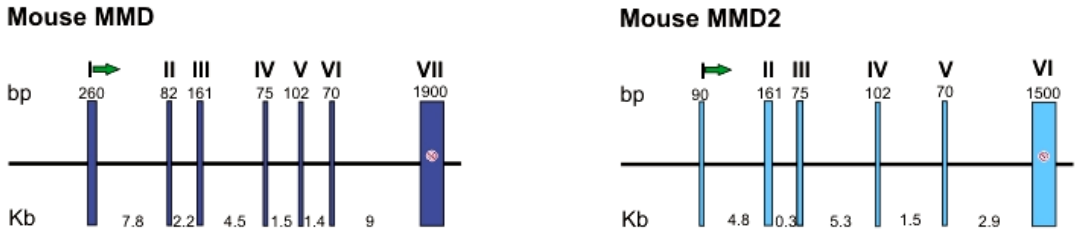

Figure 5.1 Genomic organization of mouse *MMD* and *MMD2*.
Schematic representation of the intron/exon structure of mouse *MMD* and *MMD2* as determined by BLAST. Exons are depicted as filled boxes and numbered with roman numerals, introns are represented by the connecting lines. The start codon is marked with a green arrow. The size of the exons and introns is indicated in bp or in kb, respectively.

5.1.2. Analysis of human MMD and MMD2 genes

- *Human MMD*

Human *MMD* (h*MMD*) was cloned, in our lab, from in vitro differentiated mature macrophages, and identified as monocyte to macrophage differentiation protein (Rehli et al., 1995). The full-length cDNA consists of around 2.5 kb, located on the reverse strand of chromosome 17q. It is organized in 7 exons with the ATG start codon in exon I (Figure 5.2). The protein of 238 amino acids has a predicted molecular weight of 28 kDa.

- *Human MMD2*

Human MMD2 (hMMD2) is a homologue of *hMMD*, identified at the same time as its mouse orthologue. The full-length cDNA is around 2.3 kb, located on chromosome 7p22 (Figure 5.2). The hMMD2 protein appears in the UniProt database in two alternative variants, a long isoform of 270 amino acids and a molecular weight of 31 kDa, and a short isoform missing 24 amino acid residues between position 156 and 179 of the first isoform.

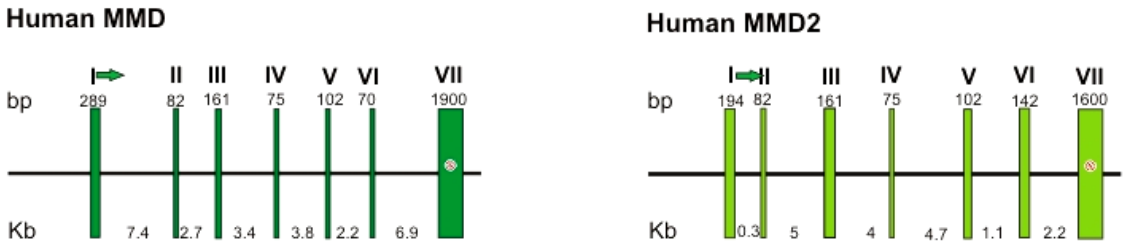

Figure 5.2 Genomic organization of human *MMD* and *MMD2*.
Schematic representation of the intron /exon structure of human *MMD* and *MMD2* as determined by BLAST. Exons are depicted as filled boxes and numbered with roman numerals, introns are represented by the connecting lines. The start codon is marked with a green arrow. The size of the exons and introns is indicated in bp or in kb, respectively.

5.1.3. Structure and sequence homology of MMD family proteins

Online database searches classified mouse and human MMD and MMD2 proteins as members of the so far uncharacterized Hemolysin-III (Hly-III) family. Based on structural similarities, both proteins were recently grouped into the Progestin and AdipoQ receptor (PAQR) family and termed as PAQR11 (MMD) and PAQR10 (MMD2) (Tang et al., 2005).

Multiple sequence alignment using ClustalW revealed 94% identity between mouse and human MMD2, and 99% between mouse and human MMD, whereas it showed about 68% identity between the paralogues in mouse and human (Figure 5.3, Table 5.1). The high range of identity found between the orthologues may suggest a similar function. On the other hand, the paralogues MMD and MMD2 may have diverged to fulfill distinctive functions in both human and mouse.

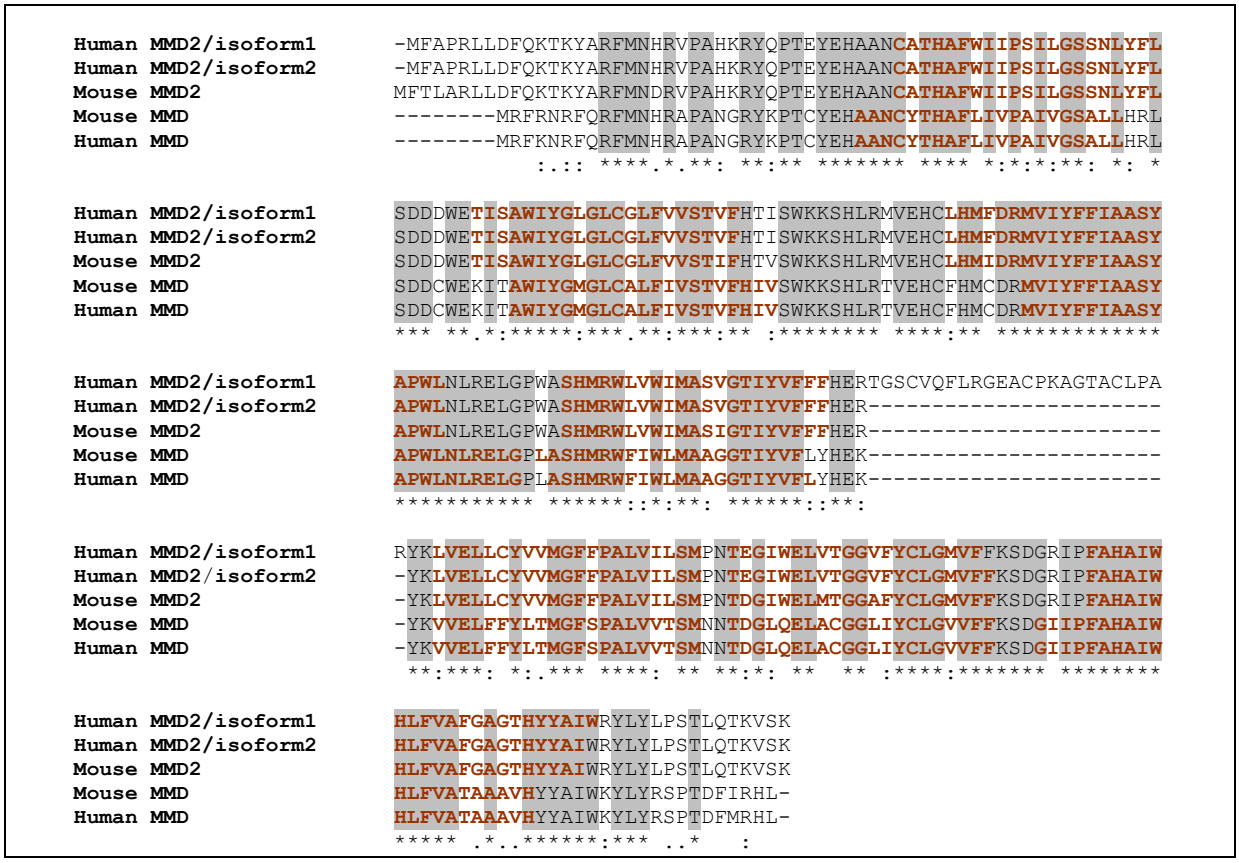

Figure 5.3 Multiple sequence alignment of mouse and human MMD and MMD2 proteins.
Identical residues are boxed in grey and marked with asterisks. Similar residues are marked with dots. Predicted transmembrane domains based on UniProt server are shown in red. The multiple protein sequence alignment was done using the ClusalW program.

Table 5.1 Multiple protein sequence alignment of mouse and human MMD and MMD2 proteins.

		Mouse		Human	
		MMD	**MMD2**	**MMD**	**MMD2**
Mouse	**MMD**	100%	69%	99%	68%
	MMD2	69%	100%	69%	94%
Human	**MMD**	99%	69%	100%	68%
	MMD2	68%	94%	68%	100%

Based on Kyte and Doolittle plots (Kyte & Doolittle, 1982), MMD and MMD2 are hydrophobic proteins with seven predicted transmembrane domains. In Figure 5.4 only the mouse MMD proteins hydropathy plots are shown.

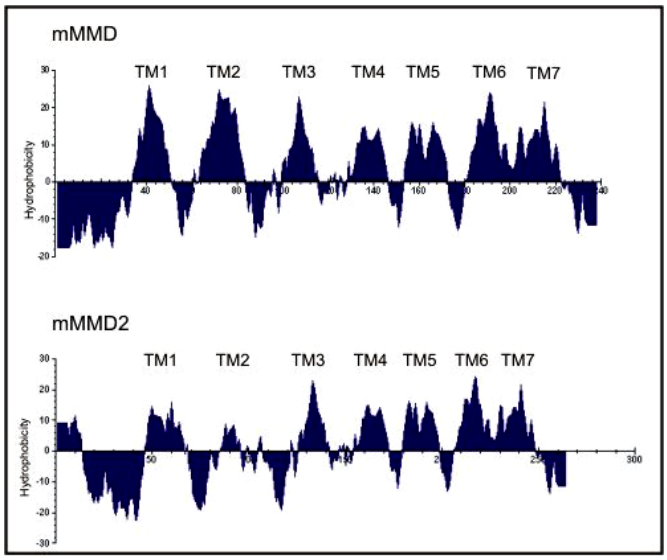

Figure 5.4 A hydropathy plot of mMMD and mMMD2 according to Kyte and Doolittle.
The predicted hydrophobic transmembrane domains (TM) are numbered with I to VII. The mMMD hydropathy plot shows 7TM domains, while mMMD2 plot shows an additional hydrophobic N-terminal tail, that does not correspond to a signal peptide (Bendtsen et al., 2004). The graphic was performed using the Gene Runner program.

A sequence alignment of mMMD and its orthologues in different species showed a markedly conserved protein sequence (Figure 5.5). The mouse protein sequence shares around 98% identity with its human (*Homo sapiens*), chimp (*Pan troglodytes*), and rat (*Rattus norvegicus*) counterparts over its entire length. The chicken (*Gallus gallus*) and the frog (*Xenopus tropicalis)* orthologues share 88% identity, followed by the zebrafish (*Danio rerio*) with 74%. Less identity was found in the fruitfly, *Drosophila melanogaster,* with 43%, and *Caenorhabditis elegans* with 36%. A similar degree of conservation between species was also seen with mMMD2 and its orthologues (data not shown).

Figure 5.5 Multiple sequence alignment of mMMD and its orthologues (ClustalW).
Predicted transmembrane (TM) regions in mMMD are depicted in black and numbered with I-VII. Conserved amino acid residues (100% identity) between the orthologues are shown in grey. Putative metal binding residues (conserved in other PAQRs including yeast YOL002c) are shown in green.

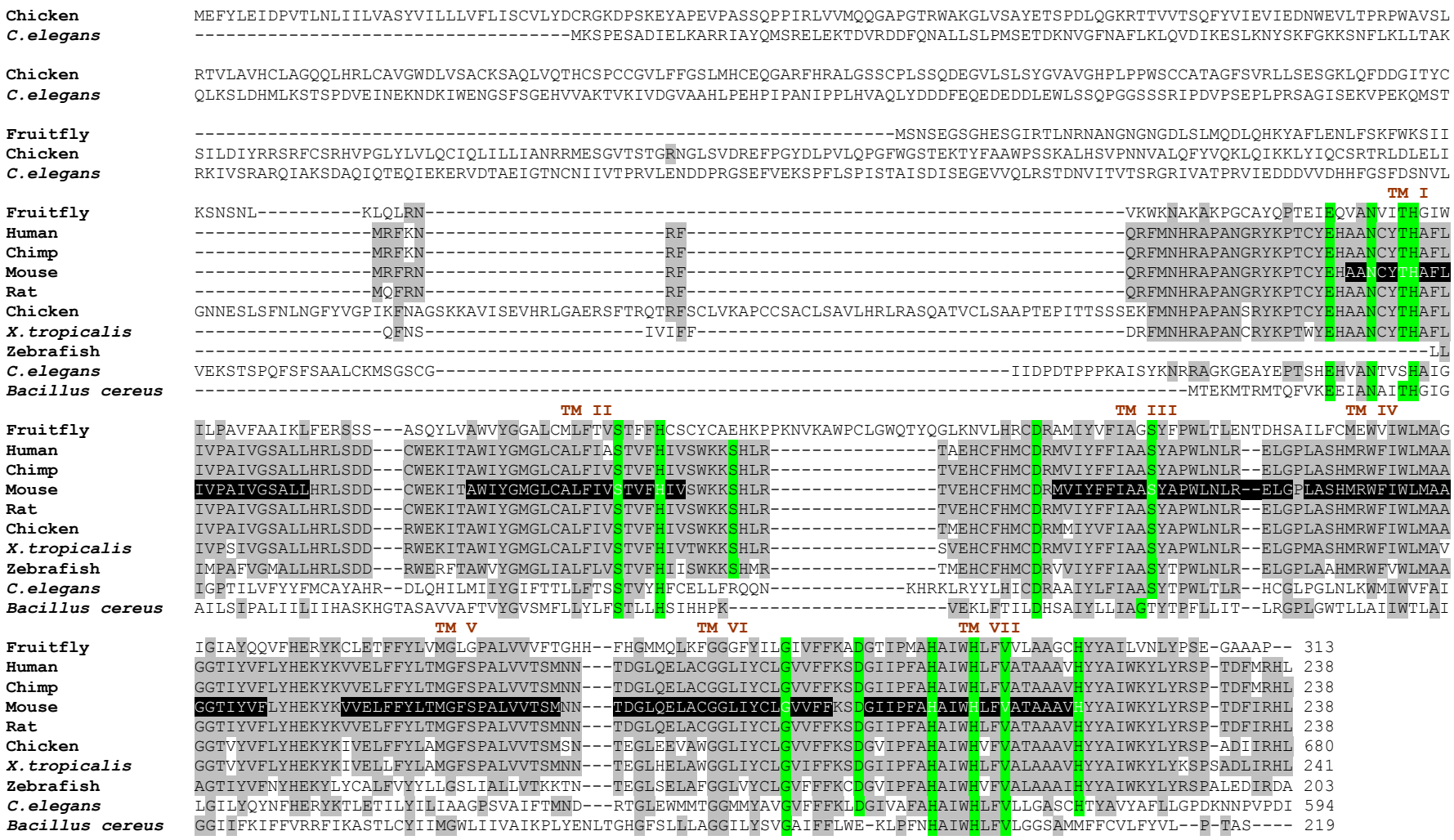

5.2. Expression analysis of MMD and MMD2 mRNA

To monitor *MMD* and *MMD2* transcription in mammalian cell lines, total RNA was isolated and Northern blot analysis was performed with specific radioactive DNA probes as described in section 4.1.4. To monitor MMD and MMD2 RNA expression in adult mouse and human tissues, multiple tissue Northern (MTN) blots (Clontech) were hybridized with the same radioactive labeled MMD and MMD2 specific DNA probes.

5.2.1. Expression patterns of human MMD and MMD2 mRNA

5.2.1.1. MMD and MMD2 expression in human cells

Northern blot analysis of various cell types confirmed hMMD expression in macrophages and not in monocytes (Rehli et al., 1995). In addition, mRNA was detected in monocyte-derived dendritic cells (DC), granulocytes and HepG2 (human hepatocellular carcinoma cell line).
Lower expression levels were found in B- and T-lymphocytes, in HUVEC (dermal fibroblasts), and NADFc (human skin fibroblast) cell lines. Although CaCo-2 and HT-29 represent two human colon carcinoma cell lines, however HT-29 expressed hMMD at lower levelsl than CaCo-2 cells (Figure 5.6A).
Human MMD2 mRNA was not detectable in all studied cell lines (data not shown). This may suggest a very low or even absence of hMMD2 expression

5.2.1.2. Multiple tissue Northern analysis in human

Multiple tissue Northern (MTN) blots showed an ubiquitous hMMD expression with the highest levels in fetal and adult liver, brain, heart and placenta (Figure 5.6B). In addition, human spleen, skeletal muscle and kidney showed an elevated expression of hMMD comparing to mMMD (Figure 5.9C).
The MTN blot was stripped and rehybridized using hMMD2 cDNA probe. Expression analysis of hMMD2 revealed that the transcript was restricted to the brain and testis (Figure 5.6C). In testis the expected transcript, described by the UCSC genome browser Database, was detected, however there is no published expressed sequence tags (ESTs) that may support the size of the brain transcripts. These different hMMD2 transcripts suggest a probably functional divergence or regulation.

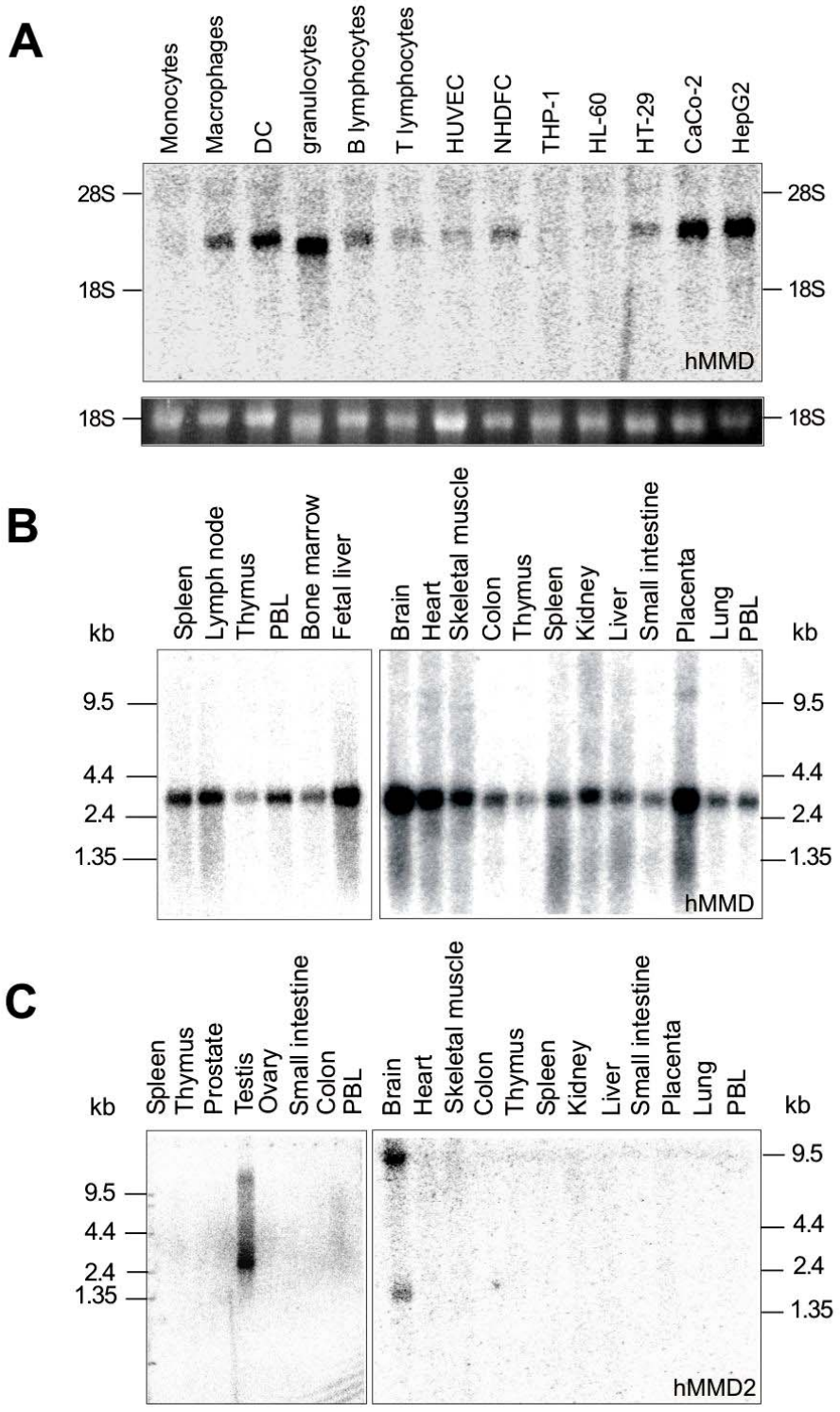

Figure 5.6 Northern blot analysis of human MMD and MMD2 mRNA expression.
(A) MMD expression in various human cells: total RNA (10 µg/lane) was hybridized with a probe positioned at the 3'-UTR region of hMMD cDNA to detect specifically hMMD expression. The positions of the 28S (5025 bp) and 18S (1868 bp) rRNA bands are indicated. The bottom inset shows the ethidium bromide-stained 18S rRNA bands before blotting. The Northern blot was kindly provided by Dr. Sven Heinz. (B) MTN blot (Clontech) analysis hybridized with the probe used in (A) generated from the 3'-UTR region of hMMD transcript. (C) MTN blot analysis hybridized with a hMMD2 probe generated from the 3'-UTR region of hMMD2 transcript, presenting little homology with the hMMD nucleotide sequence.

5.2.2. Expression patterns of mouse MMD and MMD2 mRNA

5.2.2.1. Expression of MMD and MMD2 mRNA in mouse embryo

To assess the expression pattern of MMD and MMD2 during mouse development, whole-mount in situ hybridization (ISH) was carried out on mouse embryo of different embryonic stages and on isolated embryonic brains. MMD and MMD2 sense and antisense digoxigenin (DIG)-labeled RNA probes were generated as described in section 4.1.6.2, and used to perform two independent whole-mount ISHs.

- *MMD*

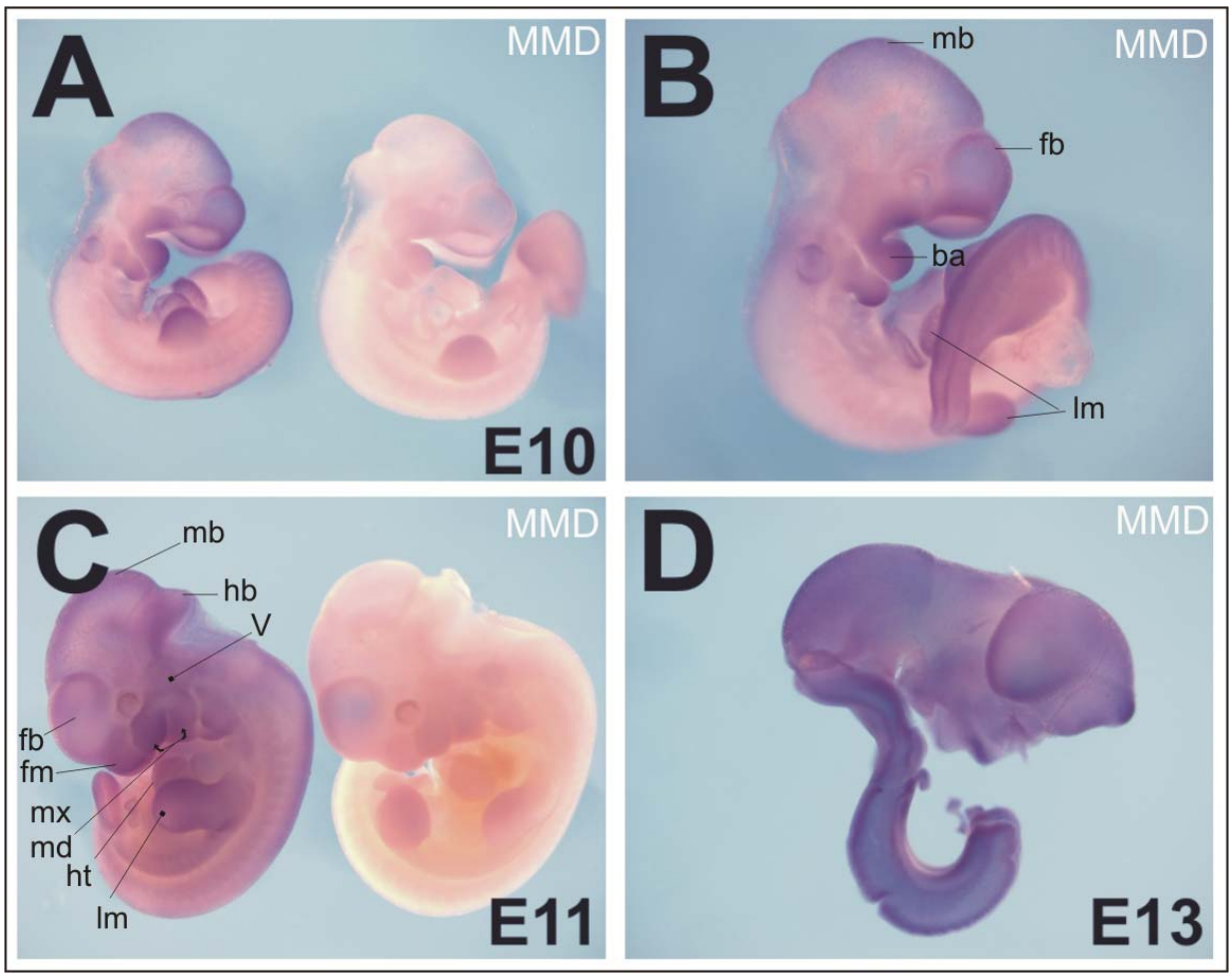

Figure 5.7 Expression of MMD mRNA in mouse by whole-mount ISH.
Side view of mouse embryos. (A) E10 embryo (on the right) shows the negative control. (B) A close-up of (A) left embryo showing positive signal in the midbrain (mb), facial mesenchyme (fm), the maxillary (mx) and mandible (md) components, branchial arches (ba) and in limb buds mesenchyme (lm). (C) The left embryo (E11) shows an almost ubiquitous expression of MMD in the brain, forebrain (fb), midbrain (mb) and hindbrain (hb), trigeminal ganglia (V), heart (ht) and limb bud mesenchyme (lm). E11 embryo on the right exhibits the negative control. (D) shows MMD ubiquitously expressed in the isolated brain of E13 embryo.

Hybridization of 10 days old embryos with an MMD antisense probe revealed a broad expression throughout the whole embryo with strong signals in the fore-, mid- and hindbrain as well as in the first and second branchial arches. In addition MMD was higher expressed in the limb bud mesenchyme (Figure 5.7A). The almost ubiquitous expression of MMD in the embryo was also seen one day later of development (Figure 5.7B andC).

Isolated brains from 13 days old embryos were also hybridized with the MMD probe and indicated signals in the whole brain. In contrast, no specific signal was detected in control hybridization with the sense probe showing its specificity (Figure 5.7A and C embryos at the right). A weak background staining could result from retained probes in embryonic cavities, due to an inappropriate perforation and permeabilization of the embryo prior to hybridization.

- *MMD2*

In contrast to MMD, MMD2 revealed an almost restricted expression pattern. At E10 embryo (Figure 5.8A), MMD2 expression was detected in the forebrain and the roof of the midbrain. Furthermore, MMD2 is also expressed in the peripheral nervous system (PNS), like the dorsal root and cranial ganglia.

The trigeminal nerve is the fifth (V) cranial nerve, contains sensory and motor fibers and is divided into three branches which are the ophthalmic, maxillary and mandible nerves. In addition, sensory branches of the trigeminal nerve enter the medulla and the spinal cord (Purves et al., 2001). In fact, at E10 embryos, MMD2 mRNA expression was prominent in the trigeminal ganglion (V). Furthermore, MMD2 was also detected in the branchial arches.

At E11(Figure 5.8B-C), this expression pattern becomes more prominent. Brain from E13 embryos revealed an MMD2 expression in the cortex and midbrain but also in the ventral spinal cord and in attached dorsal root ganglia (Figure 5.8E).

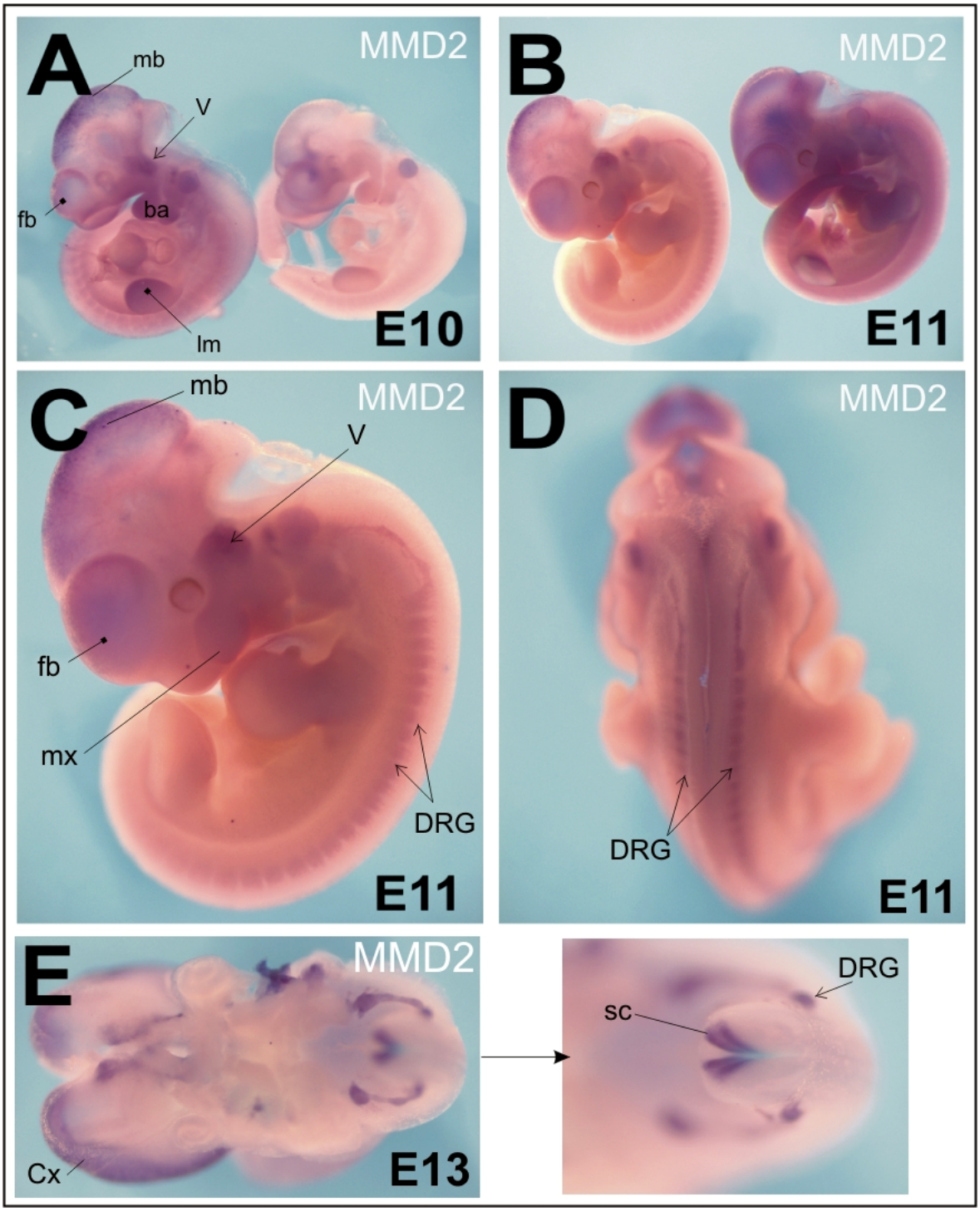

Figure 5.8 RNA expression of MMD2 in mouse embryo by whole-mount ISH.
(A, left panel) Side view of E10 showing MMD2 staining in the forebrain (fb), midbrain (mb), trigeminal ganglia (V) in branchial arches (ba) and limb bud mesenchyme (lm). (A, right panel) shows the negative control. (B, left panel) Side view of two E11 embryo. (B, right panel) shows the negative control with unspecific background staining. (C) A close-up of B showing MMD2 staining in the midbrain (mb), forebrain (fb), maxillary (mx) and mandible (md) components, trigeminal ganglia (V), and in dorsal root ganglia (DRG). (D) Dorsal view of E11 showing MMD2 expression in dorsal root ganglia. (E) Left panel: view from the ventral side of an E13 brain showing MMD2 staining in the cerebral cortex (Cx). Right panel: a close-up of the spinal cord region with MMD2 positive staining in the spinal cord (sc) and DRG.

5.2.2.2. MMD and MMD2 RNA expression in different adult mouse tissues

The analysis of MTN blots hybridized with a probe generated from the 3'-UTR region of mMMD cDNA, revealed an almost ubiquitous expression, that dominates in the brain, heart, and liver but is absent in the spleen and testis. Lower expression levels were observed in lung, kidney, and skeletal muscles. (Figure 5.9C, middle panel). Although the ubiquitous expression pattern of mouse and human MMD generally correlated, the mouse MTN blots did not include colon, thymus, lymph nodes, small intestines, placenta or peripheral blood leukocytes. It is therefore unclear if mMMD is also expressed in these tissues as its human orthologue. Interestingly, different patterns of expression, were obtained especially in liver and heart when using different probes. An additional smaller transcript was detected beside the expected 2.5 kb band, suggesting the existence of an alternative upstream polyadenylation site. This hypothesis was confirmed when the same MTN blot was hybridized with a probe generated from the 5'-coding region of MMD cDNA. A third band (around 1.35 kb) appeared revealing the transcript, which is generated when the first 5'-polyadenylation site is used (Figure 5.9C, first panel). The presence of two consensus polyadenylation sites (AATAAA) in the mMMD sequence downstream of the stop codon correlates with the presence of two transcript variants detected by MTN analysis. The third small transcript may be due to a non-typical polyadenylation site (Zhang et al., 2005).

A specific expression of mMMD2 was detected in testis, brain and kidney (Figure 5.9C, left panel). In contrast to mMMD, only one mMMD2 transcript was detected which is in line with the existence of a single polyadenylation site. Weak bands appearing in the liver and heart lanes likely correspond to background signals resulting from an inefficient removal of the mMMD probe.

5.2.2.3. MMD and MMD2 mRNA expression in different mouse cell lines

Total RNA was extracted from various mouse cell lines following the protocol described in section 4.1.4.1. Northern hybridization showed that mMMD mRNA was highly expressed in bone marrow macrophages (BMM), and weaker in RAW 264.7 (macrophage cell line), P815 (mastocytoma cell line) and HT-2 (helper T cell line), as well as in the NIH3T3 fibroblast cell line. MMD transcript was not detected in J774 (monocyte-macrophage cell line) and in BV-2 (microglia cell line). Recently, Bräuer et al. (Brauer et al., 2004) identified a MMD orthologue in rat as a macrophage/microglia activation factor (MAF). MAF/MMD transcripts were only detected in BV-2 and NIH3T3 cells (Tang et al., 2005). A more sensitive quantification of mMMD expression in BV-2 was obtained by performing a quantitative

RT-PCR analysis, showing that mMMD is expressed about 5-fold lower in BV-2 than in BMM (Figure 5.9B). This differential expression correlates with the intensity of the bands shown in Figure 5.9A demonstrating the validity of the Northern blot results.

As described for the human orthologue, mMMD2 expression was not detected in any cell line mentioned above (data not shown).

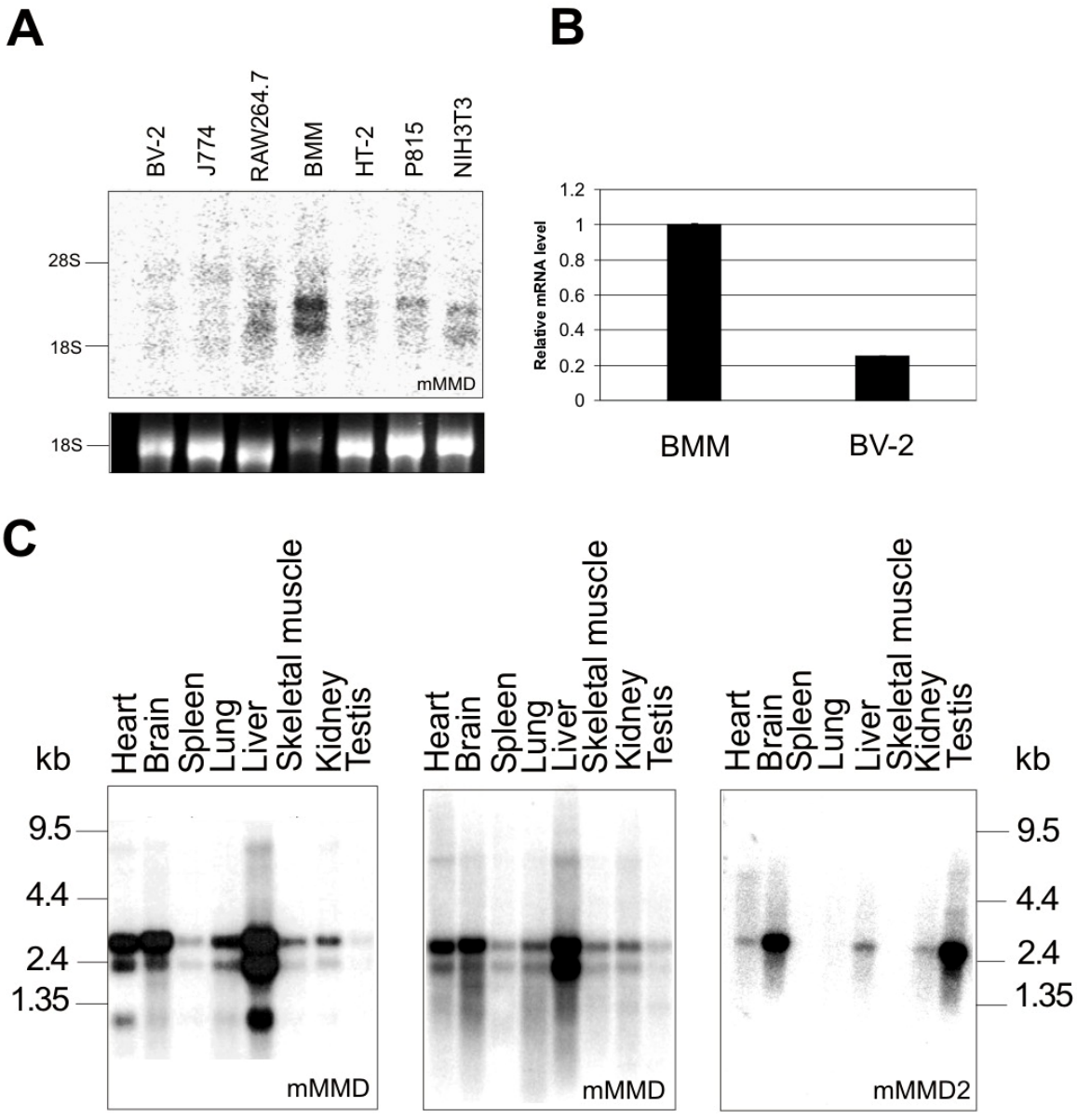

Figure 5.9 RNA expression pattern of mouse MMD and MMD2.
(A) MMD expression in mouse cell lines: total RNA (10 µg/lane) was hybridized by a probe positioned at the 3'-UTR region of mouse MMD. The positions of the 28S (5025 bp) and 18S (1868 bp) rRNA bands are indicated. The bottom inset shows the ethidium bromide-stained 18S rRNA bands before blotting. (B) Quantitative RT-PCR analysis of mMMD expression on cDNA prepared from mouse BMM and BV-2 cells. The results were normalized to HPRT expression and represent mean values ±SD of two independent qRT-PCR analyses. (C) MMD and MMD2 expression in MTN blots hybridized with a mMMD probe generated from the 5'-coding region (first panel, left), or with a probe generated from the 3'-UTR of mouse MMD (middle panel) and MMD2 (right panel) cDNA.

5.2.3. Regulation of mMMD in bone marrow macrophages

Macrophages respond to microenvironment stimuli by different activation phenotypes (see section 1.1.3). To investigate, mouse bone marrow macrophages were treated with LPS (1 µg/ml media). Afterwards, cells were harvested and total RNA was isolated at the indicated time points (30 min-25 h), reverse transcribed, and the cDNA was analysed by quantitative real time PCR (qRT-PCR) for mMMD expression.

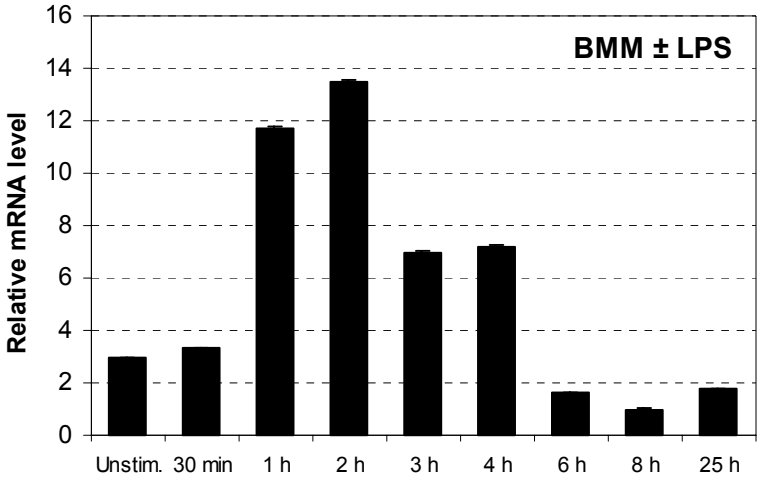

Figure 5.10 Inducible mMMD expression in BMM after LPS stimulation.
Quantitative RT-PCR analysis of mMMD expression in cDNA prepared from mouse BMM, unstimulated or stimulated with LPS (1 µg/ml media). Results were normalized to HPRT expression, and represent mean values ±SD of two independent qRT-PCR experiments.

LPS drives the innate activation of mouse macrophages mainly through TLR4 signaling (see section 1.1.3). Interestingly, mMMD transcript expression was rapidly upregulated about 7-fold after 2 h incubation with LPS. This effect was followed by a fast downregulation, reaching the lowest expression level after 8 h incubation (Figure 5.10).

While in vitro incubation of mouse BMM with INFγ influences their classical activation, incubation with IL-4 drives the development of an alternative activation phenotype (see section 1.1.3). On the other hand, the cytokine IL-10 was reported to deactivate macrophages, resulting in an anti-inflammatory phenotype different from the alternative activation.
To find out if mMMD is involved in the development of one of these macrophage subsets, isolated mouse BMM were treated with INFγ ($10x10^3$ U/ml media), IL-4 (10 ng/ml media) or IL-10 (20 ng/ml media) for 4 h. Aterwards, cells were harvested and total RNA was prepared, reverse transcribed and used for qRT-PCR analysis.

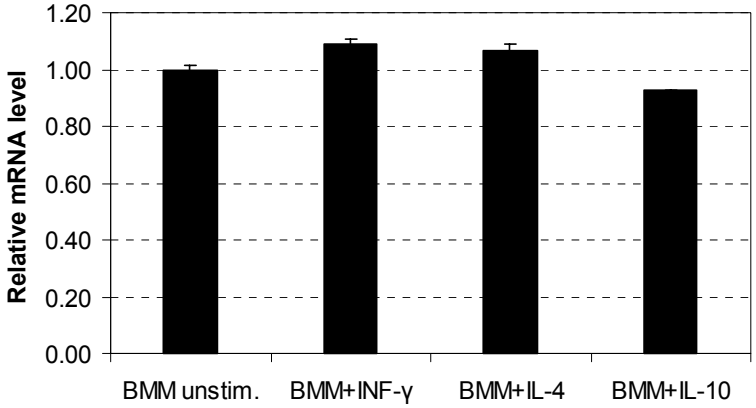

Figure 5.11 Influence of INFγ , IL-4 and IL-10 on mMMD expression in mouse BMM.
Quantitative RT-PCR analysis of mMMD expression in cDNA prepared from mouse BMM, untreated or treated for 4 h with INFγ, IL-4 or IL-10. Results were normalized to HPRT expression, and represent mean values ±SD of two independent qRT-PCR experiments.

Figure 5.11 shows that mMMD expression was not regulated by any of these cytokines, suggesting that it is neither involved in the classical or alternative activation of mouse BMM, nor in their deactivation process.

5.3. Characterization of mouse MMD

5.3.1. Mouse MMD protein expression analysis

5.3.1.1. Attempts to generate a monoclonal mMMD antibody

To investigate mMMD at the protein level, it was crucial to have an antibody targeting the protein specifically. However, it turned out to be difficult to find an appropriate peptide sequence that is specific for mMMD and capable to immunize a mammalian.

In animals like rabbit and goat, mMMD protein sequences are well conserved, and most likely not antigenic. Until recently, the lowest degree of conservation was found in the chicken orthologue before the C-terminal region of the protein was correctly sequenced. Speculating that a mMMD peptide may succeed in elucidating an immune response in chicken, the C-terminal region, KYLYRSPTDFIRHL, was chosen.

This peptide was conjugated to KLH (a highly antigenic peptide) at Davids Biotechnologie GmbH (Regensburg, Germany) and injected in chicken for immunization. Later IgG antibodies specific for this peptide were collected from egg yolks and affinity purified.

Mouse MMD specific anti-sera were tested in Western blot analyses for the detection of the endogenous protein in NIH3T3 and RAW264.7 cell lines (where the transcript was previously

detected, Figure 5.9A) and for the detection of the overexpressed, tagged protein in NIH3T3 cells (see section 5.3.2). Unfortunately, the polyclonal chicken antibody detected no mMMD protein in none of these cell lines. Recently the correct sequence of the chicken orthologue was published in the database and the C-terminal region turned out to be conserved between mouse and chicken, explaining the unsuccessful antibody production.
Because a specific antibody is an indispensable tool for investigating a proteins localization, the epitope-tagging approach was followed.

5.3.1.2. Expression of epitope-tagged mMMD protein

Epitope tagging was first described in 1984 (Munro & Pelham, 1984), and consists of fusing the protein of interest with a short peptide sequence (tag), against which an antibody exists already. Many tags are commercially available in combination with their validated antibody. Small epitopes were chosen to tag mMMD (Table 5.2), because large tags possibly interfere with the normal folding and function of the protein, thus influencing its cellular expression and localization.

Table 5.2 Epitopes used to tag MMD.

Epitope name	Size	Sequence	Antibody
3xFLAG	18 aa	3x (DYKDDDDK)	Mouse M2-anti-Flag
HA	9 aa	YPYDVPDYA	Rat anti-HA
c-myc	10 aa	EQKLISEEDL	Mouse anti-c-myc

5.3.1.3. Generation and transfection of MMD-3xFLAG construct

To tag mMMD C-terminally with 3xFLAG, it was taken advantage of the pIRES-hrGFP-1a expression vector purchased from Stratagene. This vector contains an Internal Ribosomal Entry Site (IRES) sequence which allows a simultaneous translation of two independent proteins from a single transcript under the control of one promoter. Mouse MMD cDNA was cloned into the multiple cloning site (MCS) of the vector in frame with a FLAG-tag upstream of the IRES sequence. The GFP cassette provided in the vector is located downstream (see section 4.1.3.11). In order to investigate mMMD expression in mouse macrophages, pIRES-MMD-3xFLAG was used to transiently transfect a mouse macrophage cell line, RAW264.7. A successful transfection was controlled by monitoring green cells under a fluorescence microscope and by checking the protein expression by Western blot analysis. Unfortunately, transient mMMD expression in RAW264.7 was not detected. This may be due

to a non-tolerance of these cells for an ectopic expression of mMMD. This idea was later confirmed by unsuccessful attempts to generate a cell line stably overexpressing mMMD by using a retroviral system (see section 5.3.2).

In contrast, NIH3T3, a mouse embryonic fibroblast cell line, expressed the tagged mMMD very efficiently. Although it has a non-myeloid origin, it was shown that it expresses endogenously mMMD (Figure 5.9A), suggesting that it may be an apropriate cell system to characterize the protein. After successful expression of 3xFLAG-tagged MMD in NIH3T3 cell line, eight different constructs were generated with three types of epitopes inserted at different locations in various combinations (see section 4.1.3.11). They were used to investigate the cellular localization of the protein independently from the insertion location of the tag. A summary of the generated tagged MMD variants is shown in Figure 5.12.

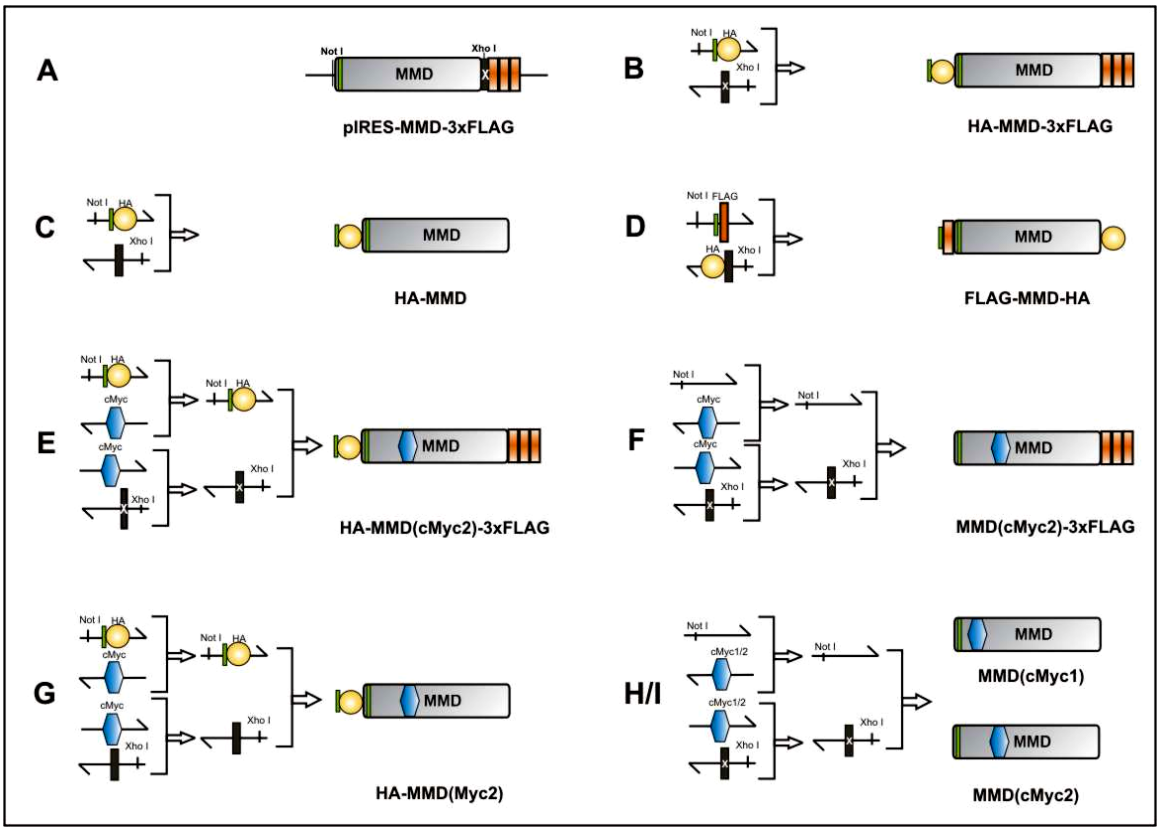

Figure 5.12 Scheme for cloning tagged MMD constructs into pIRES-hrGFP-1a vector.
Tagged MMD constructs were generated by PCR amplification using pIRES-MMD-3xFLAG as template (A). HA- (yellow circle) and FLAG- (orange rectangle) tags were introduced N- or C-terminally of MMD by PCR. c-Myc tag (blue hexagon) was incorporated either in the first (H) or the second extramembrane loop (E-G, I) by site specific mutagenesis in a three steps cloning. The stop codon (black rectangle) of MMD ORF was either mutated (white cross) to allow the translation of the downstream FLAG-tag, or inserted with the primer to prevent expression of the C-terminal tag. The ATG start codon (green rectangle) was introduced within the tag sequence at the N-terminus (B-E and G).

5.3.1.4. Expression analysis of tagged mMMD by Western blot

All tagged MMD constructs were transiently transfected in the NIH3T3 cell line using Effecten™ or Lipofectamine 2000™ following the protocols described in section 4.4.1. To monitor the expression of the tagged protein, membrane homogenates were prepared two days after transfection and analysed by Western blot analysis using specific antibodies for each tag (Table 4.5). It was noticed that whole protein lysates tended to smear in the gel, making the specific detection of defined MMD bands difficult. By preparing a membrane lysate, the genomic DNA contamination as well as the background signal was reduced.

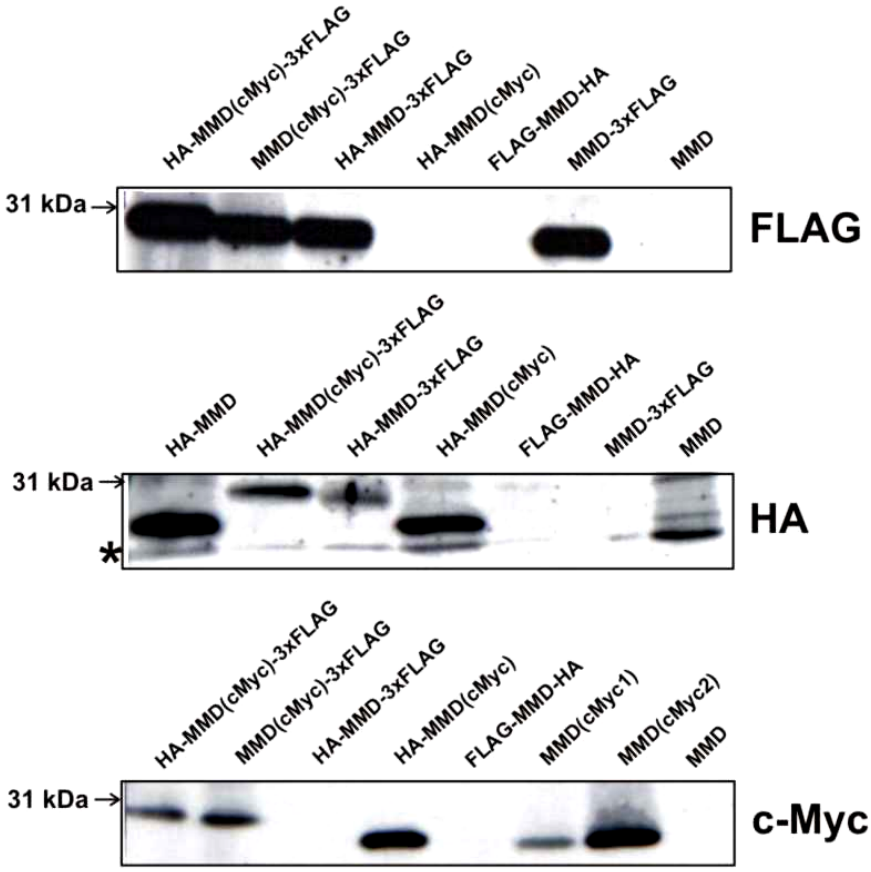

Figure 5.13 Western blot analysis showing expression of tagged MMD in NIH3T3 cell line.
Membrane cell lysats of transiently transfected NIH3T3 cell line with various tag constructs were separated by SDS gel electrophoresis and blotted. Detection of tagged-MMD protein was done using mouse anti-FLAG antibody (upper pannel), rat anti-HA antibody (middle pannel) and mouse anti-cMyc antibody (last pannel). The asterisk marks an unspecific band.

Figure 5.13 shows that almost all of the tagged constructs were expressed. As expected, the apparent molecular weight of mMMD proteins corresponds to the calculated weight of wild type MMD (28 kDa) plus the molecular weight of the incorporated tags (3xFLAG: 2.8 kDa; HA: 1.1 kDa; and c-Myc: 1.2 kDa). Furthermore, it was shown that introducing tags at the N-

or C-terminus, in the first or the second extramembrane loop of MMD, or in different combinations did not influence its expression in NIH3T3 cells.

However, when a single FLAG was incorporated at the N-terminus and an HA-tag at the C-terminus of MMD, none of these tags were detected (Figure 5.13, lane 7). This result was confirmed by immunocytochemistry (see section 5.3.1.5), suggesting that the presence of these tags in this order impaired mMMD expression.

5.3.1.5. Subcellular localization of tagged MMD in NIH3T3

Since the subcellular localization of mMMD was unknown, NIH3T3 cells transfected with tagged MMD constructs were subjected to immunostaining following the protocol described in section 4.4.1. Cells were seeded in chamber slides and transfected with the tagged constructs (see section 4.4.1). After two days, they were fixed with 2% PFA, permeabilized with methanol/acetone (1:1) and incubated with the corresponding primary and secondary antibody (see section 4.2.5.2). The *GFP* gene downstream of the IRES sequence is expressed constitutively under the control of the CMV promoter, thus the green fluorescence staining was taken as an indicator of successful transfection. In contrast, the expression of the exogenous tagged mMMD protein, shown in red, was only detected when cells were permeabilized, indicating that mMMD is localized exclusively inside the cell with one exception (MMD(cMyc1)). The staining suggests a perinuclear and probably endoplasmic reticulum (ER) and nuclear membrane localization in NIH3T3 cells.

FLAG-MMD-HA protein was not detected by immunocytochemistry as it was also seen with Western blot analysis (Figure 5.13), independently of transfection efficiency. In fact, green cells were observed (data not shown), suggesting that the expression of this variant is not controlled on the transcription level but more likely on the translational level (see section 6.2).

When c-Myc tag was incorporated in the first extramembrane loop of mMMD a vesicular localization was observed (Figure 5.14G). The different cellular localization may indicate that this region of the protein plays a crucial role in the correct integration of MMD into the lipid bilayer and its retention in the perinuclear space.

To confirm the perinuclear localization and to eliminate any possibility of an artefact due to receptor overexpression particuliary in NIH3T3 cells, human embryonic kidney cells, HEK293T, were transfected with HA-MMD, MMD-3xFLAG, or HA-MMD-3xFLAG constructs. A similar staining was obtained suggesting that the predominant perinuclear and nuclear membrane localization is not cell-line specific (data not shown).

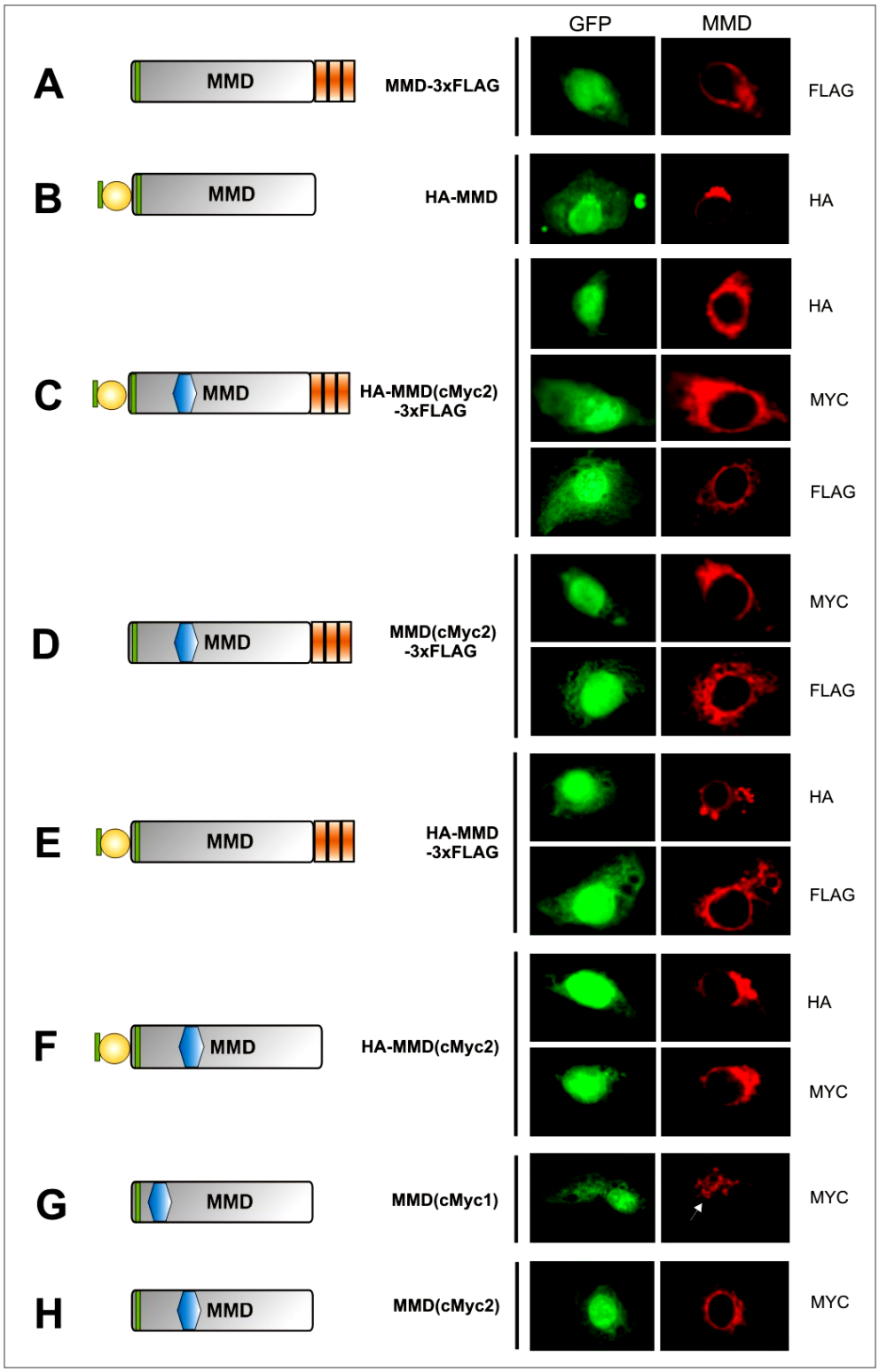

Figure 5.14 Perinuclear localization of tagged mMMD in NIH3T3 cell line.
Immunofluorescence microscopy of NIH3T3 cells transiently transfected with different tagged mMMD constructs (A-H). The GFP panel shows a diffuse staining in NIH3T3 and is a marker for transfected cells. In the MMD panel, tagged MMD protein was visualized by using mouse anti-FLAG, rat anti-HA or mouse anti-cMyc antibodies with their corresponding secondary antibodies. MMD perinuclear and membrane nuclear localization was seen with tagged MMD (A-F and H) but not in G (white arrow). No staining was observed in mock-transfected cells (data not shown) (Original magnification x400).

5.3.2. Stable overexpression of mMMD in NIH3T3 cell line

To further examine MMD localization and orientation in the membrane lipid bilayer, a NIH3T3 cell line stably overexpressing the tagged protein was generated by using a retroviral expression system. The significant advantage of stable cell lines is that once the gene of interest is transfected, it integrates into the genome of the recipient cell, leading to a constant and stable expression of the corresponding protein over many cell passages. A NIH3T3 cell line, expressing tagged mMMD stably, offers an easy model for immunocytochemistry analysis. In addition, the influence of mMMD overexpression on the cell signaling may be studied.

5.3.2.1. Stable expression of tagged mMMD in NIH3T3 cell line

The expression and the packaging plasmids (see section 4.4.2.1) were introduced into HEK293T cells as described in section 4.4.2.2. The IRES sequence in pQCXIP vector allows the generation of a single mRNA containing tagged MMD and puromycin resistance transcripts. Produced viral particles from HEK293T cells were harvested and used to transduce the NIH3T3 target cell line four times. After selection, pyromycin resistant cells, were expanded and used for further experiments. The retroviral transduction efficiency was controlled by transfecting HEK293T separately with a control vector pQCXIP-EYFP, containing an Enhanced Yellow Fluorescence Protein gene (EYFP). Transduction was monitored by fluorescence microscopy 48 h after the first infection.

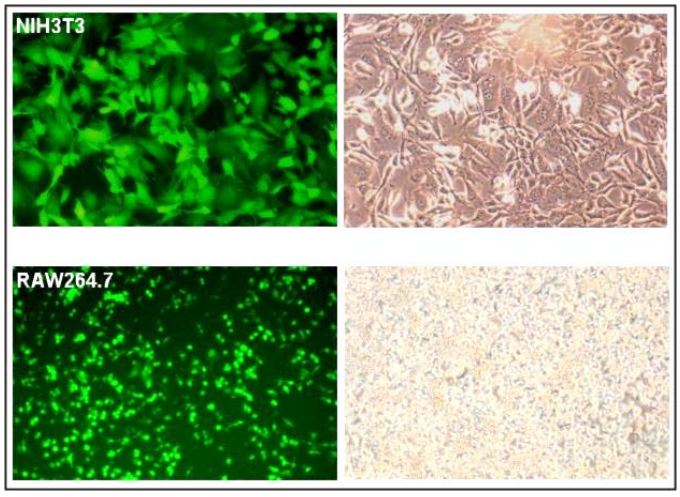

Figure 5.15 NIH3T3 and RAW264.7 cell lines transfected with pQCXIP-EYFP control vector using the retroviral system.
NIH3T3 (first row) and RAW264.7 (second row) transduction using a retroviral transfection system. Expression of EYFP protein was visualized by fluorescence microscopy, and indicated the high transduction efficiency for the target cell lines.

A high transduction efficiency of NIH3T3 and RAW264.7 cell lines was achieved (Figure 5.15), however tagged MMD expression was not detected in RAW264.7. In fact after puromycin selection the majority of the target cells died and the transduction of a mouse microglia cell line (BV-2) was unsuccessful as well (data not shown).
Taken together, this result suggests that mMMD overexpression in RAW264.7 and in BV-2 may be toxic for the cells, driving them into apoptosis or to silence the gene expression. Consequently, NIH3T3 cell line was chosen as an overexpression model for mMMD.

The stable expression of tagged mMMD in NIH3T3 cell lines was confirmed by Western blot analysis. NIH3T3 cells transduced with an empty pQCXIP vector served as a negative control cell line (Figure 5.16). The molecular weight of tagged proteins matched the one shown in section 5.3.1.4, indicating that the tagged protein was properly translated.

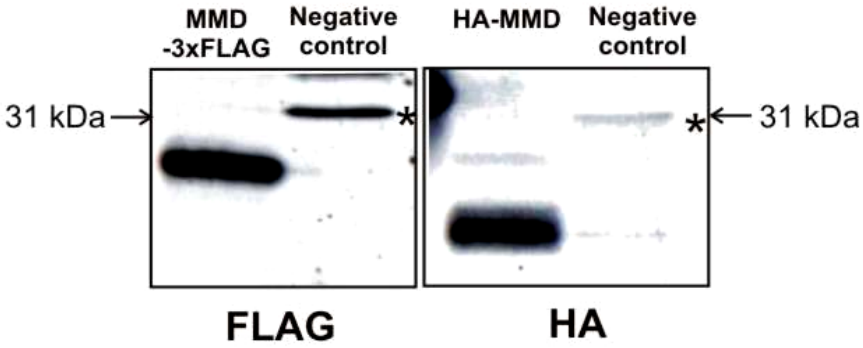

Figure 5.16 Western blot analysis showing stable tagged MMD expression in NIH3T3 cell line. Membrane lysates from NIH3T3 cells were assessed for stable expression of the tagged MMD protein. As a negative control, a cell line transduced with an empty vector was used. Detection of MMD protein in HA-MMD cells was done by using a rat anti-HA antibody (right panel), and in MMD-3xFLAG with a mouse anti-FLAG antibody (left panel). The asterisks mark an unspecific band.

Expression of tagged MMD in the stably transfected NIH3T3 cell lines was quantified on RNA level by qRT-PCR. Figure 5.17 shows about 20-fold MMD-3xFLAG and 10-fold HA-MMD transcript overexpression compared with the endogenously expressed MMD in the negative control cell line. The difference between HA- and FLAG-tagged transcript abundance may depend on a lower amount of cells expressing stably HA-MMD.

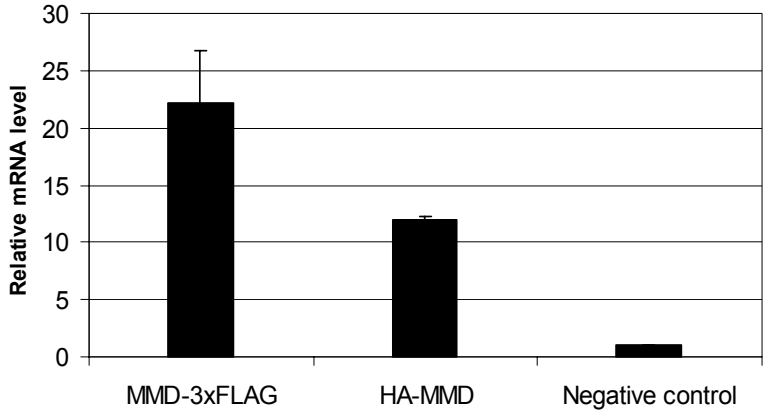

Figure 5.17 Quantitative RT-PCR analysis of tagged mMMD expression in NIH3T3 cells.
For qRT-PCR analysis, cDNA was prepared from NIH3T3 cell lines stably expressing HA-MMD or MMD-3xFLAG. The negative control cell line was generated by using the empty pQCXIP vector for transduction. Results were normalized to HPRT expression, and represent mean values ±SD of two independent qRT-PCR experiments.

5.3.3. MMD cellular localization in NIH3T3 cell line

5.3.3.1. Perinuclear localization of mMMD in NIH3T3 cells

To study mMMD cellular localization in stably transfected NIH3T3 cell lines, immunocytochemistry was performed on cells seeded on chamber slides. Again a perinuclear staining of tagged-MMD was observed (Figure 5.18A and I), which correlates with the localization described in transiently transfected cells (Figure 5.14).

Recently, Bräuer et al. reported that rat MMD protein was associated with the lysosomal associated membrane protein (LAMP)-1 in COS-7 and BV-2 cell lines (Brauer et al., 2004). To assess whether HA-MMD and MMD-3xFLAG proteins were also located in lysosomes, tagged mMMD was compared to the lysosomal marker LAMP-1.

Cell lines expressing tagged MMD were incubated with anti-FLAG and anti-HA antibodies and visualized with Alexa Fluor (red fluorescence) coupled secondary antibodies. Lysosomes were visualized using a monoclonal FITC-conjugated anti-LAMP-1 (CD107) antibody (Figure 5.18, panels B, F, J and N). Surprisingly, no lysosomal colocalization was observed with either tagged-MMD proteins (panels D and L). Staining of MMD was mainly confined at the nuclear envelope and at the reticulate network. Additional control stainings may be required to determine the exact localization of MMD, such as a costaining with specific nulear membrane and endoplasmic reticulum markers.

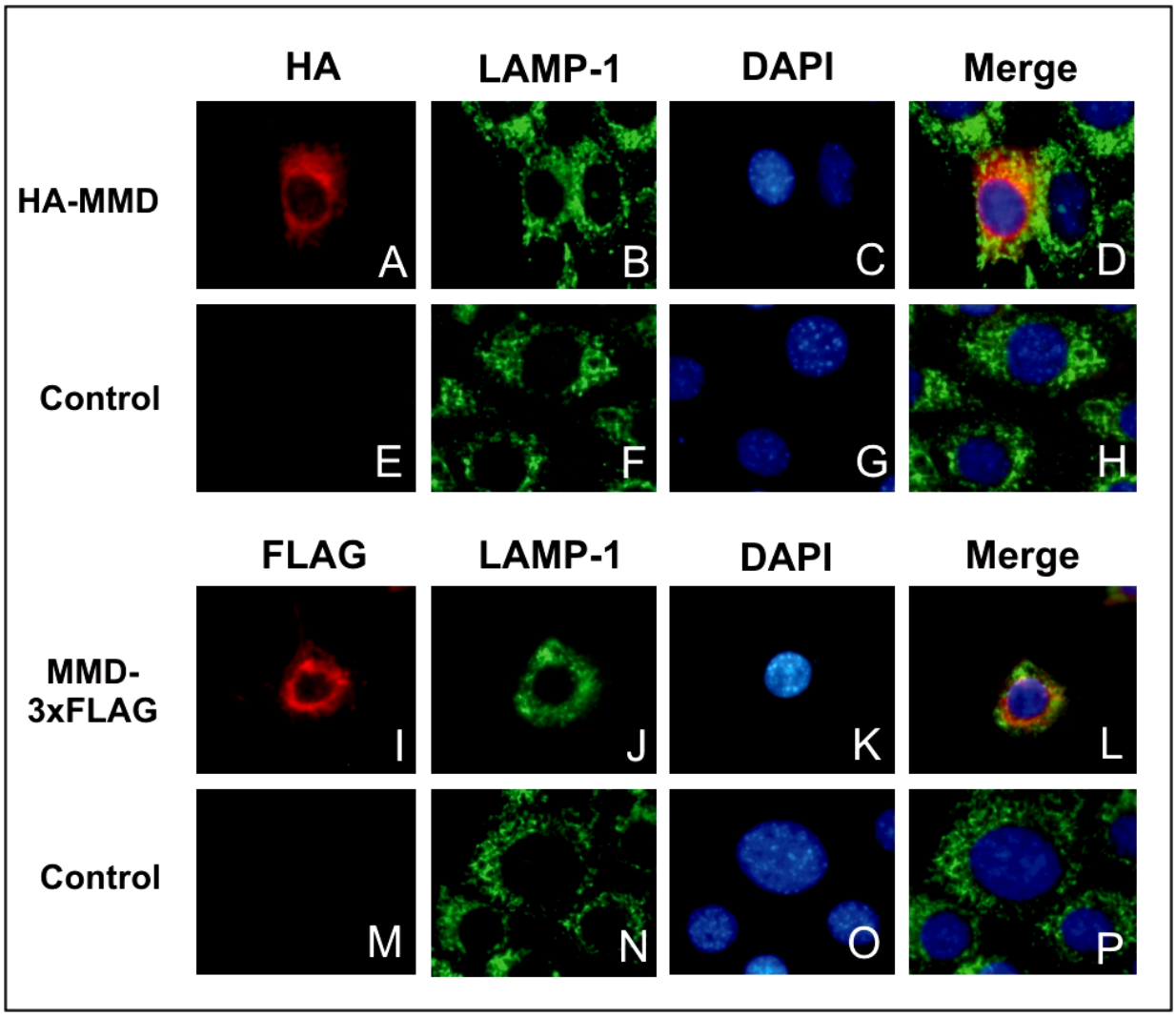

Figure 5.18 Perinuclear localization of stably expressed tagged MMD in NIH3T3 cell lines. Immunofluorescence microscopy of NIH3T3 cells stably expressing tagged MMD, seeded on chamber slides and processed for immunocytochemistry 24 h later. (A) and (I) depict NIH3T3 cell lines expressing HA-MMD and MMD-3xFLAG visualized with rat anti-HA and mouse anti-FLAG antibodies, respectively. A perinuclear staining is seen. (E) and (M) show the corresponding negative controls where NIH3T3 is transduced with the empty pQCXIP vector and thus does not express any tagged version of mMMD. Lysosomes were visualized using the anti-LAMP-1 antibody (green, B, F, J and N). The nuclei were counterstained with DAPI in blue (C, G, K and O). The last panel represents a merge of all staining, accentuating the absence of a colocalization of tagged MMD with LAMP-1 (D and L) (Original magnification x400).

5.3.3.2. Mouse MMD orientation in the lipid bilayer

Based on Kyte and Doolittle plot (Figure 5.4), it was predicted that mMMD contains a seven transmembrane domain (7TM) featuring a N-terminal tail of 28 amino acids and a smaller C-terminal domain of 19 amino acids (Figure 5.3). So far, the localization of mMMD in the lipid bilayer had not been determined. Studying the orientation of mMMD in the membrane may allow the localization of binding sites and to determine the orientation of active site

residues, relative to the membrane. This information may in turn suggest possible functions and reaction mechanisms.

To determine mMMD orientation, we took advantage of the digitonin detergent. If used at low concentrations, it permeabilizes specifically the plasma membrane leaving the nuclear membrane intact (Adam et al., 1990). The nuclear envelope is composed of two lipid bilayers, the outer nuclear membrane, which is continuous with the endoplasmic reticulum (ER) and the inner nuclear membrane. Thus by digitonin permeabilization, the entry of antibodies only to the cytoplasm and not to the nucleoplasm should allow the identification of cytoplasmic and outer nuclear membrane components.

For this purpose, immunocytochemistry was performed with NIH3T3 cell lines, stably expressing HA-MMD and MMD-3xFLAG, as described in sections 4.2.5. Briefly, one day after seeding on gelatin coated chamber slides, cells were fixed on ice with 2% PFA. Afterwards, they were either incubated on ice with acetone/methanol (1:1), or with 0.003% digitonin for different times to optimize the permeabilization conditions. Cells were then labeled with either mouse anti-FLAG or rat anti-HA. In addition, the nucleus was counterstained with DAPI.

Whereas Figure 5.19F revealed a perinuclear and nuclear membrane localization of HA-MMD after digitonin permeabilization, FLAG-MMD was only detected after methanol/acetone permeabilization (panel G and I) of the cells. These findings suggest that the N-terminal region of mMMD probably faces the cytoplasm whereas the external C-terminal tail is directed into the lumen of the ER or the inner nuclear membrane (INM).

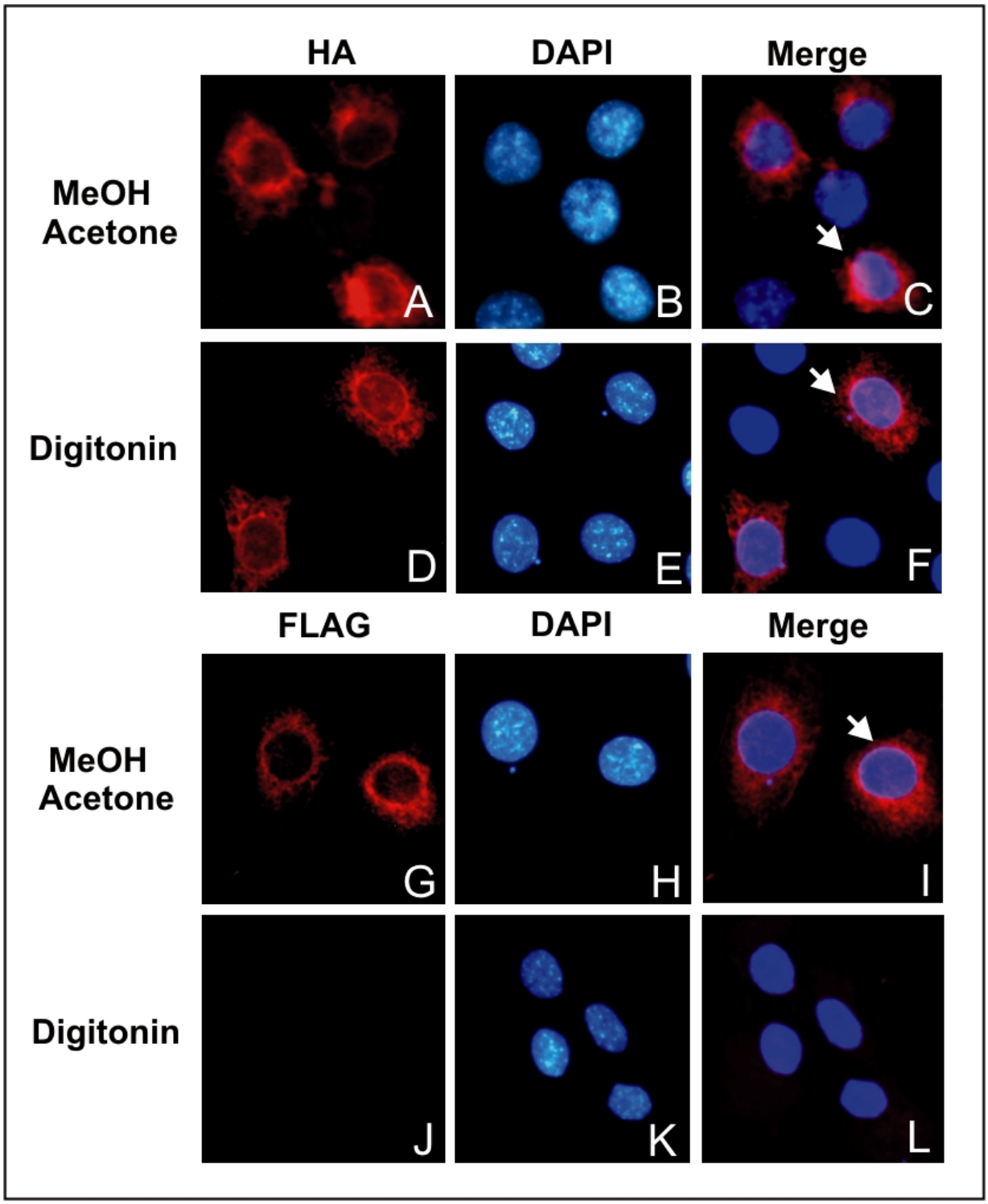

Figure 5.19 Orientation of stably expressed tagged MMD in NIH3T3 cell lines.
Immunofluorescence microscopy of NIH3T3 cells expressing stably tagged MMD. Cells were seeded on chamber slides, and after 24 h permeabilized either with acetone/methanol (panels A-C and G-I) or with 0.003% digitonin (panels D-F and J-L) before proceeding with immunostaining. Panels A-F represent cells expressing HA-MMD stained with rat anti-HA antibody (red, A and D). Panels G-L depict cells expressing MMD-3xFLAG stained with mouse anti-FLAG antibody (red, G and J). Nuclei were counterstained with DAPI (panels B, E, H, and K). HA-tag was always detected (panels C and F), whereas FLAG-tag was only stained after complete permeabilization of the cells (panels I) (Original magnification x400).

5.4. Generation of MMD knock-out ES cells

5.4.1. Gene targeting strategy

Since little is known about *mMMD* and its protein function, we followed a gene targeting approach to study *mMMD* function.

Gene targeting has become a powerful tool in the field of mouse genetics, and allows to inactivate a gene of interest at the genetic level in order to investigate its function in the context of the whole animal. Homologous recombination in mouse embryonic stem (ES) cells is the key of this concept. An artificial targeting construct, containing selectable markers surrounded by two regions of homology to the targeted locus, is electroporated into mouse ES cells. In a fraction of those cells, which were successfully transfected with the targeting construct, homologous recombination takes place at the regions of homology between the construct and the ES cells-genomic DNA. This event leads to the replacement of the intact fragment of the gene with a selectable cassette. When ES cells with the disrupted gene are injected into blastocysts, they can colonize all tissues of the future embryo including the germ line, thus giving birth to chimeras. Further breeding of chimeras may lead to homozygote knock-out mice bearing the targeted gene.

Unfortunately, in ES cells, random integration of the targeting construct happens to be the rule and not the exception. The specific integration of the vector via homologous recombination is a rare event. To be able to distinguish between homologous and non-homologous recombination, strategies are employed helping selecting positive clones. Besides the design of the targeting vector, many other factors influence the efficiency of the homologous recombination and were taken into consideration in the following section.

5.4.2. Generation of the gene targeting vectors

In the course of this work, five replacement vectors (Thomas et al., 1992), including the following elements, were designed to target MMD gene in mouse ES cells (see section 4.5.1).

- *Arms of homology*

A short and a long arm were selected on both sides of the genomic region, that should be replaced by selection markers during homologous recombination. In this work, arms of homology were generated by PCR from isogenic DNA because sequence mismatches

between the homologous arms of the vector and the target locus can reduce the efficiency of the homologous recombination (te et al., 1992).

- *GFP reporter gene*

A *GFP* reporter gene (1 kb) was cloned in frame with the ORF of *mMMD*, downstream of the left homologous arm, which contains the first ATG start codon. After successful insertion of the targeting vector into the genome of ES cells, GFP expression can be driven by the endogenous promoter of *mMMD*. This approach is also called "knock-in" and can allow the spatial and temporal tracking of *mMMD* expression in adult mice.

- *Positive selection marker*

For positive selection, a "Neo^R" cassette (2 kb) was subcloned out of a pBS vector (kindly provided by Prof. Dr. Klaus Pfeffer, Institut of Medical Microbiology, Düsseldorf, Germany). The neomycin resistance gene (*neo^r*) encodes the neomycin phosphotransferase enzyme under control of the strong PGK (phoshoglycerate kinase I) promoter. Because the constitutive translation of the selection gene is independent from its insertion location, the Neo^R cassette allows selection of both cells which integrated the cassette either via random or homologous recombination. It was reported that after homologous recombination *neo^r* expression may interfere with the expression of neighboring genes (Muller, 1999), therefore two loxP sites flank the Neo^R cassette and allow its subsequent excision by using the Cre-loxP-site-specific recombinase system.

- *Negative selection marker*

As negative selection markers, the TK (thymidine kinase)-cassette (2.8 kb) in pGEM7 vector (kindly provided by Prof. Dr. Klaus Pfeffer) or the DT-ApA (Diphterie toxin A with poly(A) signal)-cassette (1.37 kb) in pBS vector (kindly provided by Yanagawa.Y (Yanagawa et al., 1999)) were used. After homologous recombination, the negative selection cassette is not inserted and thus inactivated because of its location outside of the homologous regions. But if the targeting vector integrated randomly, the negative selection cassette will be co-inserted, and consequently its gene product is expressed. The TK of Herpes Simplex virus causes premature termination of DNA synthesis in the presence of the drug Gancyclovir driving cells into apoptosis (Nagy et al., 2003). In contrast, expression of the diphteria toxin via the DT-ApA cassette leads to the toxin accumulation, which directly inhibits chain elongation in protein synthesis without addition of drugs (Nagy et al., 2003; Yanagawa et al., 1999).

➢ *A linearization site*

In order to increase the integration efficiency of the targeting vector into the ES cell genome, the vector is linearized prior to electroporation. A NotI restriction site was chosen to linearize each targeting vector described below, because it does not cut within the whole *mMMD* locus, nor within the selection cassettes or reporter gene.

Once generated, the targeting construct was transfected into ES cells via electroporation. Homologous recombination leads to the "replacement" of the genomic region of the gene of interest with the elements located between the homologous arms of the vector. In order to disrupt the function of this gene, exons should be removed which have drastic consequences on the ORF, generating a null allele. As described in section 5.1.1, *mMMD* has 7 exons with the starting ATG codon located in exon I. In most MMD targeting constructs, (see section 4.5.1) the *GFP* reporter gene and the Neo^R cassette were inserted into the middle of exon II to ablate the intron-exon transition (Table 5.3) and thereby the transcription of *mMMD*. The targeting construct IV was the exception, where the genomic region between exons V and VI was targeted.

Table 5.3 Intron-exon boundaries in the mouse MMD.

Exon	Size (bp)	5'-splice donor	Intron (bp)	3'-splice acceptor	Amino acid interrupted
I	231	GATTCCAGCG**gt**gagagttc-	7784	-gtctccac**ag**TTTCATGAAC	Gln-Ar/g-Phe
II	82	CACACACGCA**gt**gagtacaa-	2225	-ttcctccc**ag**TTCCTCATTG	Ala-/-Phe
III	161	GCCACTTGAG**gt**atagtggg-	4515	-cccccaac**ag**AACAGTGGAG	Leu-Ar/g-Thr
IV	75	ACGCCCCATG**gt**aagatagc-	1467	-gcatctat**ag**GTTAAATCTC	Pro-Tr/p-Leu
V	102	ACCATGAAAA**gt**aagagaaa-	1365	-gtccctac**ag**GTATAAAGTG	Glu-Ly/s-tyr
VI	70	GACATCAATG**gt**gagacgtg	9082	-ctgttgac**ag**AATAACACTG	Met-/-Asn
VII	1915				-

To identify false positive Neo^R clones, which integrated the vector at random positions, the genomic DNA of every single clone was isolated, digested with an appropriate enzyme and analysed by Southern blot. Two specific external probes, 5' (of the left arm) and 3'(of the right arm), positioned outside of the homologous arms, were designed for each vector. In addition it was necessary to identify a restriction site cutting the genomic DNA outside of these homologous region and thereby giving differential band patterns after targeting.

5.4.3. ES cells transfection and screening

Generated targeting constructs were transfected into ES cells following the procedure summarized in Figure 5.20. To improve the electroporation efficiency, various protocols were followed and are described below. Results are represented in Table 5.4.

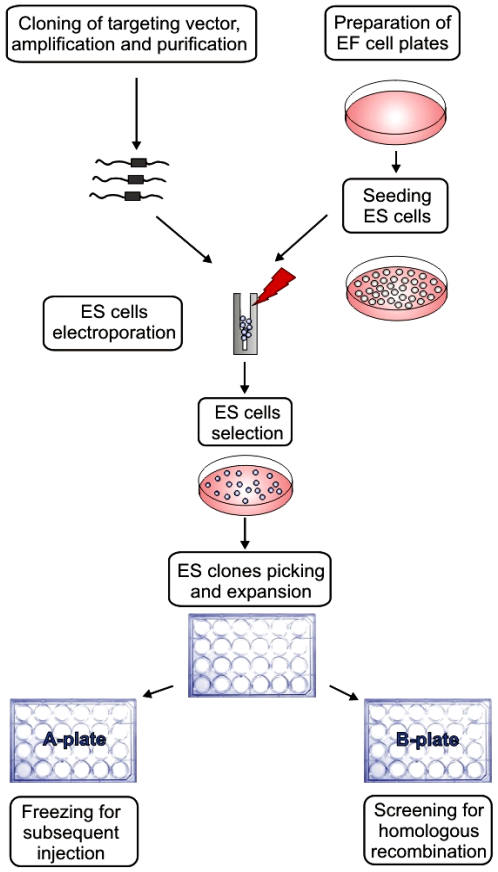

Figure 5.20 Different stages of ES cells transfection and screening.
Generated targeting construct was linearized and electroporated into ES cells, which were previously expanded on EF plates. After electroporation and selection (positive and negative selection), ES cell clones were picked into 24-well plates and expanded. Once ES cells reached confluency, they were split into an A-plate (planned for freezing) and a B-plate (used for screening).

5.4.3.1. Transfection and screening of targeting construct I

The cloning procedure of targeting construct I, TOPO-[KA-GFP-Neo-LA]-TK, was described in section 4.5.1.1, and its map is schematically depicted in Figure 5.21.

The transfection of targeting construct I into ES cells was performed as follows (Prof. Dr. Thomas Hehlgans, Institut of Immunology Regensburg, personal communication): ES cells (kindly provided by Prof. Dr. Klaus Pfeffer) were seeded on a monolayer culture of EF cells. EF CD1 cells were kindly provided by the lab of Prof. Dr. Thomas Hehlgans, and

were expanded for three weeks. Prior to electroporation, their mitosis was inactivated by incubation with Mitomycin C.

The electroporation of 20 µg linearized DNA into $5x10^6$ ES cells/cuvette was performed with Biorad electroporator (340 V, 250 µF, constant time between 5.2 and 6.4 ms). After 10 days selection (with Neomycin and Gancyclovir), 200 ES clones were picked and cultured for two weeks in ES cell medium without any selection pressure. Afterwards, ES cells plates were frozen and genomic DNA was phenol/chloroform extracted from each clone separately (see section 4.5.7.1). The screening of ES clones was performed by using a 5' and 3' DIG-labeled Southern probe. From 200 clones, only one was screened positive for homologous recombination. Unfortunately, because the whole procedure was very much time consuming (3 months), the corresponding cryo-conserved ES clone did not survive after thawing the A-plate.

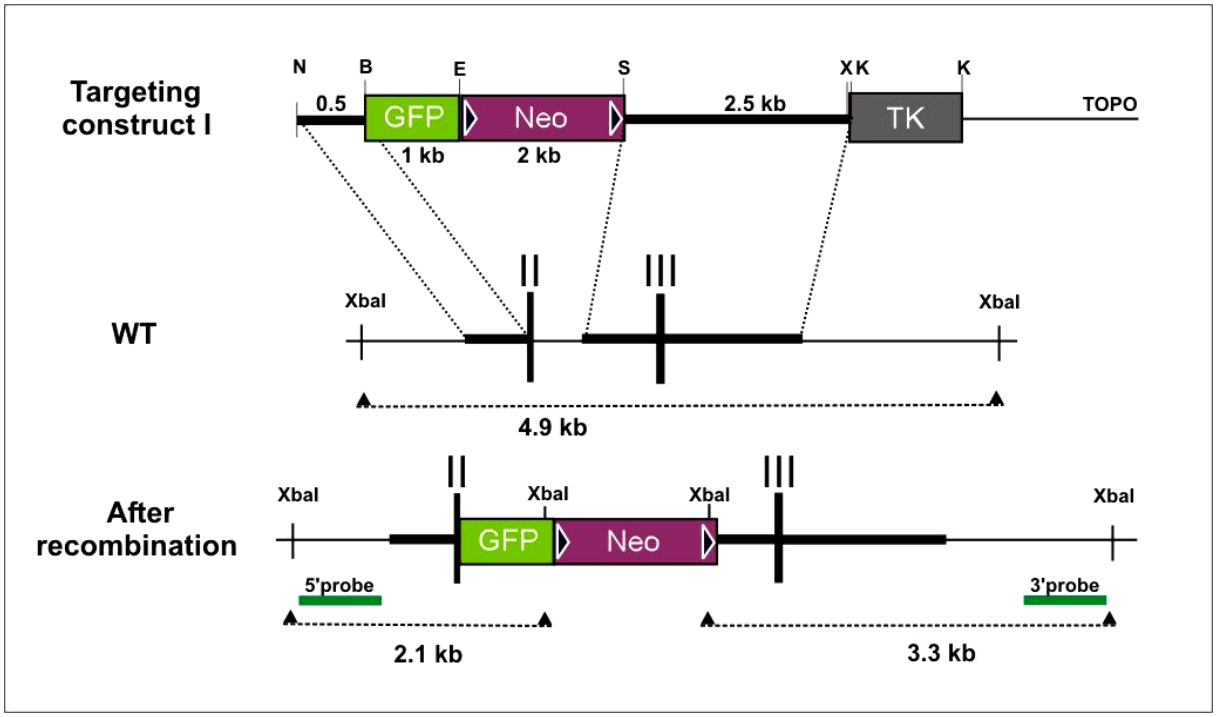

Figure 5.21 Schematic representation of MMD targeting construct I.
TOPO[KA-GFP-Neo-LA]-TK targeting vector contains a reporter cassette (GFP, in green) and a positive selection cassette (Neo^R, in pink) with loxP sites (black arrows). Both cassettes are flanked by a homologous short (0.5 kb) and long (2.5 kb) arms displayed as bold lines also on the endogenous locus. A negative selection cassette (TK, in grey) was inserted outside the homologous regions. After homologous recombination (dotted lines), part of exon II and the following intron (regular line) were replaced with Neo^R and GFP cassettes to generate the targeted locus. Southern blot analysis was performed after digestion of the genomic DNA with XbaI restriction enzyme. Detection followed by using a 5' and 3' probes (green lines). The expected size of the WT band is 4.9 kb and after recombination the 5'probe detects a 2.1 kb and the 3'probe a 3.3 kb band (dashed arrows). (B) BamHI; (E) EcoRI; (H) HindIII; (K) KpnI; (N) NotI and (S) SalI restriction sites.

5.4.3.2. Transfection and screening of targeting construct II

The recombination efficiency obtained with targeting vector I was not sufficient (Table 5.4). Possibly the length of the homology regions may have influenced the homologous recombination efficiency (Hasty et al., 1991), therefore in the second targeting construct the short 500-bp arm (KA) was replaced by a longer 4600-bp arm (see section 4.5.1.2). The map of targeting construct II is represented in Figure 5.22.

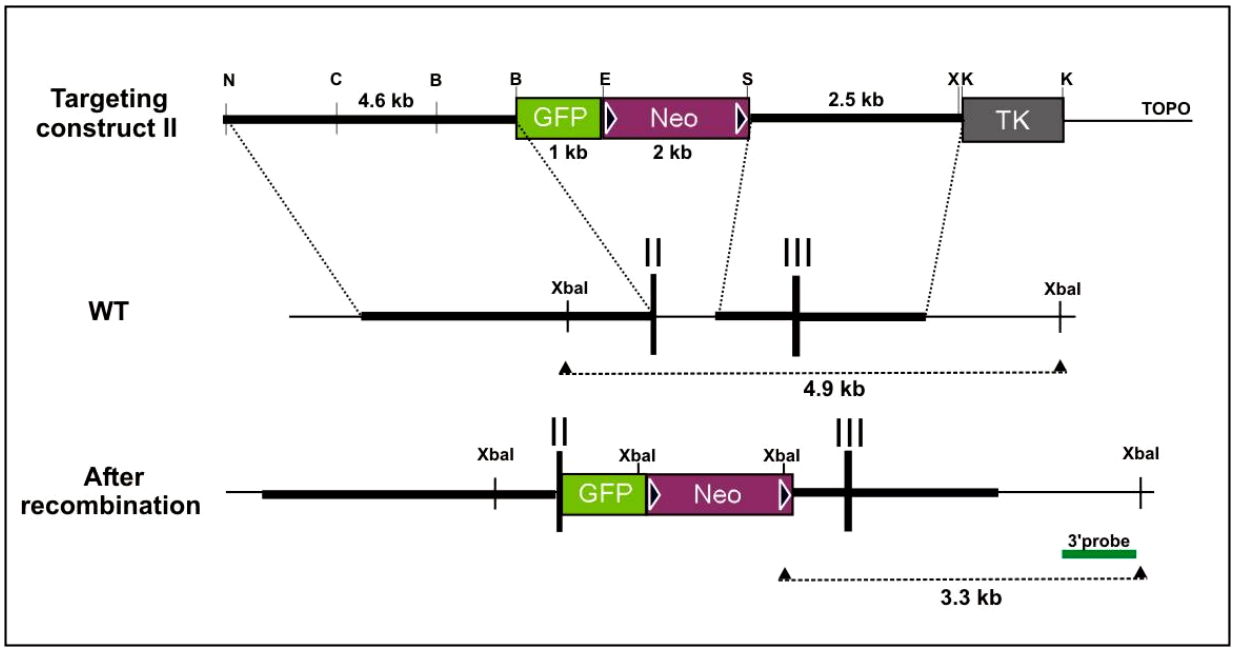

Figure 5.22 Schematic representation of MMD targeting construct II.
TOPO-[LLA-GFP-Neo-La]-TK targeting construct includes GFP, Neo and TK cassettes. The homologous regions (in bold) consist of the long (4.6 kb) and short (2.5 kb) arms. The Southern blot analysis was performed following digestion of the genomic DNA with XbaI, and screening with the 3'probe (green line). The expected WT band has the size of 4.9 kb and after homologous recombination an additional 3.3 kb band was expected. (B) BamHI; (E) EcoRI; (H) HindIII; (K) KpnI; (N) NotI and (S) SalI restriction sites.

Amplification and purification of large amounts of this construct were possible only after growing the transformed bacterial DH10B strain under non-stringent conditions (50 µg/ml ampicillin and at 32°C). Afterwards, the targeting construct II was introduced into ES cells following the protocol described in section 5.4.3.1. Additionally, an Amaxa electroporator was used to electroporate $2.5x10^6$ ES cells with 10 µg DNA following the manufacturer's instructions. Although no negative selection was done, only 60 Neo^R clones were picked and screened negative for homologous recombination. The absence of homologous recombination and a high mortality rate of the electroporated ES cells were the two main reasons to design a third targeting construct.

5.4.3.3. Transfection and screening of targeting construct III

Taking advantage from the results of previous targeting vectors, targeting construct III, pBS-[SA3-GFP-Neo-LA]-DT, was generated as described in section 4.5.1.3 (Figure 5.23).

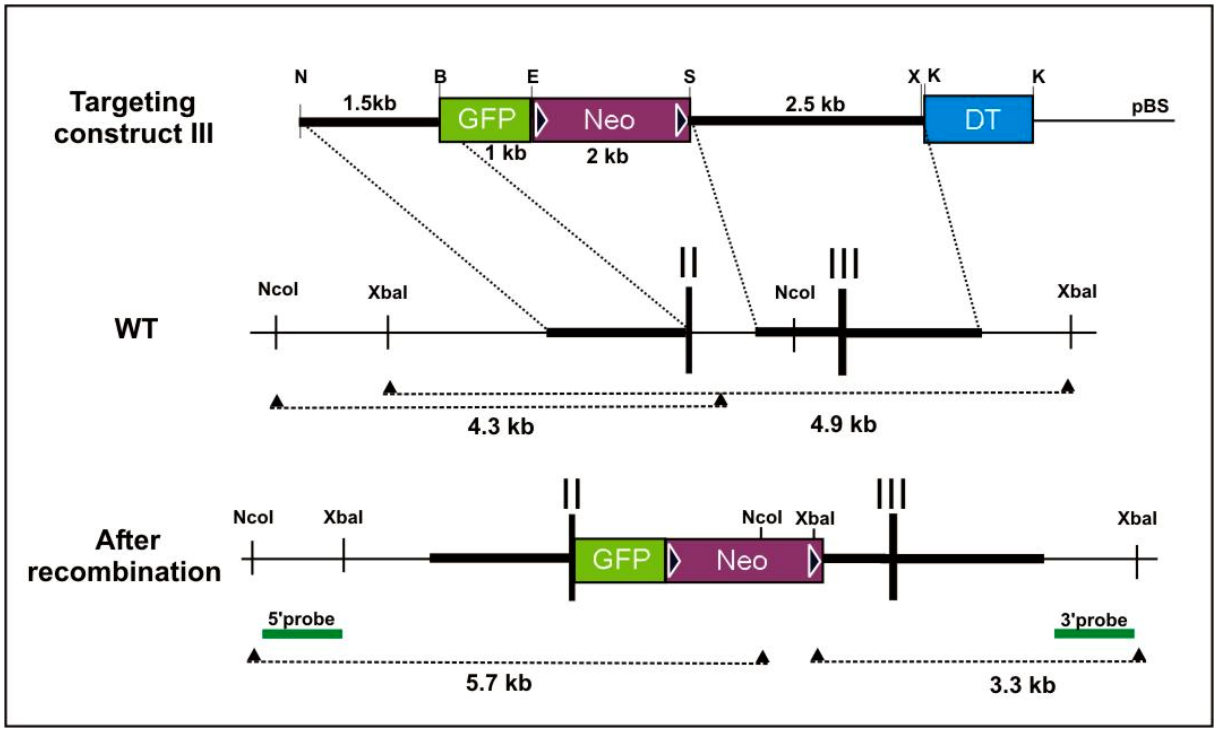

Figure 5.23 Schematic representation of MMD targeting construct III.
The pBS-[SA3-GFP-Neo-LA]-DT vector contains in addition to GFP and Neo cassette, a DT negative selection cassette (in blue). The bold lines depict the homologous short (1.5 kb) and long (2.5 kb) arms. The WT genomic DNA was digested either with NcoI or XbaI to generate a 4.3 kb or a 4.9 kb band, respectively. After homologous recombination (dotted lines), an additional band with the size of 5.7 kb by using the 5'probe, and of 3.3 kb by using the 3'probe is expected. (B) BamHI; (E) EcoRI; (H) HindIII; (K) KpnI; (N) NotI, and (S) SalI restriction sites.

pBS-[SA3-GFP-Neo-LA]-DT was electroporated into a new batch of ES cells which were kindly provided by Dr. Marina Karaghiosoff (Institut of animal breeding and genetic, Vienna, Austria). In addition, a new FCS batch was tested for these ES cells. To improve the plating and adherence of electroporated ES cells, a new batch of EF cells was prepared from inbred mice expressing the *neo*^{r} gene (see section 4.5.2.3). EFneo^r cells have the advantage to preserve the non-differentiated morphology of ES cells during their selection more efficiently. In addition, EFneo^r cells were inactivated via radiation before cryo-conservation. Whenever needed, they were thawed and directly used without expansion. In this way the targeting experiment time was reduced to at least 3 weeks.

For electroporating the targeting construct III, the Amaxa protocol described in section 5.4.3.2 was followed. Unfortunately only 29 Neo^R clones were picked from six electroporation reactions. In contrast, Biorad electroporation of 50 µg linearized DNA into $3x10^7$ ES cells (500 V, 340 µF and between 7.1 and 8.3 ms) allowed to pick 600 Neo^R clones from five electroporation reactions. Again all clones were screened negative for homologous recombination.

5.4.3.4. Transfection and screening of targeting constructs IV

Suspecting that the genomic region between exon I and II could be inappropriate for a homologous recombination event in construct IV, the short homologous arm (1.4 kb) was positioned between exons IV and V, and the long arm (4.4 kb) upstream of exon VI. Consequently, after homologous recombination exons V and VI are replaced with the Neo cassette, which disturbs the ORF of the gene. Although, the first four exons of *mMMD* will be translated, however the protein will be lacking 122 amino acids (out of 238) which may severely affect its membrane integration and therefore its functional property.

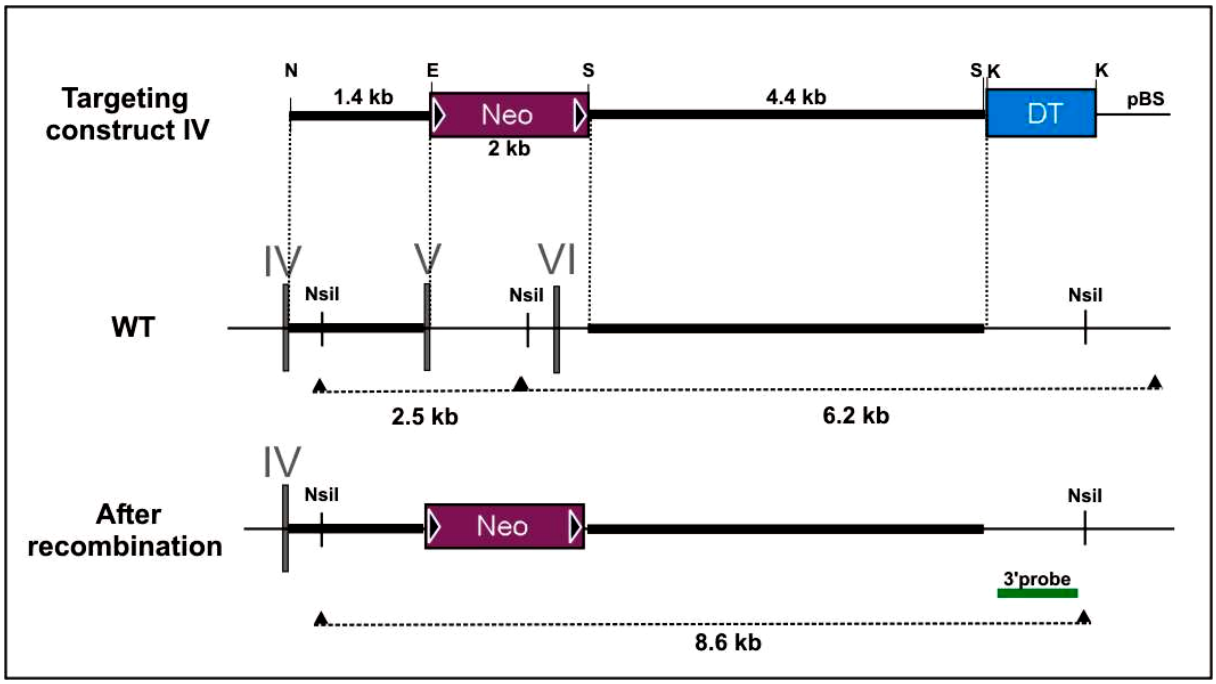

Figure 5.24 Schematic representation of the MMD targeting construct IV.
pBS-[SAex5-Neo-LAex6]-DT targeting construct contains Neo and DT cassettes. The homologous regions (in bold) consist of a short (1.4 kb) and a long (4.4 kb) arms. After homologous recombination (dotted lines), exons V and VI were replaced with the Neo cassette. A 3'southern probe (green line) was used to distinguish between a WT (6.2 kb) and knock-out (8.6 kb) band.

The targeting construct IV, pBS-[SAex5-Neo-LAex6]-DT (Figure 5.24), was cloned as described in section 4.5.1.4. It was electroporated following the instructions described in section 5.4.3.3. This led to the isolation of 551 Neo^R clones. Genomic DNA was isolated following a fast method (see section 4.5.7.1) which reduced enormously the hands-on time needed in phenol/chloroform genomic DNA extraction. The Southern blot screening was performed using radioactively labeled probes, reducing the screening procedure to 2 weeks. Again, all 551 Neo^R clones were negative for homologous recombination.

5.4.3.5. Transfection and screening of targeting vector V

The elements of targeting vector V are the same as described in Figure 5.21. However, because no enrichment of clones with a successful homologous recombination event was seen with the previously described targeting vectors, negative selection markers were omitted from construct V. This has an additional advantage, which is to reduce the size of the vector.

TOPO-[KA-GFP-Neo-LA] was chosen to electroporate ES cells because it was the only vector, which yielded to a single homologous recombination event. After isolation and expansion of 553 Neo^R clones, the genomic DNA was extracted and Southern blot analysis was carried out with radioactively labeled probes. Besides the expected wild type (WT) band, many clones displayed additional bands, which however can not be explained by a homologous recombination event. It seems that the targeting construct integrated inappropriately into the *MMD* locus.

Table 5.4 Summary of the targeting experiments

Targeting constructs	Number of isolated clones	Number of positive clones
TOPO-[KA-GFP-Neo-LA]-TK	200	1
TOPO-[LLA-GFP-Neo-LA]-TK	60	0
pBS-[SA3-GFP-Neo-LA]-DT	629	0
pBS-[SAex5-Neo-LAex6]-DT	551	0
TOPO-[KA-GFP-Neo-LA]	553	0

5.5. Mouse MMD silencing in NIH3T3 and RAW264.7 cell lines

Gene silencing using short intereference RNA (siRNA) is a more recent approach to knock-down a gene of interest. After many unsuccessful attempts to generate a mutant ES cell line by gene targeting, the next step was to silence *mMMD* in NIH3T3 and RAW264.7, which can then be used as tools for investigating mMMD function. It will be interesting, for example to study the influence of mMMD silencing on the gene expression pattern in these cells.
Four siRNA duplexes were commercially available (Qiagen, Germany):

- Mm_Mmd_1_HP siRNA: CCG GAT TAT GAT AGT ATT ATT
- Mm_Mmd_2_HP siRNA: ATG CAT GAT TCT GAA CAG TTA
- Mm_Mmd_3_HP siRNA: TTG GTG TTT AAG AGA AAT GAA
- Mm_Mmd_4_HP siRNA: CTG TGT ATA TTT GAC TTT AAA

NIH3T3 and RAW264.7 cell lines were transfected with siRNA duplexes following the procedure described in section 4.1.5. After 48, 72, and 96 h cells were harvested and mMMD transcript expression was evaluated by qRT-PCR. A complete and stable reduction of mMMD was reached only with the “Mm_Mmd_1_HP siRNA” siRNA (data not shown).

In NIH3T3 cells, mMMD expression was reduced to about 90% (Figure 5.25) and in RAW264.7 cells to about 80% of the initial level after 48 h.
However mMMD mRNA expression was remarkably lower in RAW264.7 cells and decreased after 72 h culture independently of siRNA transfection. This may have reduced the general silencing effect. It seems that stress factors (such as consumption of medium nutriments after long period of culture) may influence mMMD expression in RAW264.7 but not in NIH3T3 cell lines. No significant growth inhibition or apoptosis was observed during the culture period, suggesting that MMD knock down does not interfere with survival or proliferation of the two tested cell lines.

A

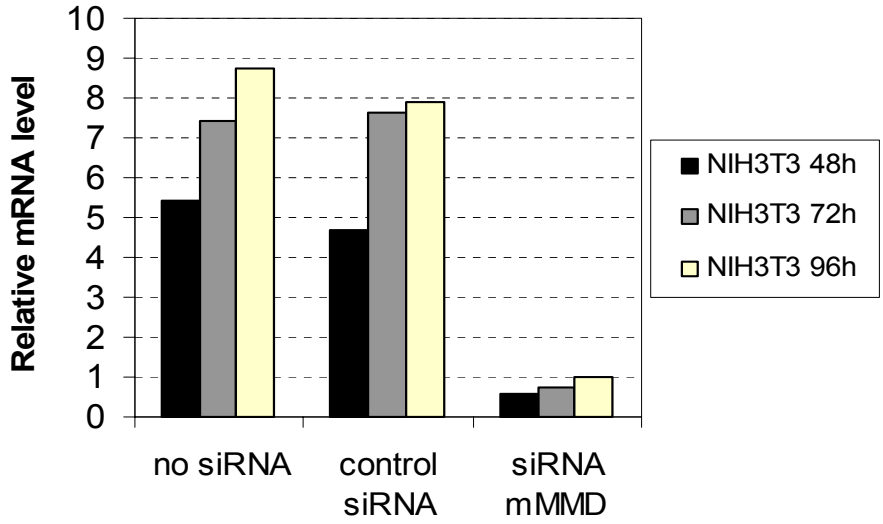

B

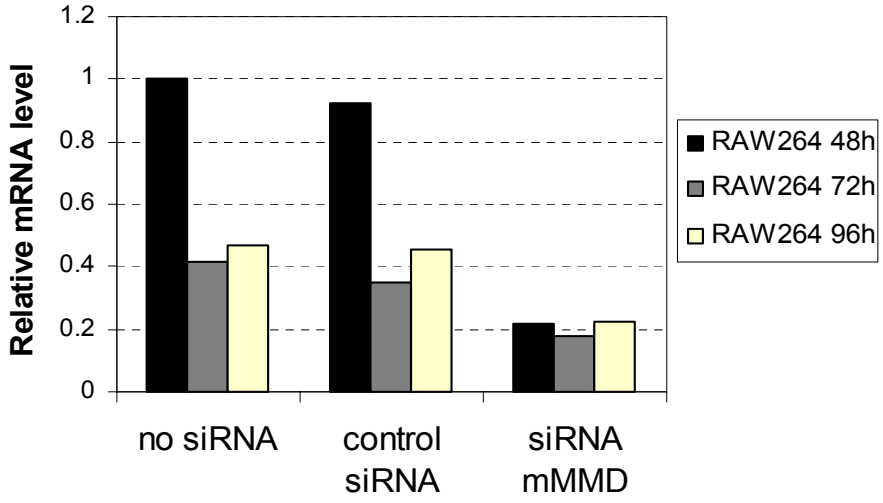

Figure 5.25 Silencing of mMMD in NIH3T3 and RAW264.7 via siRNA.
NIH3T3 and RAW264.7 cell lines were transfected with the "Mm_Mmd_1_HP siRNA" duplexes, and RNA was prepared from cells harvested after 48, 72, and 96 h. Expression of mMMD transcript was quantified with qRT-PCR. As negative control a non silencing siRNA purchased from Qiagen was transfected. Mouse MMD transcript was specifically and efficiently depleted in NIH3T3 (A) and RAW264.7 cell lines (B).

6. Discussion

Macrophages are a main cellular component of the innate immune system. They are responsible for an efficient elimination of pathogens, as well as tissues homeostasis. The *Monocyte to Macrophage Differentiation* (*MMD*) gene was identified in our lab as being up-regulated during the differentiation of human monocytes to macrophages (Rehli et al., 1995).

In this work, the expression patterns of MMD and its homologue, MMD2, were studied in cell lines and primary tissues of human and mouse origin, as well as during mouse embryogenesis. At the protein level, mouse MMD (mMMD) subcellular localization and orientation were determined.

To gain insights into mMMD function, ES cell culture was established in the course of this work, to generate a mMMD ES knock-down cell line. In addition, siRNA silencing, was considered as an alternative approach to silence the gene. Gene silencing offers many distinct advantages when investigating an unknown protein. The fact that both mouse and human MMD proteins share 99% sequence identity, makes a MMD knock-down mouse a useful tool for studying MMD function *in vivo* and its putative role in the human organism.

The recent classification of MMD and MMD2 into the newly defined Progestin and AdipoQ Receptor (PAQR) family (Tang et al., 2005) raises many questions about their functional association with these receptors. To date, PAQRs are divided into three subgroups: adiponectin receptors (AdipoRs), membrane progestin receptors (mPRs) and Hemolysin (Hly)-III related proteins. They differ in their genome and cellular localization, and in their gene organization (Tang et al., 2005), but they all share a seven transmembrane (7TM) core and conserved amino acid residues. Discussing their wide range of function may help getting more insights into MMD and MMD2 role in mammals.

6.1. Messenger RNA expression patterns

In mouse embryo, whole mount in situ hybridization showed that MMD was expressed in all tissues and brain structures, although at different expression levels (Figure 5.7). In contrast, MMD2 expression was highly restricted to certain structures of the central and peripheral nervous system such as the dorsal root ganglia and the trigeminal nerve (Figure 5.8). Dorsal root ganglia (DRG) along the spinal cord contain sensory neurons (Gilbert, 2000). The strong expression of MMD2 mRNA in these locations suggests its association with neurons.

Although both MMD and MMD2 transcripts are localized in the nervous system and brain region, MMD was absent from the spinal cord and DRG, and exhibited a rather diffused expression pattern. This finding suggests that MMD and MMD2 may be involved in different processes of the mouse development. In addition to the above, Menke et al. (Menke & Page, 2002) showed MMD2 expression in testis from E13.5 mouse embryos by whole mount in situ hybridization. In testicular cords MMD2 expression was attributed to Sertoli cells (Menke & Page, 2002), that play a pivotal role in the regulation and maintenance of spermatogenesis (Russell & Griswold , 1993), suggesting a putative role of MMD2 in this process as well.

Northern blot analyses showed that the ubiquitous MMD and restricted MMD2 expression patterns were maintained during adult age, and conserved in mouse and human (Figure 5.6B-C and Figure 5.9C).

Taking into consideration the strong expression of MMD in macrophages, it is tempting to attribute its ubiquitous expression pattern partially to resident and recruited macrophages in tissues (see section 1.1.2). Tissue macrophages are responsible for immune surveillance and maintenance of tissue homeostasis (Burke B & Lewis Claire E., 2002). Moreover they are found in different parts of the developing embryo, including the brain, the central nervous system (Lichanska et al., 1999), and in areas of active tissue remodeling such as the branchial arches (giving rise to mandibular components) and developing limbs (Lichanska et al., 1999; Hume et al., 1995). Thus the ubiquitous expression of MMD in the embryonic brain may be as well attributed to macrophages.

Nevertheless, Northern blot from different cell types showed that MMD expressions is not restricted to macrophages but is also found in other myeloid lineages (such as in T cells) and non-myeloid cell lines. The human skin (NHDFC) and dermal (HUVEC) fibroblasts, and the mouse embryonic fibroblast cell line, NIH3T3, expressed MMD as well, suggesting an involvement of this gene in connective tissues.

Moreover, CaCo-2, and HepG2, which are colon and hepatocyte carcinoma cell lines respectively, expressed strongly MMD as well. This finding is in agreement with the presence of human MMD (hMMD) transcript in colon and liver (Figure 5.6). According to the GNF SymATLAS database (Su et al., 2002), hMMD is strongly expressed in the hepatoma cell line, huh-7, various pancreatic cell lines such as Capan1 and Panc1 and in the myoblast cell line SKMC. This wide range of MMD expression emphasizes its role in several cell types.

Interestingly, multiple mouse MMD (mMMD) transcripts of different length were observed in the liver and heart, possibly resulting from the use of different polyadenylation (Poly-(A)) sites. Additionally, several ATTTA motifs are present in the 3'-untranslated region (UTR) of the mRNA. This sequence motif has been associated with mRNA stability and translational efficacity allowing fast changes in the proteins synthesis (Ross, 1995). It is therefore possible that these motifs may play a role in mMMD mRNA stability in the liver and heart.

In contrast to MMD, MMD2 transcript was not detected in any of the tested myeloid cell lines, nor in the non-myeloid fibroblasts cells (data not shown). Based on its restricted mRNA expression patterns in specific tissues, one can speculate that MMD2 may function in reproductive tissues (testis, ovary). However we cannot rule out the possibility that it may also be developmentally regulated or enriched in cell lines that have not been analysed in the present study.

Given the differential spatial expression of MMD and MMD2 despite high protein sequence homology (around 68% identical amino acids), one can speculate that these two genes arose from gene duplication of *Hly-III*. Subsequently a gene divergence occurred in regulatory elements leading to alteration of their expression pattern (Strachan T & Read A.P, 2004; Tang et al., 2005). The high degree of sequence homology shared between the orthologues results likely from a high selection pressure and suggests a conserved function among species.

As previously mentioned, mMMD was found strongly expressed in bone marrow macrophages (BMM) (Figure 5.9). Inflammatory stimuli activates macrophages and alter their gene expression pattern (see section 1.1.3). To investigate a possible regulation of mMMD expression in inflammation, mouse BMM were treated with bacterial lipopolysaccharides (LPS). LPS is a component of a Gram-negative bacteria, which binds to its receptor CD14 with the help of the soluble LPS-binding protein (LBP). The LPS-CD14 complex is then recognized by TLR4 which activates multiple signaling pathways leading to the activation of the transcription factor, NFκB (Abul K.Abbas & Andrew H.Lichtman, 2003). Consequently, a large number of genes are up- or downregulated, and their protein products provide macrophages with defense mechanisms against infection. Treatment of BMM with LPS induced a rapid increase of mMMD transcript, that reached the highest levels after 2 h, and was then downregulated 8 h after stimulation (Figure 5.10). This rapid response shows an association of mMMD with the macrophage innate activation (see section 1.1.3), which is

characterized by an increased phagocytotic capacity, and the production of cytokines and chemokines. These in turn can promote or inhibit inflammation (Burke B & Lewis Claire E., 2002). For instance IL-10, mainly produced by activated macrophages, functions as a feedback regulator, promoting their deactivation and thus protects against the damaging effects of persisting inflammation (Barsig et al., 1995; Abul K.Abbas & Andrew H.Lichtman, 2003). However, stimulation of BMM with IL-10 did not affect mMMD transcription levels, indicating that mMMD is probably not regulated by IL-10.

Cytokines, such as INFγ and IL-4, which prime macrophages towards a classical or an alternative activation phenotype respectively (see section 1.1.3), did not influence mMMD expression (Figure 5.11). These results lead to the conclusion, that mMMD expression is associated with the first phase of the macrophage activation by LPS, as it is regulated independently of IL-10, and not altered by INFγ or IL-4 priming.

6.2. Protein structure

As previously described in section 5.1.3, MMD and MMD2 were predicted to be seven transmembrane (7TM) proteins (Figure 5.4), to be highly conserved between species (Rehli et al., 1995) and to be related to Hemolysin (Hly)-III of *Bacillus cereus* (Rehli et al., 1995; Fernandes et al., 2005; Tang et al., 2005).

Hemolysin-III is one of the potential virulence factors of *Bacillus cereus*. Once secreted it binds to the cell membrane of erythrocytes and forms oligomeric pores thereby causing their lysis (Baida & Kuzmin, 1996). At present, very little is known about this protein. Multiple sequence alignment (Figure 5.5) showed significant identity with the mammalian MMD proteins especially within the transmembrane domain. It is however not clear whether MMD proteins can form oligomeric pores.

MMD and MMD2 also termed PAQR11 and 10 respectively (Tang et al., 2005), share a high degree of sequence conservation with other PAQRs within the UPF0073 motif (see section 1.3). PAQRs are characterized by the following features:

- An UPF0073 motif, which contains at least seven transmembrane (TM) domains.
- N- and C-terminal tails that vary in length and sequence between different PAQRs.
- Highly conserved protein sequence between orthologues.
- Conserved amino acid residues between all paralogues in all species.

In fact, five regions with conserved residues were first described in the yeast PAQR orthologue, YOL002c. A potential metal-binding property was attributed to these residues (Lyons et al., 2004). Four of them were found in MMD and MMD2:

- 1st region: **E**X[X_2**N**X_2**T**/**H**]$_{TM\ I}$ exhibits a truncated form of the first region in yeast.
- 2nd region: [**S**X_2**H**X_6]$_{TM\ II}$**S**.
- 3rd region: **D**[X_{10}**S**] or **D**[X_9**S**].
- 4th region of YOL002c is missing.
- 5th region: [**G**]$_{TM\ VI}$$X_6$**D**[$X_6$**H**$X_3$**H**$X_2$**V**$X_6$**H**]$_{TM\ VII}$.

Amino acid residues between brackets are located in predicted TM regions of MMD and are outlined in green in (Figure 5.5). In MMD2, some of these residues were found outside the predicted TM region such as asparagine (N) of the first region, histidine (H) of the second region and aspartate (D) of the third region. Because there is still no experimental evidence that would confirm the predicted length of the TM regions in MMD and MMD2, it is not certain whether these residues are really located in the extramembrane loops.
Interestingly, conserved residues that were predicted outside the TM domains were found located on one side of the membrane. Thereby they may play a role in the choice of physiological substrates of the MMD proteins, and influence the underlying molecular mechanisms, which have not been yet identified .

Therefore, determining the subcellular localization and orientation of mMMD constitutes an important step toward elucidating its role in the cell. The protein topology and the high level of homology existing between the ortholgues were two main hindrances for generating a specific mMMD antibody (see section 5.3.1.1). Consequently, an epitope tag strategy was employed to determine mMMD cellular localization.
Initially, a carboxy-terminally FLAG-tagged version of mMMD (MMD-3xFLAG), was transfected into a mouse macrophage cell line (RAW264.7), by using various methods without success (see section 5.3.1). The transient and stable high expression of mMMD were not tolerated by these cells (see section 5.3.2). In contrast, NIH3T3, tolerated ectopic expression of the tagged protein and was used for further experiments.
Immunocytochemistry performed on NIH3T3 cells expressing tagged versions of mMMD revealed an intracellular perinuclear localization, suggesting a reticulate network with a nuclear membrane localization. Western blot analysis confirmed the predicted size of recombinant expressed mMMD (about 28 kDa). During the course of this work, additional

seven tagged versions of the protein were generated and confirmed the mMMD perinuclear localization (Figure 5.14).

In contrast to the other seven versions of tagged recombinant mMMD proteins, for the FLAG-MMD-HA protein none of the tags were detectable neither by Western blot nor by immunocytofluorescence analyses. It seems that the N- and C-terminal tagging of mMMD with FLAG and HA respectively, influenced the protein stability. It is unlikely that the expression disturbance is on the transcriptional level, since mMMD was expressed from the first cistron of a bicistronic eGFP co-expressing construct, and the cells were eGFP-positive.
A second exception to the perinuclear localization was observed when mMMD was tagged with c-Myc at the first extramembrane loop leading to a vesicular localization. Generally, in a transmembrane proteins the first hydrophobic domain initiates the insertion of the growing peptide into the endoplasmic reticulum (ER) membrane, followed by the second TM domain, which functions as a "stop transfer" signal. After a hydrophilic stretch, the third TM domain functions again as an internal signal anchor sequence and so on, until the 7TM domains span the ER membrane (Lodish H et al., 2004). It seems that introducing a c-Myc tag in the first extramembrane loop of the protein altered its correct integration in the lipid bilayer, probably leading to its export from the ER-Golgi compartment.
In silico analysis using the SignalP program (Bendtsen et al., 2004) showed that mMMD lacks any signal sequence primary structure, supporting the notion that it is probably retained in the ER. PSORT II program (Nakai & Horton, 1999) predicted a putative cleavage site between the amino acid residues HRL and SD (Figure 5.3) located in the first extramembrane loop behind the TM I in mMMD protein sequence. However Western blot analysis of all tagged mMMD versions used for transfection experiments did not corroborate the presence of the cleavage site since none of the recombinant proteins was found to be truncated (Figure 5.16).
Based on these immunocytochemistry analyses, mMMD is an intracellular membrane protein. However, the possibility that it can be targeted to the outer cell membrane under certain conditions cannot be ruled out. It would be therefore interesting to investigate its localization, for instance, after LPS stimulation.

The rat MMD orthologue was recently identified by Bräuer et al. as a macrophage/microglia activation factor (MAF), specifically expressed in activated microglia cells after brain trauma (Brauer et al., 2004; Lunemann et al., 2006). Furthermore, they showed colocalization of

exogenous eGFP-tagged MAF with the lysosome associated membrane protein (LAMP)-1 in monkey kidney fibroblasts (COS7) and mouse microglia cells (BV-2) (Brauer et al., 2004). This result was confirmed by a generated MAF antibody, which also showed a vesicular staining pattern similar to LAMP-1. However, in Western blot analysis, a MAF antibody detected a 62 kDa band in U937 cell line (Lunemann et al., 2006), which by far exceeds the predicted molecular weight of MAF (28 kDa). From the publication is not clear if homodimers were detected, or if the protein was complexed with unknown factors, maybe helping its transport to lysosomes. Also, post-translational modifications such as glycosylation could lead to a larger apparent weight.

To explore a possible mMMD localization in lysosomes, an N-terminally HA- or a C-terminally 3xFLAG-tagged mMMD were stably expressed in NIH3T3 cells using a retroviral transfection system (see section 5.3.2). Interestingly, both tagged proteins localized mainly in the nuclear membrane (colocalization with DAPI staining) and the perinuclear region without any colocalization with the lysosomal marker LAMP-1 (Figure 5.18). The staining pattern suggests again an endoplasmic reticulum (ER) localization, however, a co-staining with an additional ER marker would be required to confirm this putative localization.

Bräuer et al. (Brauer et al., 2004) reported that addition of phorbol 12-myristate 13-acetate (PMA), an enhancer of exocytosis, drove eGFP-tagged MAF secretion in COS7 cells. However, treatment of NIH3T3, stably expressing tagged MMD proteins, with PMA did not induce changes in the protein localization. In addition, an increase in its expression was observed, resulting from an upregulation of the exogenous CMV promoter, which drove the expression of the tagged proteins (AbuBakar et al., 1990).

The discrepancy between eGFP-tagged MAF lysosomal localization (Brauer et al., 2004) and the perinuclear staining of HA or 3xFLAG tagged MMD may be partially explained by the fact that the fusion of MAF with eGFP may have influenced the correct spanning of the transmembrane domain in the lipid bilayer. This in turn may have exposed some potential domains allowing the export of the protein outside the ER. On the other hand, it is difficult to rule out the possibility that HA or 3xFLAG tags may have influenced the correct protein folding, thus leading to its accumulation in the ER. However it is unlikely that these small tags (HA, 9 aa; 3xFLAG, 18 aa) should alter mMMD localization more than the much larger eGFP tag (239 aa).

Another possible scenario to explain the observed discrepancies in localization would be that mMMD may form homodimers. The fusion with eGFP or with small tags may have influenced its lysosomal or perinuclear localization. It is difficult to confirm one scenario or the other, therefore to resolve the discrepancy between the results presented in this work and MAF staining, further experimental studies will be needed. Unfortunately, because mMMD/MAF function and its ligand identity has not yet been ascertained, it is not possible to test the functional integrity of the tagged proteins at this time.

Most 7TM proteins are classified as G-protein-coupled receptors (GPCRs), which are characterized by conserved cystein residues, a large extracellular $N_{exterior}$ and an intracellular $C_{cytosol}$ terminal domain (Bockaert & Pin, 1999). GPCRs respond to a wide range of signals such as lipids, peptides, neurotransmitters, nucleotides and are involved in numerous physiological processes. The third cytosolic intracellular loop is important for interaction with G-protein (Karnik et al., 2003; Lodish H et al., 2004). Binding of ligand induces a change in receptor conformation leading to a G-protein activation, which in turn alters the activity of a variety of downstream effector molecules (Lodish H et al., 2004). Determining the topology of mMMD in the lipid bilayer was the second approach to investigate the protein as well as the location of putative ligand binding sites but also its relation to GPCRs.

Based on the 7TM prediction (Figure 5.4), mMMD N- and C-termini have to be positioned on different sides of the lipid bilayer of perinuclear compartment. Mild permeabilizing of the plasma membrane using digitonin showed that the mMMD N-terminus faces the cytosol and the C-terminus faces the lumen of the perinuclear compartments (see section 5.3.3.2). This membrane topology that corresponds to a type IV-A multipass protein (Lodish H et al., 2004) differs from that of GPCRs.
Consequently, the predicted amino acid residues that were associated with metal-binding properties and located in predicted extramembrane loops would be all positioned at the cytosolic side of the protein (Figure 6.1). This may suggest a possible role of mMMD as cation channel in the cellular perinuclear compartments.

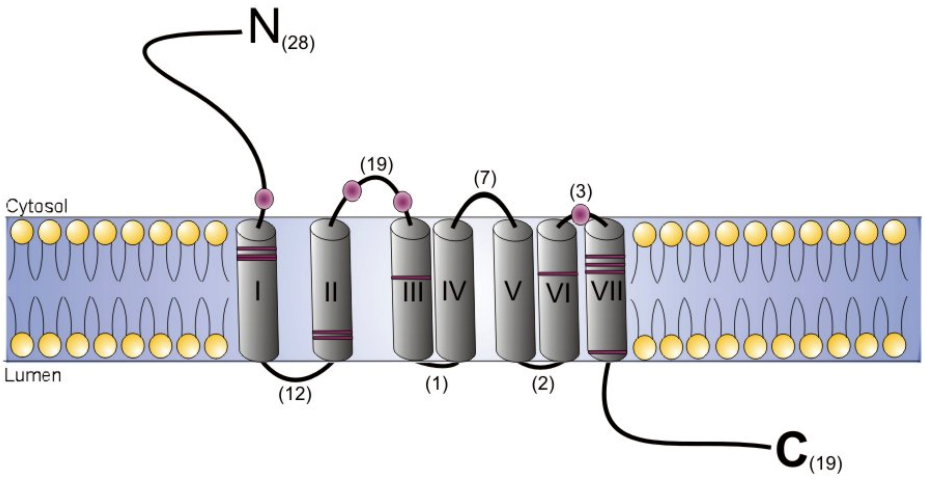

Figure 6.1 Proposed membrane topology of mMMD protein in the lipid bilayer of NIH3T3. Mouse MMD protein traverses the perinuclear (probably ER and outer nuclear) lipid bilayer seven times and has the N-terminal domain facing the cytosol. The N-, and C-terminal tails as well as extramembrane loops are depicted in bold letters and comprise the number of amino acids indicated between brackets. Conserved amino acids between mMMD and PAQRs are shown in pink, transmembrane domains in grey (I-VII).

The high protein sequence identity found between mouse and human MMD proteins, suggests a similar cellular localization and orientation. However, human and mouse MMD2 proteins differ from their MMD paralogue, both in their N- and C-teminal tail and in some amino acid residues in the extramembrane loops, which may influence their membrane topology, and probably their cellular localization and orientation. Therefore, it would be very interesting to determine MMD2 cellular localization and orientation.

6.3. Mouse MMD gene inactivation

Knocking-out MMD gene may provide valuable clues about MMD function and the processes in which it is involved.

Five attempts to knock out mMMD in ES cells were undertaken, using five different targeting vectors. However, from a total of 1993 clones isolated, only one was screened positive for homologous recombination, which unfortunately did not survive the thawing procedure from the replicate plate (see section 5.4).

Although homologous recombination at the target locus in ES cells is much more efficient than in somatic mammalian cells, it remains a rare event and the random integration of the targeting vector into the ES cell genome is rather the rule than the exception (Joyner, 2001). Numerous factors influencing gene targeting efficiency were taken into consideration for the construction of the different targeting vectors, in addition to various ES cell electroporation

methods that were tested in this work (see section 5.4.3.4). The unsuccessful attempts to generate an mMMD deficient ES cell line remains a problem to be resolved. One can speculate that the mMMD locus may be inaccessible for the recombination machinery in ES cells (Muller, 1999). One clue supporting this assumption, was provided by a qRT-PCR analysis showing that mMMD mRNA endogenous expression in ES cells was very low when compared to its expression in BMM (data not shown). In many cases, unexpressed genes are associated with a tightly packed chromatin organization (Strachan T & Read A.P, 2004). If this is the case with mMMD, the gene locus would be inaccessible for the recombination machinery, and therefore the efficiency of the homologous recombination would be affected negatively.

The second approach for silencing mMMD gene was to employ RNA interference (iRNA). After transfection into RAW264.7 and NIH3T3, mMMD-specific small interference RNA (siRNA) mediated a successful degradation reaching a transcript reduction of 90% in NIH3T3, and 80% in RAW264 7. Interestingly, the mMMD mRNA level in RAW264.7 decreased after 72 h cell culture, independently of siRNA transfection. One explanation may be the rapid nutrient depletion in RAW264.7 low glucose medium. In contrast NIH3T3 were grown in DMEM high glucose medium and did not show any reduction in mMMD transcript levels over time. It remains to be determined whether mMMD is involved in glucose uptake or energy metabolism, and whether this effect is cell type-specific.
Recently, it has been reported that using a lentiviral shRNA vector, stable transgenic knock-down mice can easily be produced from infected transgenic ES cells (Szulc et al., 2006; Tiscornia et al., 2003). Consequently, the identified siRNA can be further used to generate a mMMD knock-down mouse by expressing a short hairpin-forming RNA (shRNA) containing the sequences of the siRNA duplex.

6.4. Possible functions

To date there is no published data for MMD and MMD2 protein functions. In mouse BMM, the rapid increase of mMMD transcript expression upon LPS stimulation suggests an association of the protein with the first phase of the immune response. This latter involves pro-inflammatory processes and the activation of transcription factors such as NFκB, which in turn promotes gene transcription and expression. It is not known whether the increase in mMMD expression is directly induced by NFκB or by other unknown factors, or whether it

contributes to the inflammatory response mediated by NFκB (Abul K.Abbas & Andrew H.Lichtman, 2003).

A second hint involving MMD in activated macrophages processes was provided by Sawcer S. et al. (Sawcer et al., 2002), who classified hMMD as a susceptibility gene for Multiple Sclerosis (MS). MS is a chronic inflammatory demyelinating disease of the central nervous system, resulting in impaired nerve conduction. The keys to the pathophysiology are activated lymphocytes, macrophages, astrocytes and microglia. Activated microglia/macrophages are involved in the demyelination and secrete inflammatory cytokines such as TNFα, IL-1 and IL-6 which additionally contribute to the formation of free radicals and tissue damage (Burke B & Lewis Claire E., 2002). The involvement of hMMD in these processes suggests either a role in inflammation or as protector against brain damage.

Recently, Lünemann et al. (Lunemann et al., 2006) showed that MAF/MMD (rat MMD orthologue) was upregulated in regions of the brain after an entorhinal cortex lesion (ECL). ECL models post-traumatic tissue remodeling of neuronal structure and connectivity (Lunemann et al., 2006). The early phase of this process is characterized by the recruitment, into the lesion site, of inflammatory cells such as microglia and newly infiltrated macrophages, whichs produce IL-1β. In the late phase of ECL (two days later), tissue repair and remodeling are initiated, where microglia were shown to play a crucial role (Mabuchi et al., 2000). MMD/MAF expression in this latter stage of ECL suggests its role in tissue remodeling rather than inflammation (Lunemann et al., 2006). However, Lünemann et al. did not investigate whether MAF/MMD was also expressed during the early phase of ECL.
Taken together, MMD function may be associated with immediate post-stimulatory activation of macrophages, and is likely associated with tissue remodeling.

The recent classification of MMD and MMD2 into PAQRs family (Tang et al., 2005) shed more light into their putative functions, however few clues are available linking MMD proteins to these receptors.
On the transcript level, Northern blot analysis showed that both MMD and AdipoRs mRNA were expressed in macrophages but also in liver, skeletal muscle, adipose tissue and placenta (Yamauchi et al., 2003a). On the other hand, MMD2 shared with mPRα (PAQR7) the expression in testis and with mPRβ and MMD the expression in brain. However, apart from

the similar expression pattern, there is no other evidence which relates functionally MMD proteins to PAQRs.

Interestingly, in the placenta in addition to hMMD and AdipoRs (Yamauchi et al., 2003a), mPRα and PAQR9 were expressed (Fernandes et al., 2005; Zhu et al., 2003a) and functionally associated with the onset of pregnancy. PAQR3 was also strongly and constantly expressed in the endometrium during the cycle and upon pregnancy, where it was predicted to responsible for the maintenance of the tissue homeostasis (Fernandes et al., 2005). In fact, in the early phases of pregnancy, a balance between pro- and anti-oxidant factors is important in the placenta microenvironment for the trophoblast invasion (Biondi et al., 2005). Macrophages, which are in close contact with trophoblasts, play a pivotal role in this process by supporting a certain grade of inflammation (Mor & Abrahams, 2003; Zhu et al., 1997). Interestingly, PAQR3 orthologue in *Drosophila melanogaster*, CG7530, was identified as a resistant gene against oxidative stress (Monnier et al., 2002). It is therefore likely that PAQR3 may play the same role in the placenta during the pregnancy. The next question would be if hMMD can also be involved in the onset of pregnancy and in oxidative stress as well.

On the protein level, PAQRs differ in their subcellular localization. PAQR1 and PAQR2 (Yamauchi et al., 2003a) as well as the yeast YOL002c (Narasimhan et al., 2005) were defined as plasma membrane proteins (Zhu et al., 2003b). PAQR8 was located in lysosomes (Suzuki et al., 2001) and only mPRα (PAQR7) shares with mMMD the perinuclear and nuclear membrane localization (Fernandes et al., 2005). However, amino acid residues with a predicted metal-binding property were found conserved in all PAQRs (see section 6.2) (Tang et al., 2005; Lyons et al., 2004).

In the yeast PAQR orthologue, YOL002c, the metal-binding amino acid residues were associated with zinc metabolism. YOL002c, also termed “Implicated in Zinc Homeostasis” (IZH)-2 was found to be induced by a zinc limited environment. Its function was also associated with lipid metabolism (Karpichev et al., 2002). Additionally, it has been speculated that IZH-2 could be an ion channel (Lyons et al., 2004).

In AdipoRs and mMMD proteins, where the membrane topology was determined, the metal-binding residues, located outside the TM regions, face the cytosol. It is therefore tempting to propose that both proteins may be implicated in the cellular zinc homeostasis.

An ion channel property was proposed for the human PAQR8 (mPRβ, also termed as lysosomal membrane protein brain (LMPB)-1). PAQR8 was associated with a brain

pathology, namely juvenile myoclonic epilepsy (JME), which is characterized by seizures without detectable brain lesions (Suzuki et al., 2001). Defects in ion channel proteins were implicated in JME.
One can assume that MMD proteins could be an ion channels as well. The fact that they were defined as related to Hly-III (Rehli et al., 1995; Tang et al., 2005), which was shown to form membrane pores in erythrocytes (Baida & Kuzmin, 1996), may support this assumption.

Taken together, MMD and MMD2 expressed in different tissues, are likely to be involved in different processes. Mouse MMD intracellular localization and topology suggest a putative role in maintenance of the cellular homeostasis. Whether the metal-binding property of the conserved amino acid residues plays a role in oxidative stress, or whether MMD protein are ion channels, remains to be determined.

6.5. Outlook

After assessing MMD and MMD2 expression patterns, in human and mouse adult tissues, there are still fairly many unanswered questions.
At the protein level, the finding that mMMD is a perinuclear transmembrane protein, whose transcript is rapidly induced by stimulation with LPS, paves the way for more interesting experiments, such as determining in which signaling pathway mMMD may be involved.
On the other hand, the finding that MMD2 is specifically expressed in brain and testis of mouse and human, and not in macrophages or any other tested cell line, raises many questions on its role in these tissues. Therefore, in situ hybridization in brain and testis, in addition to its subcellular localization and orientation have to be assessed prior to the search for its ligand.
Although the generation of a MMD knock-down mouse may offer many advantages, this technology still has some limitations, which have been encountered particularly in cases of genes expressed ubiquitously in adult animals and in embryonic tissues. Whole mount ISH showed early expression of MMD in mouse embryo that becomes ubiquitous after 13 dpc, indicating the importance of this gene during the embryogenesis and mouse development. Thus, inactivating MMD may have dramatic consequences and cause early lethality, which makes difficult the analysis of its function in adult tissues.
On the other hand, in cases of genes ubiquitously expressed at an adult age, alteration of its expression at early embryonic stages is more likely to activate compensatory pathways, leading to complicated phenotypes (Gerlai, 2001). Taken these into consideration, the

generation of a MMD deficient mice using the Cre/lox recombinase system under temporal control would be the most promising approach.

Generating a MMD2 conditional knock-out mouse is as well of great interest to investigate MMD2 function.

Finally, the established siRNA against mMMD can be further used to silence MMD in various cell lines. Additionally this approach, when coupled to microarray gene expression analysis, may help to gain insight into mMMD association in different processes such as lipid and glucose metabolism as well as the nongenomic action of progestin. Through this approach putative genes regulated by mMMD can be identified.

7. Summary

During the course of this work the monocyte to macrophage differentiation factor (*MMD*) and its homologue *MMD2* were characterized. Both genes encodes for orphan proteins with a predicted seven transmembrane domain very well conserved between species.

MMD mRNA expression could be shown to be upregulated in macrophages and to be ubiquitously distributed in mouse and human. In contrast, MMD2 mRNA was only detected in brain and testis and in none of the tested cell lines. This differential expression pattern indicates differences in gene regulation although MMD and MMD2 share about 68% sequence identity at the protein level.
Furthermore, mouse MMD (mMMD) regulation on the mRNA level was investigated in bone marrow macrophages and found to be rapidly induced by LPS, associating MMD function with processes that occur during the first stage of the macrophage innate activation.

At the protein level, mMMD cellular localization and topology were determined. For this purpose various tagged versions of the protein were generated, and used to determine its subcellular localization. Additionally, a retroviral transfection system was established in our lab, and used to generate two cell lines stably expressing two tagged versions of MMD. By performing immunocytochemistry, tagged MMD proteins were localized in perinuclear compartments with an $N_{cytosol}$ and C_{lumen} orientation.

The second and main aim of this project was to investigate the effect of a MMD null-mutation in mice in an attempt to elucidate its function. For this purpose ES cell culture was established, MMD targeting constructs were generated and transfected into ES cells with the aim to generate an ES knock-out cell line and to establish an MMD knock-out mouse line by blastocyst injection.
As an alternative to gene targeting, an siRNA sequence was determined that can be used for further analysis of MMD function.

8. References

AbuBakar,S., Boldogh,I., & Albrecht,T. (1990). Human cytomegalovirus stimulates arachidonic acid metabolism through pathways that are affected by inhibitors of phospholipase A2 and protein kinase C. *Biochem.Biophys.Res.Commun.*, 166(2), 953-959.

Abul K.Abbas and Andrew H.Lichtman. Cellular and molecular immunology. Fifth Edition. 2003. Saunders.

Adam,S.A., Marr,R.S., & Gerace,L. (1990). Nuclear protein import in permeabilized mammalian cells requires soluble cytoplasmic factors. *J.Cell Biol.*, 111(3), 807-816.

Altschul,S.F., Madden,T.L., Schaffer,A.A., Zhang,J., Zhang,Z., Miller,W., & Lipman,D.J. (1997). Gapped BLAST and PSI-BLAST: a new generation of protein database search programs. *Nucleic Acids Res.*, 25(17), 3389-3402.

Arita,Y., Kihara,S., Ouchi,N., Takahashi,M., Maeda,K., Miyagawa,J., Hotta,K., Shimomura,I., Nakamura,T., Miyaoka,K., Kuriyama,H., Nishida,M., Yamashita,S., Okubo,K., Matsubara,K., Muraguchi,M., Ohmoto,Y., Funahashi,T., & Matsuzawa,Y. (1999). Paradoxical decrease of an adipose-specific protein, adiponectin, in obesity. *Biochem.Biophys.Res.Commun.*, 257(1), 79-83.

Ausubel Frederick, M, Brent R, and Kington , RE. Current Protocols in Molecular Biology. 2006. John Wiley & Sons, Inc. 2000.

Baetselier,P.D., Namangala,B., Noel,W., Brys,L., Pays,E., & Beschin,A. (2001). Alternative versus classical macrophage activation during experimental African trypanosomosis. *Int.J.Parasitol.*, 31(5-6), 575-587.

Baida,G.E. & Kuzmin,N.P. (1996). Mechanism of action of hemolysin III from Bacillus cereus. *Biochim.Biophys.Acta.*, 1284(2), 122-124.

Bar-Or,A., Oliveira,E.M., Anderson,D.E., & Hafler,D.A. (1999). Molecular pathogenesis of multiple sclerosis. *J.Neuroimmunol.*, 100(1-2), 252-259.

Barsig,J., Kusters,S., Vogt,K., Volk,H.D., Tiegs,G., & Wendel,A. (1995). Lipopolysaccharide-induced interleukin-10 in mice: role of endogenous tumor necrosis factor-alpha. *Eur.J.Immunol.*, 25(10), 2888-2893.

Bender,A., Sapp,M., Schuler,G., Steinman,R.M., & Bhardwaj,N. (1996). Improved methods for the generation of dendritic cells from nonproliferating progenitors in human blood. *J.Immunol.Methods.*, 196(2), 121-135.

Bendtsen,J.D., Nielsen,H., von Heijne,G., & Brunak,S. (2004). Improved prediction of signal peptides: SignalP 3.0. *J.Mol.Biol.*, 340(4), 783-795.

Berrebi,D., Bruscoli,S., Cohen,N., Foussat,A., Migliorati,G., Bouchet-Delbos,L., Maillot,M.C., Portier,A., Couderc,J., Galanaud,P., Peuchmaur,M., Riccardi,C., & Emilie,D. (2003). Synthesis of glucocorticoid-induced leucine zipper (GILZ) by macrophages: an anti-inflammatory and immunosuppressive mechanism shared by glucocorticoids and IL-10. *Blood.*, 101(2), 729-738.

Biondi,C., Pavan,B., Lunghi,L., Fiorini,S., & Vesce,F. (2005). The role and modulation of the oxidative balance in pregnancy. *Curr.Pharm.Des.*, 11(16), 2075-2089.

Bockaert,J. & Pin,J.P. (1999). Molecular tinkering of G protein-coupled receptors: an evolutionary success. *EMBO J.*, 18(7), 1723-1729.

Boring,L., Gosling,J., Cleary,M., & Charo,I.F. (1998). Decreased lesion formation in CCR2-/- mice reveals a role for chemokines in the initiation of atherosclerosis. *Nature.*, 394(6696), 894-897.

Brauer,A.U., Nitsch,R., & Savaskan,N.E. (2004). Identification of macrophage/microglia activation factor (MAF) associated with late endosomes/lysosomes in microglial cells. *FEBS Lett.*, 563(1-3), 41-48.

Burke B and Lewis Claire E. The macrophage. Second. 2002. Oxford University Press.

Chapman,N.R., Kennelly,M.M., Harper,K.A., Europe-Finner,G.N., & Robson,S.C. (2006). Examining the spatio-temporal expression of mRNA encoding the membrane-bound progesterone receptor-alpha isoform in human cervix and myometrium during pregnancy and labour. *Mol.Hum.Reprod.*, 12(1), 19-24.

Charles A.Janeway, Paul Travers, Mark Walport, and Mark J.Shlomchik. Immunobiology. Fifth Edition. 2001. Garland Publishing.

Chinetti,G., Zawadski,C., Fruchart,J.C., & Staels,B. (2004). Expression of adiponectin receptors in human macrophages and regulation by agonists of the nuclear receptors PPARalpha, PPARgamma, and LXR. *Biochem.Biophys.Res.Commun.*, 314(1), 151-158.

Combs,T.P., Pajvani,U.B., Berg,A.H., Lin,Y., Jelicks,L.A., Laplante,M., Nawrocki,A.R., Rajala,M.W., Parlow,A.F., Cheeseboro,L., Ding,Y.Y., Russell,R.G., Lindemann,D., Hartley,A., Baker,G.R., Obici,S., Deshaies,Y., Ludgate,M., Rossetti,L., & Scherer,P.E. (2004). A transgenic mouse with a deletion in the collagenous domain of adiponectin displays elevated circulating adiponectin and improved insulin sensitivity. *Endocrinology.*, 145(1), 367-383.

Dalton,D.K., Pitts-Meek,S., Keshav,S., Figari,I.S., Bradley,A., & Stewart,T.A. (1993). Multiple defects of immune cell function in mice with disrupted interferon-gamma genes. *Science.*, %19;259(5102), 1739-1742.

Dickensheets,H.L., Venkataraman,C., Schindler,U., & Donnelly,R.P. (1999). Interferons inhibit activation of STAT6 by interleukin 4 in human monocytes by inducing SOCS-1 gene expression. *Proc.Natl.Acad.Sci.U.S.A.*, 96(19), 10800-10805.

Elbashir,S.M., Lendeckel,W., & Tuschl,T. (2001). RNA interference is mediated by 21- and 22-nucleotide RNAs. *Genes Dev.*, 15(2), 188-200.

Fadok,V.A., Bratton,D.L., Konowal,A., Freed,P.W., Westcott,J.Y., & Henson,P.M. (1998). Macrophages that have ingested apoptotic cells in vitro inhibit proinflammatory cytokine production through autocrine/paracrine mechanisms involving TGF-beta, PGE2, and PAF. *J.Clin.Invest.*, 101(4), 890-898.

Fearon,D.T. & Locksley,R.M. (1996). The instructive role of innate immunity in the acquired immune response. *Science.*, 272(5258), 50-53.

Fernandes,M.S., Pierron,V., Michalovich,D., Astle,S., Thornton,S., Peltoketo,H., Lam,E.W., Gellersen,B., Huhtaniemi,I., Allen,J., & Brosens,J.J. (2005). Regulated expression of putative membrane progestin receptor homologues in human endometrium and gestational tissues. *J.Endocrinol.*, 187(1), 89-101.

Geissmann,F., Jung,S., & Littman,D.R. (2003). Blood monocytes consist of two principal subsets with distinct migratory properties. *Immunity.*, 19(1), 71-82.

Gerlai,R. (2001). Gene targeting: technical confounds and potential solutions in behavioral brain research. *Behav.Brain Res.*, 125(1-2), 13-21.

Gilbert,S. (2000). *Developmental biology*. Sinauer Associates, INC.

Gordon,S. (2003). Alternative activation of macrophages. *Nat.Rev.Immunol.*, 3(1), 23-35.

Gordon,S., Perry,V.H., Rabinowitz,S., Chung,L.P., & Rosen,H. (1988). Plasma membrane receptors of the mononuclear phagocyte system. *J.Cell Sci.Suppl.*, 9:1-26., 1-26.

Gordon,S. & Taylor,P.R. (2005). Monocyte and macrophage heterogeneity. *Nat.Rev.Immunol.*, 5(12), 953-964.

Gosling,J., Slaymaker,S., Gu,L., Tseng,S., Zlot,C.H., Young,S.G., Rollins,B.J., & Charo,I.F. (1999). MCP-1 deficiency reduces susceptibility to atherosclerosis in mice that overexpress human apolipoprotein B. *J.Clin.Invest.*, 103(6), 773-778.

Gu,L., Okada,Y., Clinton,S.K., Gerard,C., Sukhova,G.K., Libby,P., & Rollins,B.J. (1998). Absence of monocyte chemoattractant protein-1 reduces atherosclerosis in low density lipoprotein receptor-deficient mice. *Mol.Cell.*, 2(2), 275-281.

Hasty,P., Rivera-Perez,J., & Bradley,A. (1991). The length of homology required for gene targeting in embryonic stem cells. *Mol.Cell Biol.*, 11(11), 5586-5591.

Hu,E., Liang,P., & Spiegelman,B.M. (1996). AdipoQ is a novel adipose-specific gene dysregulated in obesity. *J.Biol.Chem.*, 271(18), 10697-10703.

Hume,D.A., Monkley,S.J., & Wainwright,B.J. (1995). Detection of c-fms protooncogene in early mouse embryos by whole mount in situ hybridization indicates roles for macrophages in tissue remodelling. *Br.J.Haematol.*, 90(4), 939-942.

Joyner, A. L. Gene targeting, a practical approach. Second edition. 2001. Oxford University Press.

Karnik,S.S., Gogonea,C., Patil,S., Saad,Y., & Takezako,T. (2003). Activation of G-protein-coupled receptors: a common molecular mechanism. *Trends Endocrinol.Metab.*, 14(9), 431-437.

Karpichev,I.V., Cornivelli,L., & Small,G.M. (2002). Multiple regulatory roles of a novel Saccharomyces cerevisiae protein, encoded by YOL002c, in lipid and phosphate metabolism. *J.Biol.Chem.*, 277(22), 19609-19617.

Katabuchi,H., Yih,S., Ohba,T., Matsui,K., Takahashi,K., Takeya,M., & Okamura,H. (2003). Characterization of macrophages in the decidual atherotic spiral artery with special reference to the cytology of foam cells. *Med.Electron Microsc.*, 36(4), 253-262.

Kawanami,D., Maemura,K., Takeda,N., Harada,T., Nojiri,T., Imai,Y., Manabe,I., Utsunomiya,K., & Nagai,R. (2004). Direct reciprocal effects of resistin and adiponectin on vascular endothelial cells: a new insight into adipocytokine-endothelial cell interactions. *Biochem.Biophys.Res.Commun.*, 314(2), 415-419.

Kraal,G. (1992). Cells in the marginal zone of the spleen. *Int.Rev.Cytol.*, 132:31-74., 31-74.

Kubota,N., Terauchi,Y., Kubota,T., Kumagai,H., Itoh,S., Satoh,H., Yano,W., Ogata,H., Tokuyama,K., Takamoto,I., Mineyama,T., Ishikawa,M., Moroi,M., Sugi,K., Yamauchi,T., Ueki,K., Tobe,K., Noda,T., Nagai,R., & Kadowaki,T. (2006). Pioglitazone ameliorates insulin resistance and diabetes by both adiponectin-dependent and -independent pathways. *J.Biol.Chem.*, 281(13), 8748-8755.

Kumada,M., Kihara,S., Ouchi,N., Kobayashi,H., Okamoto,Y., Ohashi,K., Maeda,K., Nagaretani,H., Kishida,K., Maeda,N., Nagasawa,A., Funahashi,T., & Matsuzawa,Y. (2004). Adiponectin specifically increased tissue inhibitor of metalloproteinase-1 through interleukin-10 expression in human macrophages. *Circulation.*, 109(17), 2046-2049.

Kyte,J. & Doolittle,R.F. (1982). A simple method for displaying the hydropathic character of a protein. *J.Mol.Biol.*, 157(1), 105-132.

Lea,R.G. & Clark,D.A. (1989). The immune function of the endometrium. *Baillieres Clin.Obstet.Gynaecol.*, 3(2), 293-313.

Li,X., Lonard,D.M., & O'Malley,B.W. (2004). A contemporary understanding of progesterone receptor function. *Mech.Ageing Dev.*, 125(10-11), 669-678.

Lichanska,A.M., Browne,C.M., Henkel,G.W., Murphy,K.M., Ostrowski,M.C., McKercher,S.R., Maki,R.A., & Hume,D.A. (1999). Differentiation of the mononuclear phagocyte system during mouse embryogenesis: the role of transcription factor PU.1. *Blood.*, 94(1), 127-138.

Lodish H, Berk A, Zipursky L.S, Matsudaira P., Kaiser C.A, Krieger M, Scott M.P, and Darnell J. Molecular cell biology. Fifth edition. 2004.

Lunemann,A., Ullrich,O., Diestel,A., Jons,T., Ninnemann,O., Kovac,A., Pohl,E.E., Hass,R., Nitsch,R., & Hendrix,S. (2006). Macrophage/microglia activation factor expression is restricted to lesion-associated microglial cells after brain trauma. *Glia.*, 53(4), 412-419.

Lyons,T.J., Villa,N.Y., Regalla,L.M., Kupchak,B.R., Vagstad,A., & Eide,D.J. (2004). Metalloregulation of yeast membrane steroid receptor homologs. *Proc.Natl.Acad.Sci.U.S.A.*, 101(15), 5506-5511.

Mabuchi,T., Kitagawa,K., Ohtsuki,T., Kuwabara,K., Yagita,Y., Yanagihara,T., Hori,M., & Matsumoto,M. (2000). Contribution of microglia/macrophages to expansion of infarction and response of oligodendrocytes after focal cerebral ischemia in rats. *Stroke.*, 31(7), 1735-1743.

Matsuda,M., Shimomura,I., Sata,M., Arita,Y., Nishida,M., Maeda,N., Kumada,M., Okamoto,Y., Nagaretani,H., Nishizawa,H., Kishida,K., Komuro,R., Ouchi,N., Kihara,S., Nagai,R., Funahashi,T., & Matsuzawa,Y. (2002). Role of adiponectin in preventing vascular stenosis. The missing link of adipo-vascular axis. *J.Biol.Chem.*, 277(40), 37487-37491.

McGeer,P.L., Kawamata,T., Walker,D.G., Akiyama,H., Tooyama,I., & McGeer,E.G. (1993). Microglia in degenerative neurological disease. *Glia.*, 7(1), 84-92.

Menke,D.B. & Page,D.C. (2002). Sexually dimorphic gene expression in the developing mouse gonad. *Gene Expr.Patterns.*, 2(3-4), 359-367.

Monnier,V., Girardot,F., Cheret,C., Andres,O., & Tricoire,H. (2002). Modulation of oxidative stress resistance in Drosophila melanogaster by gene overexpression. *Genesis.*, 34(1-2), 76-79.

Mor,G. & Abrahams,V.M. (2003). Potential role of macrophages as immunoregulators of pregnancy. *Reprod.Biol.Endocrinol.*, 1:119., 119.

Mora,A.L., Torres-Gonzalez,E., Rojas,M., Corredor,C., Ritzenthaler,J., Xu,J., Roman,J., Brigham,K., & Stecenko,A. (2006). Activation of Alveolar Macrophages via the Alternative Pathway in Herpesvirus-induced Lung Fibrosis. *Am.J.Respir.Cell Mol.Biol.*, .

Mourot,B., Nguyen,T., Fostier,A., & Bobe,J. (2006). Two unrelated putative membrane-bound progestin receptors, progesterone membrane receptor component 1 (PGMRC1) and membrane progestin receptor (mPR) beta, are expressed in the rainbow trout oocyte and exhibit similar ovarian expression patterns. *Reprod.Biol.Endocrinol.*, 4:6., 6.

Muller,U. (1999). Ten years of gene targeting: targeted mouse mutants, from vector design to phenotype analysis. *Mech.Dev.*, 82(1-2), 3-21.

Munro,S. & Pelham,H.R. (1984). Use of peptide tagging to detect proteins expressed from cloned genes: deletion mapping functional domains of Drosophila hsp 70. *EMBO J.*, %20;3(13), 3087-3093.

Nagy, A, Gertsenstein, M, Vintersten, K, and Gehringer, R. Manipulating the mouse embryo, a laboratory manual. 2003. Cold Spring Harbor Laboratory Press.

Nakai,K. & Horton,P. (1999). PSORT: a program for detecting sorting signals in proteins and predicting their subcellular localization. *Trends Biochem.Sci.*, 24(1), 34-36.

Narasimhan,M.L., Coca,M.A., Jin,J., Yamauchi,T., Ito,Y., Kadowaki,T., Kim,K.K., Pardo,J.M., Damsz,B., Hasegawa,P.M., Yun,D.J., & Bressan,R.A. (2005). Osmotin is a homolog of mammalian adiponectin and controls apoptosis in yeast through a homolog of mammalian adiponectin receptor. *Mol.Cell.*, 17(2), 171-180.

O'Riordain,M.G., Falconer,J.S., Maingay,J., Fearon,K.C., & Ross,J.A. (1999). Peripheral blood cells from weight-losing cancer patients control the hepatic acute phase response by a primarily interleukin-6 dependent mechanism. *Int.J.Oncol.*, 15(4), 823-827.

Orchinik,M., Murray,T.F., Franklin,P.H., & Moore,F.L. (1992). Guanyl nucleotides modulate binding to steroid receptors in neuronal membranes. *Proc.Natl.Acad.Sci.U.S.A.*, 89(9), 3830-3834.

Ouchi,N., Kihara,S., Arita,Y., Maeda,K., Kuriyama,H., Okamoto,Y., Hotta,K., Nishida,M., Takahashi,M., Nakamura,T., Yamashita,S., Funahashi,T., & Matsuzawa,Y. (1999). Novel modulator

for endothelial adhesion molecules: adipocyte-derived plasma protein adiponectin. *Circulation.*, 100(25), 2473-2476.

Ouchi,N., Kihara,S., Arita,Y., Nishida,M., Matsuyama,A., Okamoto,Y., Ishigami,M., Kuriyama,H., Kishida,K., Nishizawa,H., Hotta,K., Muraguchi,M., Ohmoto,Y., Yamashita,S., Funahashi,T., & Matsuzawa,Y. (2001). Adipocyte-derived plasma protein, adiponectin, suppresses lipid accumulation and class A scavenger receptor expression in human monocyte-derived macrophages. *Circulation.*, 103(8), 1057-1063.

Purves,D., Augustine,G.J., Fitzpatrick,D., Katz,L.C., LaMantia,A.-S., McNamara,J.O., & Williams,S.M. (2001). *Neuroscience*. Sinauer Associates, Inc.

Randolph,G.J., Beaulieu,S., Lebecque,S., Steinman,R.M., & Muller,W.A. (1998). Differentiation of monocytes into dendritic cells in a model of transendothelial trafficking. *Science.*, 282(5388), 480-483.

Rehli M (1996). Klonierung und charakterisierung von reifungsassoziierten, makrophagenspezifischen proteinen.

Rehli,M., Krause,S.W., Schwarzfischer,L., Kreutz,M., & Andreesen,R. (1995). Molecular cloning of a novel macrophage maturation-associated transcript encoding a protein with several potential transmembrane domains. *Biochem.Biophys.Res.Commun.*, 217(2), 661-667.

Rehli,M., Sulzbacher,S., Pape,S., Ravasi,T., Wells,C.A., Heinz,S., Sollner,L., El Chartouni,C., Krause,S.W., Steingrimsson,E., Hume,D.A., & Andreesen,R. (2005). Transcription factor Tfec contributes to the IL-4-inducible expression of a small group of genes in mouse macrophages including the granulocyte colony-stimulating factor receptor. *J.Immunol.*, 174(11), 7111-7122.

Revelli,A., Modotti,M., Piffaretti-Yanez,A., Massobrio,M., & Balerna,M. (1994). Steroid receptors in human spermatozoa. *Hum.Reprod.*, 9(5), 760-766.

Rezaie,P. & Male,D. (1999). Colonisation of the developing human brain and spinal cord by microglia: a review. *Microsc.Res.Tech.*, 45(6), 359-382.

Rodriguez,N.E., Chang,H.K., & Wilson,M.E. (2004). Novel program of macrophage gene expression induced by phagocytosis of Leishmania chagasi. *Infect.Immun.*, 72(4), 2111-2122.

Ross,J. (1995). mRNA stability in mammalian cells. *Microbiol.Rev.*, 59(3), 423-450.

Russell,L. & Griswold ,M. (1993). *The Sertoli Cell.* Cache River Press, Clearwater FL.

Sallusto,F. & Lanzavecchia,A. (1994). Efficient presentation of soluble antigen by cultured human dendritic cells is maintained by granulocyte/macrophage colony-stimulating factor plus interleukin 4 and downregulated by tumor necrosis factor alpha. *J.Exp.Med.*, 179(4), 1109-1118.

Sambrook, J and Russel, DW. Molecular cloning: a laboratory manual. Third Edition. 2001. New York, Cold Spring Harbor Laboratory Press.

Sawcer,S., Maranian,M., Setakis,E., Curwen,V., Akesson,E., Hensiek,A., Coraddu,F., Roxburgh,R., Sawcer,D., Gray,J., Deans,J., Goodfellow,P.N., Walker,N., Clayton,D., & Compston,A. (2002). A whole genome screen for linkage disequilibrium in multiple sclerosis confirms disease associations with regions previously linked to susceptibility. *Brain.*, 125(Pt 6), 1337-1347.

Scherer,P.E., Williams,S., Fogliano,M., Baldini,G., & Lodish,H.F. (1995). A novel serum protein similar to C1q, produced exclusively in adipocytes. *J.Biol.Chem.*, 270(45), 26746-26749.

Schneider-Brachert,W., Tchikov,V., Neumeyer,J., Jakob,M., Winoto-Morbach,S., Held-Feindt,J., Heinrich,M., Merkel,O., Ehrenschwender,M., Adam,D., Mentlein,R., Kabelitz,D., & Schutze,S. (2004). Compartmentalization of TNF receptor 1 signaling: internalized TNF receptosomes as death signaling vesicles. *Immunity.*, 21(3), 415-428.

Stanley,E.R., Berg,K.L., Einstein,D.B., Lee,P.S., Pixley,F.J., Wang,Y., & Yeung,Y.G. (1997). Biology and action of colony--stimulating factor-1. *Mol.Reprod.Dev.*, 46(1), 4-10.

Stein,M., Keshav,S., Harris,N., & Gordon,S. (1992). Interleukin 4 potently enhances murine macrophage mannose receptor activity: a marker of alternative immunologic macrophage activation. *J.Exp.Med.*, 176(1), 287-292.

Strachan T & Read A.P (2004). *Human molecular genetics 3*. Garland Science.

Su,A.I., Cooke,M.P., Ching,K.A., Hakak,Y., Walker,J.R., Wiltshire,T., Orth,A.P., Vega,R.G., Sapinoso,L.M., Moqrich,A., Patapoutian,A., Hampton,G.M., Schultz,P.G., & Hogenesch,J.B. (2002). Large-scale analysis of the human and mouse transcriptomes. *Proc.Natl.Acad.Sci.U.S.A.*, 99(7), 4465-4470.

Suzuki,T., Ganesh,S., Agarwala,K.L., Morita,R., Sugimoto,Y., Inazawa,J., Delgado-Escueta,A.V., & Yamakawa,K. (2001). A novel gene in the chromosomal region for juvenile myoclonic epilepsy on 6p12 encodes a brain-specific lysosomal membrane protein. *Biochem.Biophys.Res.Commun.*, 288(3), 626-636.

Szulc,J., Wiznerowicz,M., Sauvain,M.O., Trono,D., & Aebischer,P. (2006). A versatile tool for conditional gene expression and knockdown. *Nat.Methods.*, 3(2), 109-116.

Takahashi,K., Umeda,S., Shultz,L.D., Hayashi,S., & Nishikawa,S. (1994). Effects of macrophage colony-stimulating factor (M-CSF) on the development, differentiation, and maturation of marginal metallophilic macrophages and marginal zone macrophages in the spleen of osteopetrosis (op) mutant mice lacking functional M-CSF activity. *J.Leukoc.Biol.*, 55(5), 581-588.

Tang,Y.T., Hu,T., Arterburn,M., Boyle,B., Bright,J.M., Emtage,P.C., & Funk,W.D. (2005). PAQR proteins: a novel membrane receptor family defined by an ancient 7-transmembrane pass motif. *J.Mol.Evol.*, 61(3), 372-380.

Tauber,A.I. (2003). Metchnikoff and the phagocytosis theory. *Nat.Rev.Mol.Cell Biol.*, 4(11), 897-901.

Taylor,P.R., Martinez-Pomares,L., Stacey,M., Lin,H.H., Brown,G.D., & Gordon,S. (2005). Macrophage receptors and immune recognition. *Annu.Rev.Immunol.*, 23:901-44., 901-944.

te,R.H., Maandag,E.R., & Berns,A. (1992). Highly efficient gene targeting in embryonic stem cells through homologous recombination with isogenic DNA constructs. *Proc.Natl.Acad.Sci.U.S.A.*, 89(11), 5128-5132.

Thomas,K.R., Deng,C., & Capecchi,M.R. (1992). High-fidelity gene targeting in embryonic stem cells by using sequence replacement vectors. *Mol.Cell Biol.*, 12(7), 2919-2923.

Tiscornia,G., Singer,O., Ikawa,M., & Verma,I.M. (2003). A general method for gene knockdown in mice by using lentiviral vectors expressing small interfering RNA. *Proc.Natl.Acad.Sci.U.S.A.*, 100(4), 1844-1848.

Tsatsanis,C., Zacharioudaki,V., Androulidaki,A., Dermitzaki,E., Charalampopoulos,I., Minas,V., Gravanis,A., & Margioris,A.N. (2005). Adiponectin induces TNF-alpha and IL-6 in macrophages and promotes tolerance to itself and other pro-inflammatory stimuli. *Biochem.Biophys.Res.Commun.*, 335(4), 1254-1263.

Tsuchida,A., Yamauchi,T., Takekawa,S., Hada,Y., Ito,Y., Maki,T., & Kadowaki,T. (2005). Peroxisome Proliferator-Activated Receptor (PPAR){alpha} Activation Increases Adiponectin Receptors and Reduces Obesity-Related Inflammation in Adipose Tissue: Comparison of Activation of PPAR{alpha}, PPAR{gamma}, and Their Combination. *Diabetes.*, 54(12), 3358-3370.

van Furth,R. (1982). Current view on the mononuclear phagocyte system. *Immunobiology.*, 161(3-4), 178-185.

Yamauchi,T., Kamon,J., Ito,Y., Tsuchida,A., Yokomizo,T., Kita,S., Sugiyama,T., Miyagishi,M., Hara,K., Tsunoda,M., Murakami,K., Ohteki,T., Uchida,S., Takekawa,S., Waki,H., Tsuno,N.H., Shibata,Y., Terauchi,Y., Froguel,P., Tobe,K., Koyasu,S., Taira,K., Kitamura,T., Shimizu,T., Nagai,R., & Kadowaki,T. (2003a). Cloning of adiponectin receptors that mediate antidiabetic metabolic effects. *Nature.*, 423(6941), 762-769.

Yamauchi,T., Kamon,J., Waki,H., Imai,Y., Shimozawa,N., Hioki,K., Uchida,S., Ito,Y., Takakuwa,K., Matsui,J., Takata,M., Eto,K., Terauchi,Y., Komeda,K., Tsunoda,M., Murakami,K., Ohnishi,Y., Naitoh,T., Yamamura,K., Ueyama,Y., Froguel,P., Kimura,S., Nagai,R., & Kadowaki,T. (2003b). Globular adiponectin protected ob/ob mice from diabetes and ApoE-deficient mice from atherosclerosis. *J.Biol.Chem.*, 278(4), 2461-2468.

Yanagawa,Y., Kobayashi,T., Ohnishi,M., Kobayashi,T., Tamura,S., Tsuzuki,T., Sanbo,M., Yagi,T., Tashiro,F., & Miyazaki,J. (1999). Enrichment and efficient screening of ES cells containing a targeted mutation: the use of DT-A gene with the polyadenylation signal as a negative selection maker. *Transgenic Res.*, 8(3), 215-221.

Yokota,T., Oritani,K., Takahashi,I., Ishikawa,J., Matsuyama,A., Ouchi,N., Kihara,S., Funahashi,T., Tenner,A.J., Tomiyama,Y., & Matsuzawa,Y. (2000). Adiponectin, a new member of the family of soluble defense collagens, negatively regulates the growth of myelomonocytic progenitors and the functions of macrophages. *Blood.*, 96(5), 1723-1732.

Zhang,H., Hu,J., Recce,M., & Tian,B. (2005). PolyA_DB: a database for mammalian mRNA polyadenylation. *Nucleic Acids Res.*, 33(Database issue), D116-D120.

Zhu,X.D., Bonet,B., & Knopp,R.H. (1997). 17beta-Estradiol, progesterone, and testosterone inversely modulate low-density lipoprotein oxidation and cytotoxicity in cultured placental trophoblast and macrophages. *Am.J.Obstet.Gynecol.*, 177(1), 196-209.

Zhu,Y., Bond,J., & Thomas,P. (2003a). Identification, classification, and partial characterization of genes in humans and other vertebrates homologous to a fish membrane progestin receptor. *Proc.Natl.Acad.Sci.U.S.A.*, 100(5), 2237-2242.

Zhu,Y., Rice,C.D., Pang,Y., Pace,M., & Thomas,P. (2003b). Cloning, expression, and characterization of a membrane progestin receptor and evidence it is an intermediary in meiotic maturation of fish oocytes. *Proc.Natl.Acad.Sci.U.S.A.*, 100(5), 2231-2236.

Ziegler-Heitbrock,H.W. (2000). Definition of human blood monocytes. *J.Leukoc.Biol.*, 67(5), 603-606.

9. Abbreviations

AA	Acrylamide
AP	Alakaline Phosphatase
BLAST	Basic Local Alignment Search Tool
BSA	Bovine Serum Albumine
cDNA	complementary DNA
CFU	Colony Forming Unit
cpm	count per minute
DAPI	4',6'-diamidino-2-phenylindol
DC	Dendritic cell
DEPC	Diethyl Pyrocarbonate
DIG	Digoxigenin
DMEM	Dulbecco's Modified Eagle Medium
DMSO	Dimethyl Sulfoxyde
DNA	Deoxyribonucleic Acid
dNTP	deoxinucleotide Triphosphate
dpc	day post coitus
DTT	Dithiothreitol
ECL	Enhanced Chemiluminescence
EDTA	Ethylenediaminetetraacetic Acid
ES	Embryonic stem cell
EST	Expressed Sequence Tag
EtOH	Ethanol
FCS	Fetal calf serum
FITC	Fluorescein Isothiocyanate
GM-CSF	Granulocyte Macrophage Colony Stimulating Factor
HA	Hemaglutanin
HRP	Horseradish Peroxidase
IL	Interleukin
INFγ	Interferon gamma
INM	Internal nuclear membrane
ISH	In situ hybridization

LAMP	Lysosomal-associated membrane protein
LB	Luria Bertani
M-CSF	Macrophage Colony Stimulating Factor
MEF	Mouse Embryonic Fibroblast
MHC	Major Histocompatibility Complex
MMD	Monocyte to Macrophage Differentiation
MMD2	Monocyte to Macrophage Differentiation 2
MNC	Mononuclear cell
MOPS	3-(N-Morpholino) Propanesulfonic acid
mRNA	messenger RNA
NaOAc	Sodium Acetate
Neo	Neomycin
NP-40	Nonidet P-40
OD	Optical Density (Absorbance)
PBS	Phosphate Buffered Saline
pBS	Plasmid Bluescript
PCR	Polymerase Chain Reaction
PEG	Polyethyleneglycol
PFA	Paraformaldehyde
qRT-PCR	Quantitative Real-time PCR
RNA	Ribonucleic Acid
rpm	round per minute
RT	Room Temperature
SDS	Sodium Dodecyl Sulfate
siRNA	small interference RNA
SSC	Saline Sodium Citrate
TAE	Tris Acetate /EDTA electrophoresis buffer
TE	Tris-EDTA
TEMED	N,N,N’,N’,-Tetramethylenediamine
tRNA	transfer RNA
UV	Ultraviolet
WB	Washing Buffer
WT	Wild Type

10. Eidesstattliche Erklärung

Ich erkläre hiermit an Eides statt, daß ich die vorliegende Arbeit ohne unzulässige Hilfe Dritter und ohne Benutzung anderer als der angegebenen Hilfsmittel angefertigt habe; die aus anderen Quellen direct oder indirect übernommenen Daten und Konzepte sind unter Angabe des Literaturzitats gekennzeichnet.

Weitere Personen waren an der inhaltlich-materiellen Herstellung der vorliegenden Arbeit nicht beteiligt. Insbesondere habe ich hierfür nicht die entgeltliche Hilfe eines Promotionsberaters oder anderer Personen ins Anspruch genommen. Niemand hat von mir weder unmittelbar noch mittelbar geldwerte Leistungen für Arbeiten erhalten, die im Zusammenhang mit dem inhalt der vorgelegten Dissertation stehen.

Die Arbeit wurde bisher weder im In- noch im Ausland in gleicher oder ähnlicher Form einer anderen Prüfungsbehörde vorgelegt.

---------- ----------

(Carol El Chartouni)